New insights into assembly dynamics of the axoneme in Trypanosoma brucei

Daniel Abbühl

Thèse de doctorat

De Sorbonne Université

École doctorale Complexité du Vivant

Présentée par

M. Daniel Abbühl

Pour obtenir le grade de
Docteur de Sorbonne Université

New insights into assembly dynamics of the axoneme in *Trypanosoma brucei*

Soutenue le 29 septembre 2023

Devant le jury composé de :
Sylvie SCHNEIDER-MAUNOURY, Présidente du jury
Aminata TOURÉ, Rapporteuse
Keith MATTHEWS, Rapporteur
Alice MEUNIER, Examinatrice
Yurchenko VYACHESLAV, Examinateur
Philippe BASTIN, Directeur de thèse
Serge BONNEFOY, Co-Directeur de thèse

För mini Eltere, well ihr mich bedingigslos unterstützet

Acknowledgements

As I consider the Master's degree the start of my scientific journey I want to first thank Isabel, Nagul and the whole Roditi lab for igniting the spark and pointing me in the direction of Paris. Without your initial guidance, this adventure would have been so much harder and might not have been undertaken in the first place.

My gratitude goes out to the members of the thesis committee.
I want to thank Aminata Touré and Keith Matthews for accepting to read and evaluate the manuscript as well as their valuable comments on how to improve its quality and presentation. I am grateful to Slava Yurchenko and Alice Meunier for challenging me and the presented work during the defense procedure. For presiding over the jury and the bureaucratic effort entailed by this task, I thank Sylvie Schneider-Manoury. Lastly, I want to thank all of the jury members for their collaborative effort, on making the thesis defense a scientific discussion I will remember.

Dear Philippe, I thank you wholeheartedly for accepting me as a PhD student.
Thank you for giving me the opportunity of developing and discussing my ideas and driving this project in a satisfying direction. Thank you for always being available for questions and discourse and for being so resourceful with literature suggestions. Finally, I want to thank you for the way you accept the strength and weakness of all your lab members, allowing us to pour some of our personality into our research.

Dear Serge, thank you for providing me with the freedom I enjoy when approaching new techniques and experiments. Thank you for always being open for questions or listening to my theories.

I want to thank Anne for being the administrative backbone of this lab and being a big help during the initial bureaucracy involved in signing up for the CDV.

Next, I of course want to thank all the members of Philippes lab. Anais, Brice, Christine, Hashem, Héloise, Thierry, Christelle and Sabie. I also want to thank Karinna, Elena and the rest of Lucys lab. Before I started, someone told me that the best thing about a PhD will be the people you meet along the way. This is true.

A special thanks I want to extend to Aline and Jean-Marc for all the scientific and not so scientific discussions, for all the beers we shared, lunches we ate and world cups we watched. Thank you Parul for all of the above and being the best PhD buddy and a friend that was always listening to my ideas, ramblings and opinions.

Thank you, Tutu, for being my best friend in this city even when times were most difficult.

Viele Dank a all mini fründe i de Schwiz wo mi us de ferni unterstützt hend ond devör sorge dasi au miteme lachende auge Paris verlo welli zu euch zrugg chume.

Min grösste Dank goht a mini schwöster, mini eltere, s grosi ond s Karin. Euche bedingigslose Rückhalt het mir so viel Druck weggnoh, weli gwüsst ha dasi immer uf euch chan zähle au wenn das abentüür nid set klappe.

Abbreviations

AA	Amino Acids
AAT	Animal African Trypanosomiasis
AE	Adhering Epimastigotes
BB	Basal Body
BP	Basal Plate
BSF	Bloodstream Forms
cNMP	cyclic Nucleotide Monophosphate
CP	Central Pair
DE	Dividing Epimastigotes
ER	Endoplasmatic Reticulum
FAZ	Flagellar Attachment Zone
FC	Flagellar Connector
FG	Foregut
FP	Flagellar Pocket
FPC	Flagellar Pocket Collar
FRAP	Fluorescence Recovery After Photobleaching
GDP	Guanosine Diphosphate
GTP	Guanosine Triphosphate
HAT	Human African Trypanosomiasis
HSP	Heat Shock Protein
IDA	Inner Dynein Arm
IFA	Immunofluorescence Assay
IFT	Intraflagellar Transport
kDa	Kilodalton
kDNA	kinetoplast DNA
LS	Long Slender
MAP	Microtbubule Associated Protein
MG	Midgut
MS	Mesocyclic
MT	Metacyclic
MTOC	Microtubule Organising Center
MtQ	Microtubule Quartet
MTs	Microtubules

NDRC	Nexin Dynein Regulatory Complex
NF	New Flagellum
ODA	Outer Dynein Arm
OF	Old Flagellum
ORF	Open Reading Frame
PAC	PFR Axoneme Connectors
PC / PCF	Procyclic Forms / Procyclic Culture Forms
PCM	Pericentriolar Matrix
PFR	Paraflagellar Rod
Pol I/II	DNA-dependent RNA-polymerase I/II
PTM	Post-translational Modification
PTU	Polycistronic Transcription Unit
RNAi	RNA interference
SEM	Scanning Electron Microscopy
ST / SS	Stumpy / Short Stumpy
TAC	Tripartite Attachment Complex
TEM	Transmission Electron Microscopy
TET/ tet	Tetracycline
tetO	Tetracycline Operator
tetR	Tetracycline Repressor
TF	Transition Fibers
TLF	Trypanosome Lytic Factor
TTLL	Tubulin Tyrosine Ligase Like
TZ	Transition Zone
UTR	Untranslated Region
VSG	Variable Surface Glycoprotein
WB	Western Blot
WT	Wild Type
YFP	Yellow Fluorescent Protein

Table of Contents

Introduction

The parasite *Trypanosma brucei brucei*

At the end of the year 1895, Scottish pathologist David Bruce published the first report that described the agent responsible for the "tsetse fly disease" (Bruce, 1915). He noted the presence of a pathogen in the blood of cattle affected by this condition, that the local population called nagana ("depressed in spirit"). The parasite is now recognized by the name *Trypanosoma brucei*. They are transmitted by the bite of the tsetse fly and shuttle between the insect vector and a mammalian host. On their journey through the two hosts, parasites differentiate between multiple stages that are adapted to the respective environment. This process includes substantial changes in metabolism, gene expression and most importantly for this work, morphology (Rotureau and Van Den Abbeele, 2013; Vickerman, 1985). The disease is restricted to the habitats of these insects. An area spanning from Gambia in the west towards Mozambique in the east of the African continent is often referred to as the "tsetse-belt'. When a tsetse-fly infected with trypanosomes takes a bloodmeal, it injects the parasites into the mammalian host. There, the trypanosomes live extracellularly in the blood as well as in extravascular compartments (Capewell et al., 2016; Vickerman, 1985). The stage that proliferates in the mammal is called slender bloodstream forms (slender BSFs). BSFs exhibit an extremely densely packed coat of surface proteins, called various surface glycoproteins (VSGs). Around ~2000 different genes code for these highly variable proteins, that serve the purpose of evading the mammalian hosts immune response(Cross et al., 2014). Progressively the infected individual will mount antibodies against a certain VSG and eliminate parasite that carry it. The parasite load decreases until a subpopulation with a different VSG emerges. This vicious cycle repeats until the parasite eventually overpowers the mammalian hosts immune system. Upon increasing parasitemia the slender BSFs turn into the cell cycle arrested stumpy BSFs. The metabolism of this stage is pre-adapted for the life in the insect vector. When a

tsetse fly takes a bloodmeal on an infected mammal, it will ingest a mix of slender and stumpy BSF. In the fly's midgut these cells then differentiate into procyclic forms that marks the first stage that is specific to the insect vector. In the fly parasites will migrate through the digestive tract and finally end up in the salivary glands. There the metacyclic trypomastigote stage is ready for the next infectious bite.

Three subspecies have been described from which two are human pathogens that cause "sleeping sickness" (Human African Trypanosomiasis (HAT)), a devastating ailment that results in the patient's death if left untreated. The name derives from the observation, that many afflicted by this disease, demonstrated a disrupted circadian cycle. This manifests in patients being awake during the night and asleep at daytime. *Trypanosoma brucei gambiense* causes the chronic form of the disease predominantly present in western and central Africa. The incubation time ranges from weeks to months and in some cases years. This time is much shorter for the acute form caused by *Trypanosoma brucei rhodesiense* and parasites are found to cross the blood brain barrier as short as one month post infection. The presence of *Trypanosoma brucei* in a patient's brain leads to lethargy, coma and ultimately death (reviewed in Despommier et al., 2017). Human African Trypanosomiasis (HAT) is targeted for elimination in the coming decade and significant advances have been achieved in the last 20 years. Undoubtedly, a continuous effort of researchers towards this goal is indispensable (Franco et al., 2022), as resurgence of HAT cases remains a threat (Camara et al., 2017).

Humans possess an innate immune response that eliminates trypanosomes, based on Apolipoprotein 1 (ApoL-1), also called the trypanosome lytic factor (TLF). This protein integrates in the membrane of the cell and the mitochondrion where it acts as a channel. The exact mechanism by which TLF kills trypanosomes is not clear (O'Toole et al., 2017). *T.b.gambiense and T.b.rhodesiense* have separately evolved resistance to the TLF that is present in human serum (Thomson et al., 2014; Thomson and Finkelstein, 2015; Uzureau et al., 2013; Vanhamme et al., 2003). The third subspecies Trypanosoma *brucei brucei* is pathogen of cattle and other livestock, presenting a substantial economic burden in infested

regions. However, it did not evolve resistance to human serum and is therefore not a human pathogen. Much of the trypanosome research is carried out with this subspecies. Although the focus on the disease and how to combat it remains sharp, *T.b.brucei* has gained popularity as a model organism during the past decades for multiple practical and biological reasons.

First, the trypanosome genome has been sequenced (Berriman et al., 2005) which opened the door to dissect its molecular biology. Secondly, the parasite is readily cultured *in vitro* and very amenable to genetic manipulation. A non-exhaustive list of available tools includes the knockout and *in situ* tagging of genes, RNA interference (Huan et al., 1998; Shi et al., 2009), CRISPR-Cas mediated DNA editing (Beneke et al., 2017; Rico et al., 2018), as well as the introduction of transgenes and their inducible ectopic expression (Wirtz and Clayton, 1995)(Poon et al., 2012).

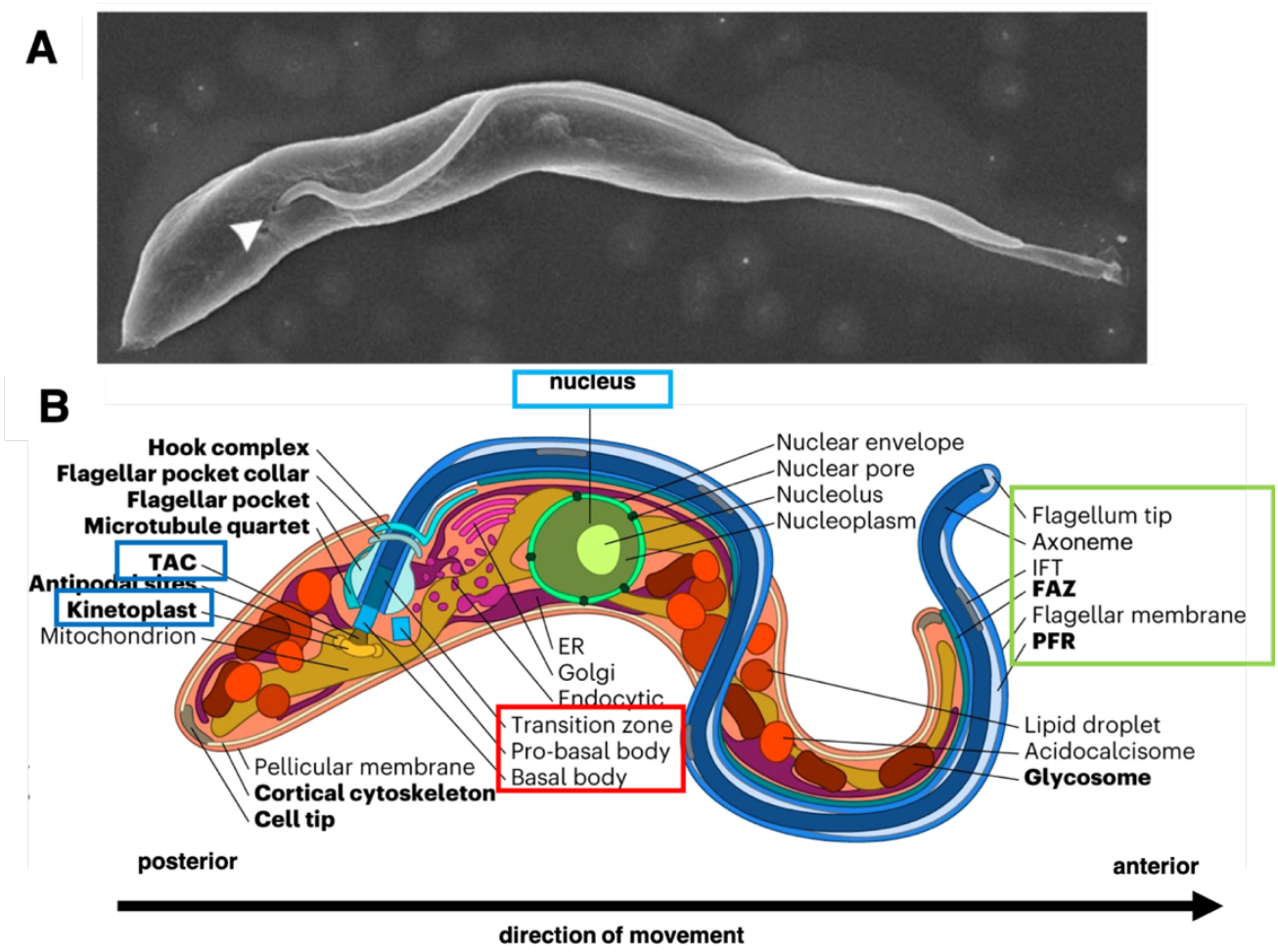

Figure 1: Image of a procylic form trypanosome. A: SEM image from Buisson and Bastin 2010. The single flagellum emerges posterior out of the flagellar pocket and is attached alongside the cell apart from a short portion at the distal tip that goes beyond the cell body. B: Cartoon of the intracellular architecture of a procyclic trypanosome adjusted from Billington et al. 2023. Some of the cell compartments are highlighted in colors. Dark blue: tripartite attachment complex (TAC) that attaches the kinetoplast to the basal body(BB). Light blue: the nucleus. Red: the start of the flagellum with the two basal bodies (BB), the transition zone (TZ). Green: the flagellum and the flagellar membrane including the flagellar tip, the axoneme, IFT particles and the flagellar attachment zone that spans the flagellar and cell membrane as well as the extra-axonemal paraflagellar rod (PFR).

A unique cell

It is not just the relative ease of experimental procedures that makes the African trypanosome a worthwhile model to study, but also its unique architecture and biology. Fig.1a depicts an image of a procyclic form trypanosome acquired by scanning electron microscopy (SEM). It highlights the elongated "screw"-like shape of this cell. The cell posterior is relatively thicker than the anterior. Depending on the life cycle the unicellular eukaryote is 10 – 30μm long and 2 - 3μm thick. Attached to the cell body is a single flagellum that exits the cell body at the posterior and that drags the cells forward in the direction of the flagellar tip (Fig. 1B, arrow). Apart from the single flagellum, they possess one nucleus, one golgi-apparatus and one mitochondrion that contains one additional structure called the kinetoplast, a dense network of DNA (Fig. 1b). These structures duplicate before the trypanosome cell divides and each daughter inherits one copy of each. It is this "singularity" that makes trypanosomes a formidable tool to study the function of organelles and structures as well as their duplication and segregation during the cell cycle. Importantly, their number, size, shape and positioning provide useful markers to understand the state of the cell cycle in which any given cell is at a specific point in time. The assembly and division of the flagellum, nucleus and the kinetoplast follows a highly orchestrated program and its timing is vital for parasite survival (Woodward and Gull, 1990). Broadly understanding the configuration of each of these three structures is therefore paramount, even when the focus lies on only on one of them.

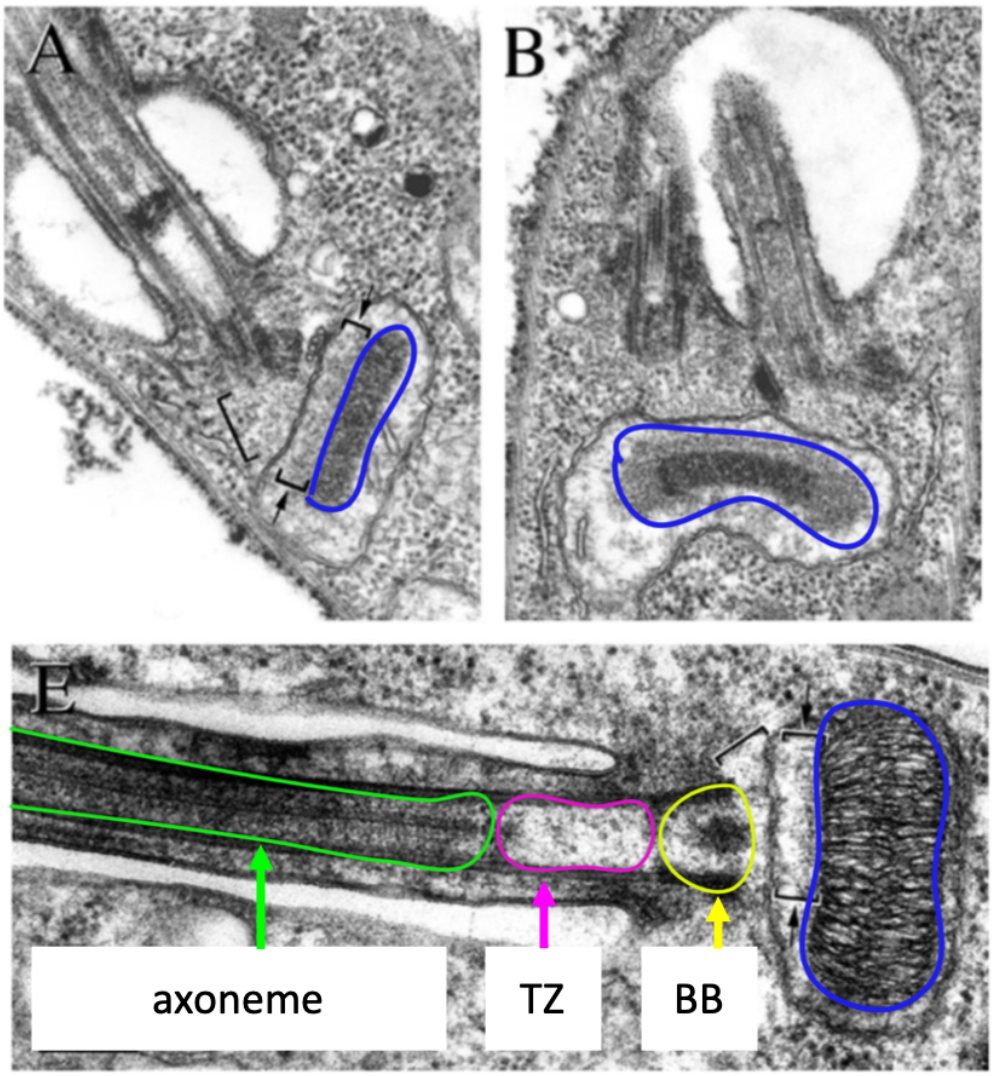

Figure 2: longitudinal sections aquired by TEM of the flagellum, the kinetoplast and surrounding structures. Highlighted in blue is the dense DNA network of the kinetoplast inside the mitochondrion. A: longitudinal section of a cell with one flagellum, the arrows indicate the structure that connects the base of the flagellum to the kinetoplast (tripartite attachment complex or TAC, (Ogbadoyi et al., 2003)). B: longitudinal section of a cell with an old and a very short new flagellum that still shares a flagellar pocket with the old flagellum. C: longitudinal section highlighting the densily packed DNA inside the kinetoplast and the connecting structure indicated by arrows. Highlighted in blue: kinetoplast, yellow: basal body (BB), magenta: transition zone (TZ), green: axoneme. Figure adjusted from Ogbadoyi et al., 2003.

The kinetoplast

Trypanosoma belong to the class of the Kinetoplastea whose name was coined by the presence of a specialized structure called the kinetoplast (Fig. 1b, Fig 2), a dense network of DNA made from intertwined mini and maxi-circles that lies inside the single mitochondrion. Maxi-circles are substantially larger and code mostly for genes of the respiratory chain (Hajduk and Ochsenreiter, 2010). To process transcripts that are ready for translation, kinetoplast RNAs are subject to substantial editing. Indeed, RNA-editing was first described for transcripts from the kinetoplast DNA (Hajduk and Ochsenreiter, 2010; Stuart et al., 1997). A majority (~95%) of the kinetoplastid DNA (kDNA) consists of the mini-circles that code for regulatory RNAs. Duplication relies on a concatenation/de-concatenation process that dis-entangles the complex network ahead of segregation.

The nucleus: Gene expression

A second home to the trypanosomes genes is the nucleus that houses a diploid genome. It has been sequenced and codes for roughly 9000 genes (Berriman et al., 2005). The genome is organized into 11 megabase chromosomes, 5 intermediate chromosomes and approximately 100 mini chromosomes. A majority of protein coding genes are transcribed by RNA-polymerase II (Pol II). They are transcribed as polycistronic transcription units (PTUs) and then processed and spliced into monocistronic transcripts corresponding to the individual genes. The individual genes on a given PTU are not functionally related to each other, apart from a few exceptions, like the tandem repeats of the genes that code of alpha and beta-tubulin (Thomashow et al., 1983).

Initiation of Pol II transcription at the PTUs remains a topic under investigation. Previously thought to predominantly rely on chromatin modifications, the identification of sequence specific promoters has only started very recently (Clayton, 2016; Cordon-Obras et al., 2022; Daniels et al., 2010; Wedel et al., 2017). Trypanosomes evolved a simple strategy to achieve

the expression of high quantities of certain proteins. They simply duplicated genes that code for proteins in high demand. One example are the roughly forty identical copies of alternating beta and alpha-tubulin genes, that are found in the trypanosome genome (Berriman et al., 2005; Clayton, 2016; Daniels et al., 2010; Ersfeld et al., 1999; Thomashow et al., 1983).

Excessive post-transcriptional regulation is a necessity for faithful gene expression of the individual genes transcribed from the PTUs. The 3' untranslated region (UTR) and its interaction with a plethora of RNA binding proteins plays a major role in the control mRNA decay and translation. The length of the 3' UTR often spans over of several hundred nucleotides and its sequence integrity therefore important for gene regulation (Clayton, 2016).

A limited set of promoters has been described which are mainly responsible for the transcription of surface proteins. Surprisingly, these are transcribed by Pol I which is unusual for eukaryotes (Clayton, 2016; Daniels et al., 2010).

Some of these such as the procyclin promoter are very active transcription initiators. This is frequently exploited in trypanosome research, especially for the ectopic (over)-expression of trans-genes (Biebinger et al., 1996; Pays et al., 1990). To circumvent the absence of gene-specific promoters, an exogenous polymerase derived from bacteriophages (T7-polymerase) was succesfully introduced. When a trypanosome cell line possesses the T7 polymerase, one can introduce a transgene under the regulation of a T7 promoter, allowing the expression of high amounts of RNA, suitable for ectopic (over)-expression (Poon et al., 2012; Wirtz et al., 1998).

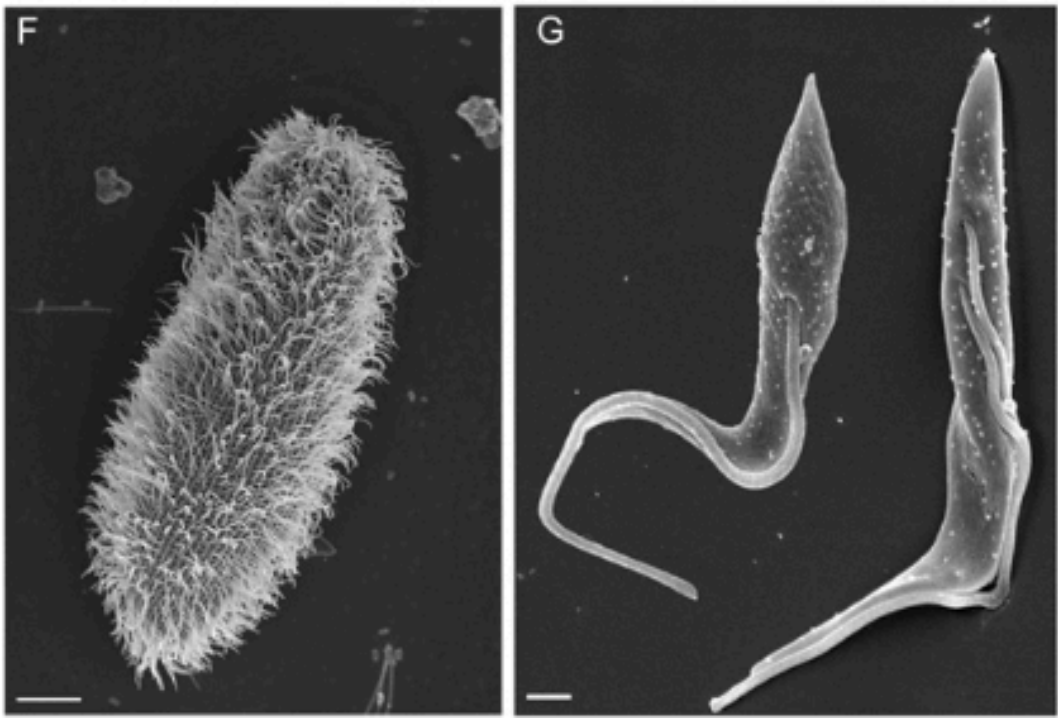

Figure 3 : SEM images of cilia and flagella present on different organisms with variable number and length. F: numerous cilia of *Paramecium tetraurelia* scale bar: 10 μm. G: flagella of Trypanosoma brucei of a mono-flagellated cell (left) and a bi-flagellated cell that is assembling a new flagellum in the same cell as it maintains an old flagellum, scale bar: 1 μm. Images adapted from (Vincensini et al., 2011)

The flagellum

Flagella also called cilia are highly organized cell protrusions that are present in many organisms of the eukaryotic lineage. They can be present on their own or in copies of several hundreds. In eukaryotes two main types of flagella are distinguished: the primary cilium as well as the motile cilium. The core of both these structures is made from long filaments called microtubules (MTs). MT's constitute a vital part of the eukaryotic cytoskeleton and give rise to a variety of specialized structures aside from flagella. The core of primary cilia is built from nine regularly interspaced MT doublets that are arranged in a cylinder. In motile cilia, an additional pair of single MTs is found in the center surrounded by the nine outer MT doublets. The central pair plays and important role in a cilium's motility. The motile cilium (9+2 MTs) is what is present on the trypanosome cell. We will henceforth refer to this organelle with the term flagellum.

A non-exhaustive list of the roles of flagella includes:

Locomotion refers to the ability of cells to move through the environment. For many cells, displacement is paramount for survival or to fulfill their role. One example is a spermatozoon that needs motility to reach the egg for fertilization.

Formation of flagella can be paramount for cellular morphogenesis and cell division. The connecting cilium for example is indispensable for the formation of photoreceptor cells. Many human diseases are indeed associated with ciliary defects (Rachel et al., 2012). In trypanosomes, mutants that assemble shorter flagella generate shorter cells and can display severe defects in cytokinesis (Kohl et al., 2003).

Flagella can be sensory organelles that detect and respond to cues from the environment. Some of these signals can be molecules such as cyclic nucleotide mono-phosphates (cNMP) or environmental stimuli of physical nature like light and temperature. These signals can provide the cells with cues for where they have to move to or how they respond to the environment.

In some organisms' flagella can be very numerous so their collective beating will govern the flow of the fluid that surrounds them. This process may serve the acquisition of nutrients or the distribution of molecules that affect a cells fate. Flagellar beating has for example been implicated in the organization of the Left/Right axis in vertebrate embryos development (Buceta et al., 2005).

In summary, flagella are highly ordered arrays of microtubules that are wrapped into a specialized extension of the cell membrane. (Fig. 5). The flagellum is anchored in the cell via the basal body (BB) which is followed by the transition zone (TZ) and then the axoneme. MTs are made from two very conserved proteins called alpha and beta-tubulin.

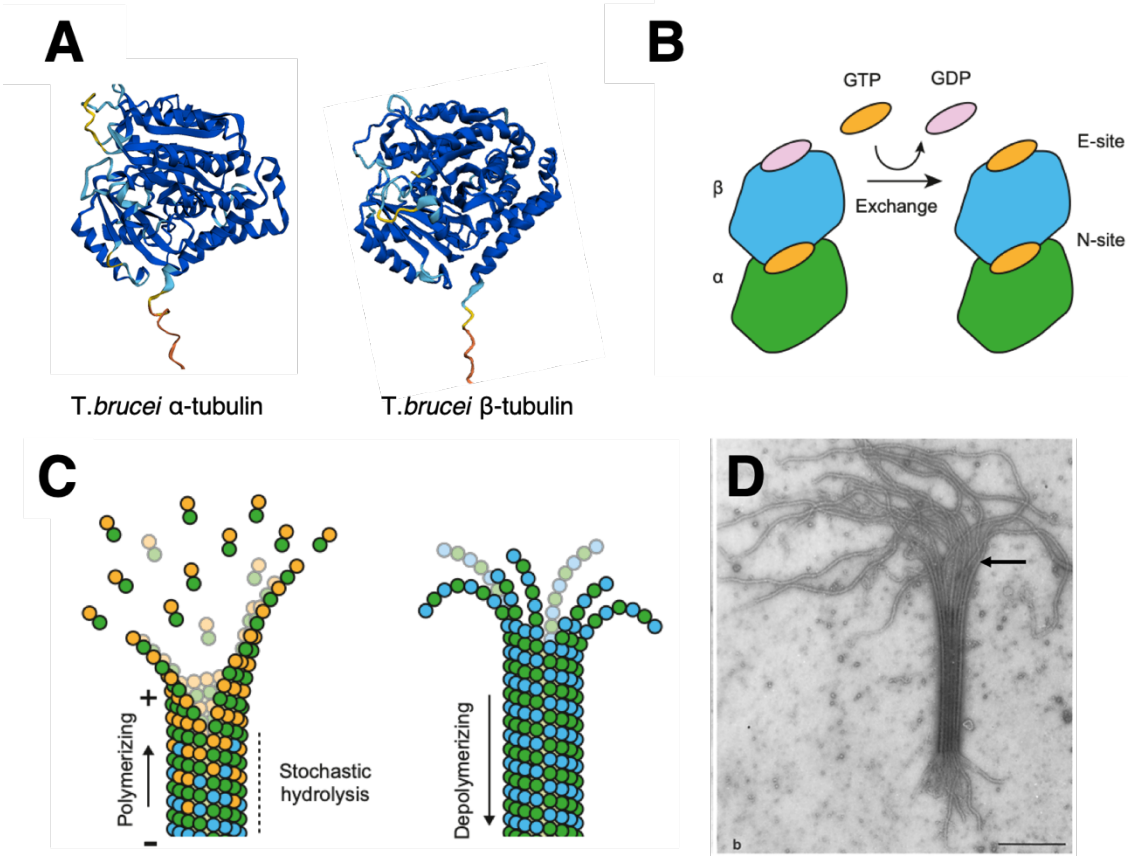

Figure 4: Images highlighting tubulin and its assembly into microtubules. A: Alpha-fold prediction of the three-dimensional structure of alpha and beta-tubulin from *Trypanosoma brucei*. The predicted protein structures obtained from http://wheelerlab.net/alphafold/index.php. (Richard Wheeler, 2021). Structures predicted by AlphaFold (Jumper et al. 2021). The color code indicates prediction confidence. C-terminal tails (orange, pointing towards the bottom of the image) of trypanosome tubulins are disordered.

B: Beta-tubulin is a GTPase capable of *hydrolyzing* GTP. C: Assembly of microtubules is a polarized process and new dimers are added at the plus end. Images were taken from Alushin et al. 2014 (A+B). D: MT doublets of Chlamydomonas polymerizing into an axoneme, adapted from (Binder and Rosenbaum, 1978), the arrow indicates the fork of an A and B-tubule that connect to form a doublet.

The main building block of microtubules: Tubulin

Tubulin is one of the most conserved proteins across the eukaryotic lineage. It is a globular protein with a molecular weight of approximately 50kDa. The most prominent role of tubulin is the assembly into MTs, that are a major part of the cytoskeleton. Only two tubulin proteins, alpha and beta-tubulin are capable of forming the dimers that are incorporated into MTs. The predicted three-dimensional structures of alpha and beta-tubulin from T.*brucei* can be seen in Fig. 4A (Jumper et al., 2021; Wheeler, 2021). Generally, MT assembly is a polarized process and the growing end is referred to as plus end while the more stable end is called minus end. Nucleation is the term that refers to the addition of new tubulin subunits to the growing end of microtubules. To assemble into MTs, it is important that alpha and beta-tubulin can bind to GTP. Furthermore, Beta-tubulin has GTPase activity, meaning it can hydrolyze GTP (Bramhill and Thompson, 1994; Nogales et al., 1998) (Fig. 4B). When the tubulin dimer is assembled into MT's, GTP remains bound to alpha-tubulin at all times but can be hydrolyzed to GDP bound to beta-tubulin (Fig. 4B). This process changes tubulin conformation and alters the nature of how individual dimers are connected to each other. When more GDP is bound at the end of a microtubule, the individual filaments tend to curve outwards, favoring de-polymerization (disassembly) (Fig. 4 C, (Alushin et al., 2014)). Contrarily, increased presence of double GTP-positive dimers (one GTP on both alpha and beta-tubulin) results in straight filaments that are laterally connected and organized into the characteristic tubules. This organization promotes the extension of microtubules, which is dependent on the availability of tubulin-dimers and guanosine nucleotides. The switch towards disassembly (named "catastrophe") is more stochastic (Fig. 4C) (Höög et al., 2011; Mandelkow et al., 1991; Nogales and Wang, 2006; Wang and Nogales, 2005). The balance between spontaneous disassembly and reassembly is often referred to as dynamic instability.

In vivo, a full single microtubule is built from 13 protofilaments. Which are longitudinal chains made from α/β-tubulin-dimers that get laterally connected to form a hollow tube (Tilney et al., 1973) (Fig. 4). Cilia and flagella are made of doublet MTs where a complete A-tubule of 13 protofilaments is joined by an incomplete B-tubule amounting to 10 protofilaments (Nogales et al., 1998). Fig. 4D depicts multiple MTs of Chlamydomonas assembling into a dedicated structure, predominantly made from MT doublets. The arrow indicates the fork at which an A-tubule is connected to B-tubule. The depicted structure, called the axoneme, is the flagellums core component and described in more detail in a later section.

Microtubule organizing centers (MTOCs) are the specific sites in the cell where the minus ends of many microtubules are bundled to and/or spread from.

The three most prominent MT based structures in trypanosomes are the flagellum, the MTs of the subpellicular array which are forming the cell body (Schneider et al., 1986), and the mitotic spindle. The trypanosome flagellum is anchored in the cell by its MTOC, called the basal body.

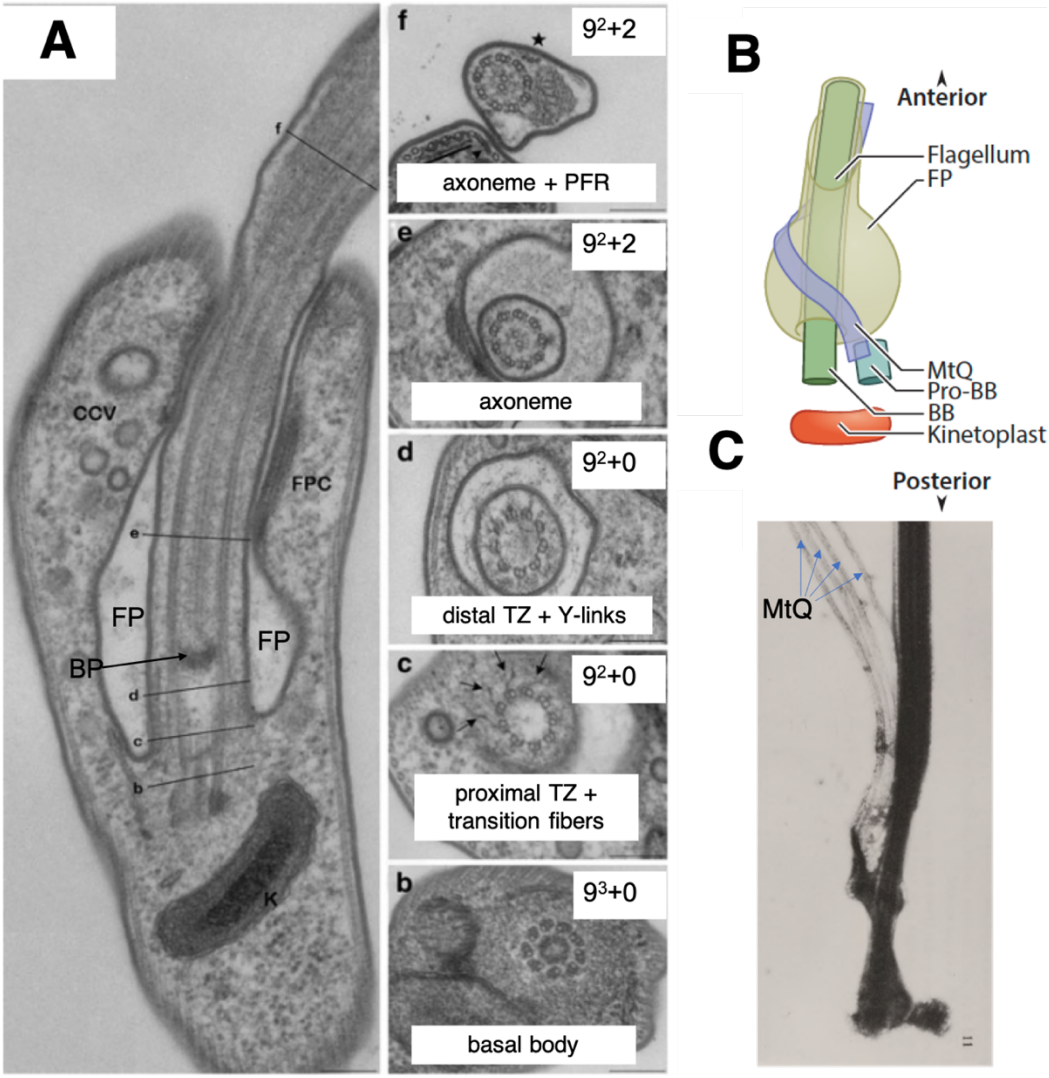

Figure 5: Longitudinal section through the flagellum root and stem, exiting the flagellar pocket (FP) that wraps around the flagellar membrane with the FP collar (FPC). A: Series of transversal sections through different parts of the flagellum. b) the basal body (BB) that anchors the flagellum in the cell c) proximal transition zone (TZ) with the transition fibers (arrows) that connect the intersection between BB and TZ to the flagellar pocket (FP). d) distal part of the TZ with the characteristic Y-links extending from the doublets towards the membrane. This section ends in the basal plate (BP) e) axoneme inside the FP. The nine outer doublets are now accompanied by the central pair in the middle. f) The axoneme outside the FP is joined by the extra-axonemal PFR. B: Cartoon illustrating a single flagellum inside the FP the mature BB that gives rise to the flagellum as well as the pro-BB. In the space between the two BBs the MT-quartet originates. C: SEM image of the MT quartet attached to the BB. Arrows indicate the four individual MTs of the quartet. Images were adjusted from: A: Buisson and Bastin, 2010 B: Wheeler et al., 2019, C: Sherwin and Gull, 1989.

The basal body

The basal body is a protein complex with a cylindrical shape that marks the short initial portion of the flagellum (Fig. 5a). Its core is formed by nine MT-triplets made from a complete A-tubule (13 protofilaments), an incomplete B-tubule (10 protofilaments) as well as a third, also incomplete (10 protofilaments), C-tubule. The BB anchors the flagellum in the cell and nucleates the MTs of the transition zone and then the axoneme (Fig. 5A, b). In essence this means, the BBs A and B-tubule continue as the MT doublet of the next part of the flagellum, the transition zone. At its end, the BB is attached with a set of fibers (transition fibers (TF)) to the flagellar pocket (FP) membrane (Fig. 5A, c). The FP is an invagination of the cell membrane through which the trypanosome flagellum leaves the cell body. It is the cell compartment that is responsible for endo- and exocytosis. A set of four MTs, (MT quartet) originates next to the basal body, wraps around the FP and then extends inside the cell towards the anterior cell tip (Lacomble et al., 2010; Taylor and Godfrey, 1969) (Fig. 5 B+C). The quartet runs in proximity to multiple structures that abide in the spatial coordination of cytoskeletal structures during flagellum formation and cell division and helps to facilitate these two processes.

The transition zone

The transition zone is made of nine cylindrically arranged MT doublets in continuation of the BB. It has a length of approximately 300nm and can be divided into a proximal and a distal portion. Analysis by electron microscopy revealed that in the distal portion each MT doublet possesses a Y-link that extends from the intersection of the two connected tubules outwards to form a bridge with the flagellar membrane (Fig. 5A, d). These links are likely present in the proximal portion as well but are obscured by an accumulation of electron dense material between the MT doublets cylinder and the membrane (Dean et al., 2016; Trépout et al., 2018). It is assumed that the TZ, together with the TF that connect its base to the membrane, act as a barrier that governs the access to the flagellum. FTZC is a highly repetitive protein of

unknown function that surrounds the MT doublets of the transition zone (Bringaud et al., 2000). Many studies that focus on protein localization in the area of the BB and the TZ utilized FTZC as a marker.

The TZ ends with an electron dense disk that separates this zone from the axoneme. This region is called the basal plate and thought to play a role in the nucleation of the two MTs that form the central pair (CP) inside the axoneme. Mutants of basal plate components exhibit defects in CP formation and motility (Dean et al., 2019).

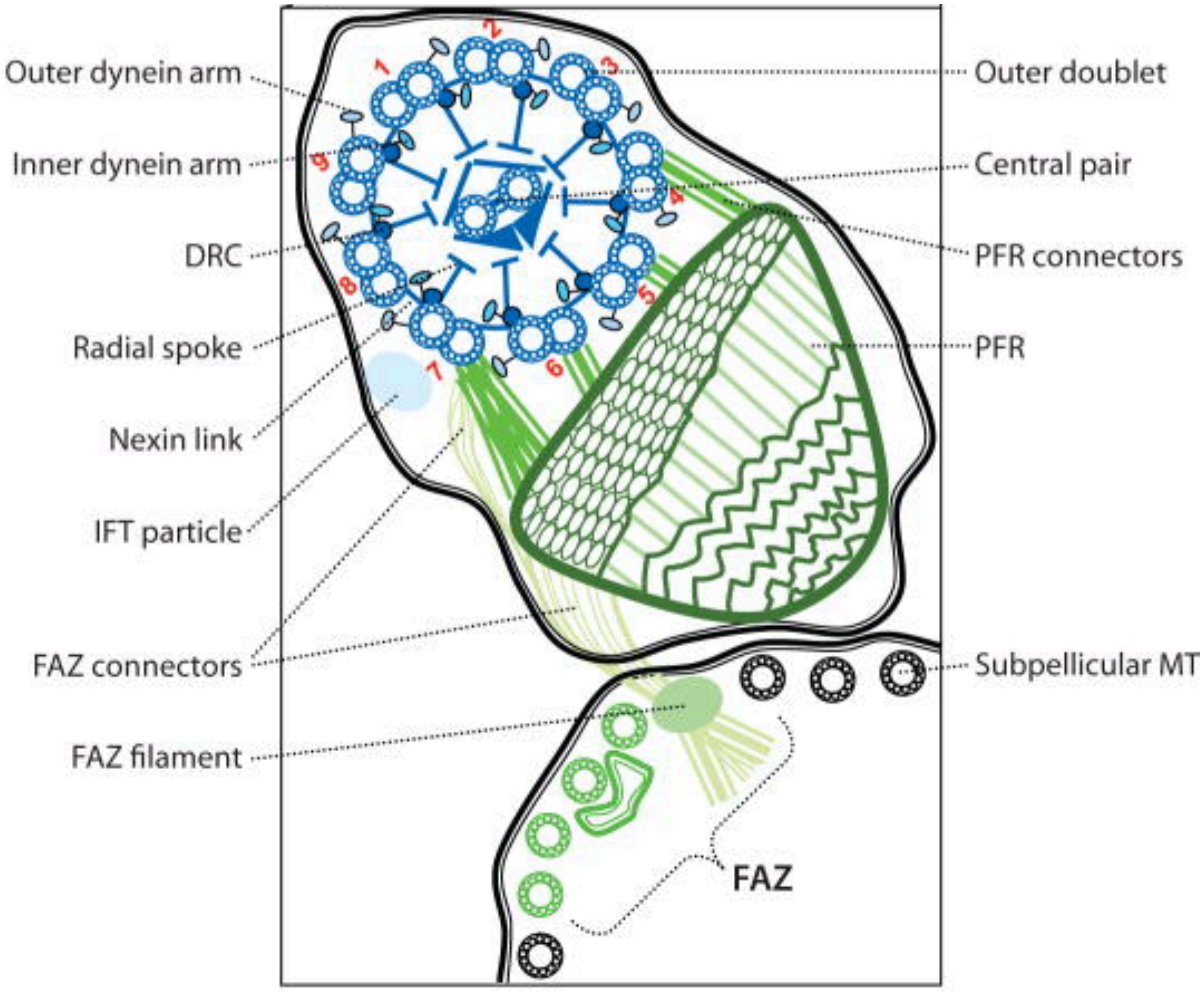

Figure 6 : Illustration of the axoneme and its components. Between MT doublets 4 and 7 the axoneme is connected to the largest accessory structure, the PFR. Filaments of the FAZ span the membranes of the flagellum and the cell. Image adapted from Ralston et al. 2009.

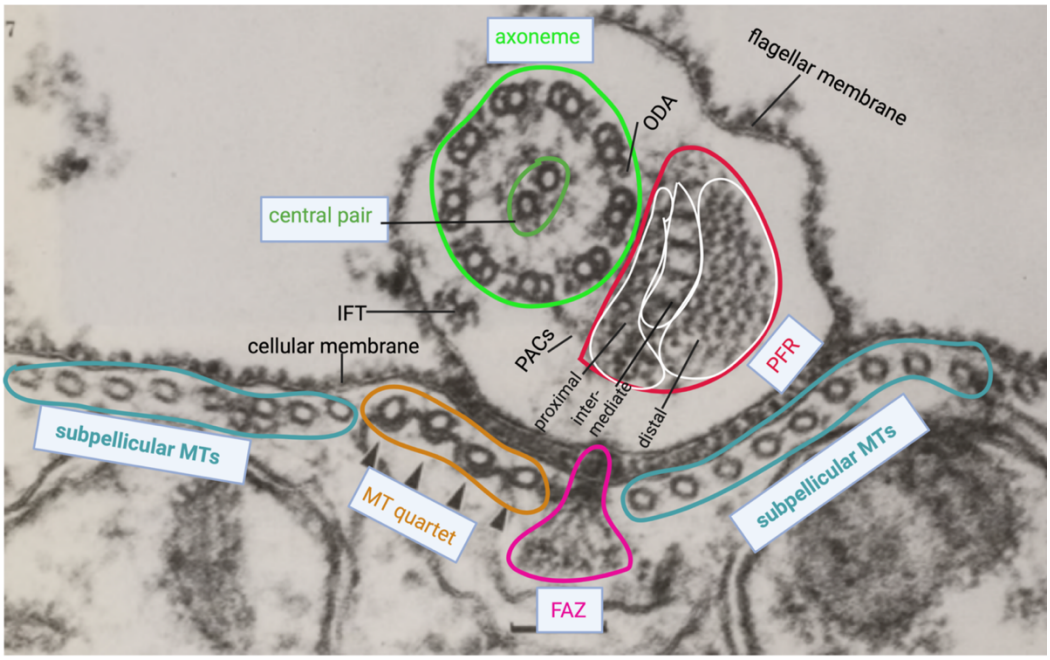

Figure 7: Transversal section of the dorsal side of a trypanosome cell and the attached flagellum. In light green and green: The axoneme and the central pair and outer dynein arms in clockwise direction as well as an IFT train between the axoneme and the flagellar membrane. Red: The extra-axonemal PFR with its three layers and the proteins above that connect it to the axoneme (PACs). Inside the cell that is wrapped in the cellular membrane: in turquoise the MTs of the subpellicular array that wrap around the entire cell, with the exception of a gap that is occupied by the flagellar attachment zone (FAZ), that spans the flagellar and the cellular membrane, as well as the microtubule quartet (MT quartet.) Both FAZ and quartet run along the length of the flagellum towards the anterior cell tip. In terms of cell orientation, this is the perspective from which the viewer sees this image (posterior to anterior-axis), indicated by the clockwise orientation of the outer dynein arm (ODA) that decorates the complete B-tubule. The image was modified from a transversal section acquired by Sherwin and Gull, 1989.

The axoneme

In close proximity to the basal plate two microtubules are nucleated that form the central pair (CP) of the axoneme. At this point the highly conserved structure is complete and nine outer doublet microtubules surround the central pair of single MTs in the middle. Several proteins that abide in spatial organization and flagellum motility are connected on the outside of the MT doublets Fig. 6 + 7).

As previously mentioned the doublet consists of a complete A-tubule that is joined by an incomplete B-tubule (Nogales et al., 1998). In the axoneme, from every B-tubule a radial spoke extends towards the central pair. Also positioned on the A-tubule are a set of dynein arms. One sits on the outside relatively closer to the membrane (outer dynein arm or ODA) and one on the inside of the A-tubule relatively closer to the CP (inner dynein arm or IDA). Together they generate the force necessary for flagellum beating. The doublets are connected to each other via the Nexin-dynein regulatory complex (NDRC) that extends from every incomplete B-tubule towards the complete A-tubule of the neighboring doublet. This connection ensures that the cylindrical arrangement of the MT doublets remains intact during the physical stress caused by the flagellar beat (Langousis and Hill, 2014). Radial spokes originate in close proximity where the IDA is connected to the A-tubule towards the central pair in the middle.

In figure 6 + 7 and additional structure is visible that is connected to the axoneme between the doublets four and seven. This extra-axonemal structure is unique to the euglenozoa including trypanosomes.

The paraflagellar rod (PFR)

The PFR is a sophisticated structure that accompanies the axoneme after the flagellum exits the FP and then extends for almost the entire length of the flagellum. By electron microscopy two rope-like structures are visible that attach the MT doublets 4 and 7 to the PFR (Farina et al., 1986). Its structure is separated into three layers. The first is the proximal layer that further connects PFR and axoneme between the doublets 4 and 7 via a zone that is rich in PFR-axoneme connecting proteins (PACs). From this zone a set of wires extend towards the distal layers of the PFR (Fig. 6 + 7, intermediate zone). The most distal layer is a paracrystalline network of repeating subunits that is predominantly filled with what appears to be empty space (Zhang et al., 2021). Two proteins PFR 1 and 2 are mainly responsible for the formation of the PFR. A combination of immunofluorescent analysis (IFA), RNAi mutants and proteomic approaches has revealed that the PFR is a network of roughly 200 genes. This entails structural components, genes involved in calcium modulation and other components of signaling pathways (Alves et al., 2020; Dean et al., 2017; Portman et al., 2009; Sunter et al., 2023).

The incorporation of new PFR material was measured with a tagged PFR 2 protein whose expression could be induced by the addition of a compound called tetracycline. After expression was induced the tagged PFR protein was expressed and the addition of PFR 2 could be monitored. Approximately 3.6μm of new PFR material was added along the length of the flagellum every hour at a linear rate. A gradient of tagged PFR2 was visible that increased in intensity towards the distal tip of the flagellum. This gradient could be separated by its intensity into two distinct parts. The section with higher intensity was found at the distal part of the flagellum towards the tip and the less intense section found more proximal. The authors concluded that the latter probably corresponded to the completion of segments in which PFR assembly had begun before induction of tagged PFR material (Bastin et al., 1999).

Assembly and structure of the PFR is still subject to investigation but its role remains even more enigmatic. So far, it is clear that the PFR is important for parasite motility (Bastin et al., 1998) and that it possibly assists in shaping the flagellar beat (Cicconofri et al., 2021; Zhang et al., 2021).

In brief, the PFR is the largest structure that decorates the axoneme. Without the flagellum's main component however, there is no PFR, no dynein arms or other extra-axonemal proteins.

The flagellar attachment zone (FAZ)

The FAZ is an electron dense cytoskeletal structure whose shape resembles a tower that intersects and thereby connects the membrane of the flagellum with the membrane of the cell (Fig. 7, FAZ). Its exact position can be seen in a transversal section by trans-emission electron microscopy (TEM), highlighted in Fig. 7. If the FAZ is followed through transversal sections from the posterior towards the anterior it runs along the longitudinal axis on the right side of the MT quartet (Fig. 7). Electron densities can be observed connecting the quartet to the "cell body membrane junctional complex", that is found very close to the cellular membrane. Fibers connect the complex to a filamentous plate, that is located in close proximity to the smooth endoplasmatic reticulum (ER) membrane and anchors the FAZ inside the cell body. In conjunction with the flagellum it governs cell morphology and length during assembly. Additionally, it helps to maintain the cells shape during movement and especially cell division.

Intraflagellar transport (IFT)

MT's provide the tracks for motor proteins to move cargo through the cell. Kinesins transport vesicles, organelles and other macromolecules towards the growing end (plus end) of microtubules while dyneins move in the opposite direction (Gennerich and Vale, 2009). In the

case of flagella, kinesins are responsible for the anterograde transport towards the tip of the axoneme, while dyneins move retrograde to its base reviewed in (Pigino, 2021).

This active transportation has been discovered and termed intraflagellar transport in 1993 (Kozminski et al., 1993). The authors discovered a protein that moves particles towards the distal tip of the flagellum and back. This protein, called FLA10, is a molecular motor of the kinesin family (Kozminski et al., 1993). As an intermediate between the cargo and the motor proteins serve two large protein complexes termed IFT-A and IFT-B. The latter is assembled first and serves as the platform for the assembly of the IFT-A complex and its binding to the dynein as well as the kinesin motors. Together these complexes are often referred to as IFT trains (Fig. 6 + 7, IFT) as they mediate the shuttling of cargo between flagellar tip and base (Lacey et al., 2023; Van Den Hoek et al., 2022). The area between BB and the TZ is a hub for the IFT machinery that is also responsible for the injection of trains into the flagellum to transport cargo towards the flagellum tip and back (Jung et al., 2021). This transport machinery ensures that new building blocks arrive at the tip where they can then be incorporated during flagellar elongation. IFT is essential for the construction of flagella of normal length and function. Depletion of IFT proteins can result in flagella being constructed to short or ablate flagellar morphogenesis altogether. As mis-regulation of flagellar length or absence of flagella severely impacts cell shape, size and division, many IFT mutants of trypanosomes display aberrant cells. (Absalon et al., 2007; Bertiaux et al., 2018; Davidge et al., 2006; Huet et al., 2019; Kohl et al., 2003).

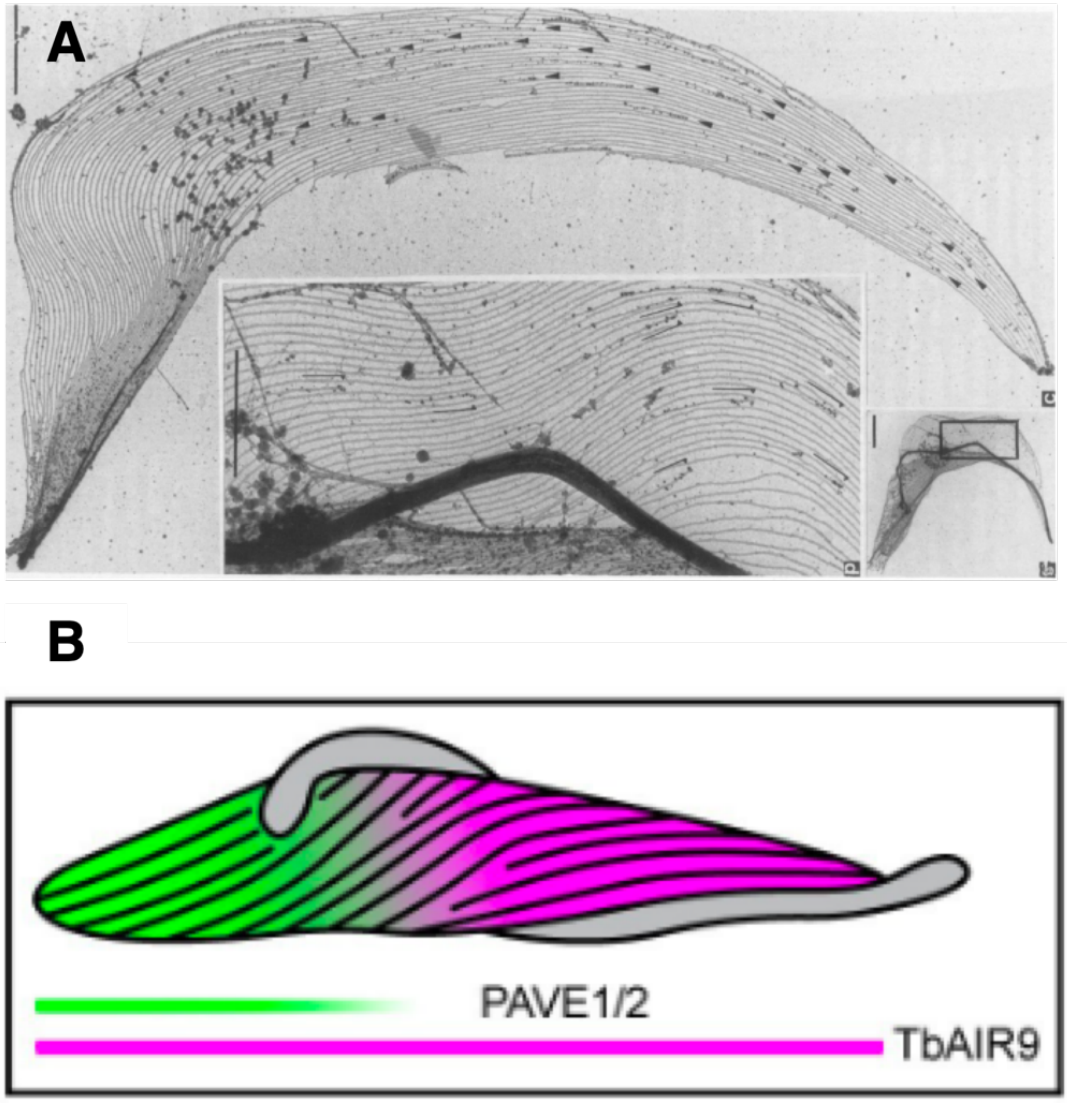

Figure 8 : The cytoskeleton of T.brucei. A: TEM longitudinal section depicting one layer of the subpellicular array of regularly interspaced MT singlets with an average distance of 20nm. Immunogold particles show staining with the YI1/2 antibody. Arrows indicate newly polymerizing MT intertwined with older MT singlets. Image modified from Sherwin and Gull 1989. B: Cartoon indicating the organization of new MTs at the posterior and relatively older MTs anterior as well as associated binding proteins. Image modified from Sinclair et al. 2021.

The subpellicular array of MTs in the trypanosome cell body

Basal bodies, the transition zone and the axoneme are all MT based structures ultimately made from tubulin. They have been described in previous sections, which leaves the MTs of the cell body for discussion. These form a very distinct array of MTs also found in apicomplexans and other kinetoplastids. The “subpellicular” MTs lie just beneath the cell membrane and are the source of the characteristic screw-like cell shape of trypanosomes. It is this morphology that makes trypanosomes motile swimmers in environments of different viscosities. The subpellicular MTs of trypanosomes are an example of a very uniform, specialized and sturdy array. Individual tubules are crosslinked to each other and the cell membrane above (Hemphill et al. 1991). Together, they form one single stable layer throughout the entire cell that is extremely resistant and durable (Robinson et al., 1995; Sherwin & Gull, 1989; Sherwin & Gull’, 1989). This is needed to withstand the continuous forces exerted by the flagellar beat (Sun et al., 2018). One isolated layer of the subpellicular array can be seen in Fig. 8A.

A thin filament called flagellar attachment zone (FAZ) is found in a gap between MT singlets of the subpellicular array. There it attaches the flagellar and the cell membrane to each other. It connects the flagellum where it exits the cell body along the longitudinal axis up to the anterior tip (Sunter & Gull, 2016). Stability of the subpellicular array derives from the extensive cross-linking between the regularly interspaced (~20nm distance) individual tubules. In stark contrast to MT arrays of other organisms, dynamic instability is not reported for the subpellicular array of trypanosomatids (Sinclair et al., 2021) and these polymers may last many cell cycles (Sheriff et al., 2014; Sherwin & Gull’, 1989; Sinclair et al., 2021). Different subdomains of the subpellicular array have been described with the aid of associated proteins (MAPs) and the presence of antibodies that recognize posttranslational modifications of tubulin. At the posterior cell tip plus ends of newly polymerized MTs (Sheriff et al., 2014; Sherwin & Gull’, 1989) are found in close proximity to each other and form a tapering end

supported by posterior and ventral edge proteins 1 and 2 (PAVE1 and PAVE2) (Fig. 8B). This region is nicely co-stained with antibodies that recognize newly synthesized tubulin (Sherwin & Gull', 1989). Another protein, TbAIR9, is distributed in the whole array and plays a role in maintaining interaction of associated proteins (Fig. 8B) (Sinclair et al., 2021). Two related, but life cycle stage dependent proteins (CAP15, CAP17), stabilize MTs and display a more anterior localization that excludes the relatively newer posterior (Vedrenne et al., 2002). These microtubules of the anterior part of the "corset" are more stable and older (Sheriff et al., 2014; Vedrenne et al., 2002).

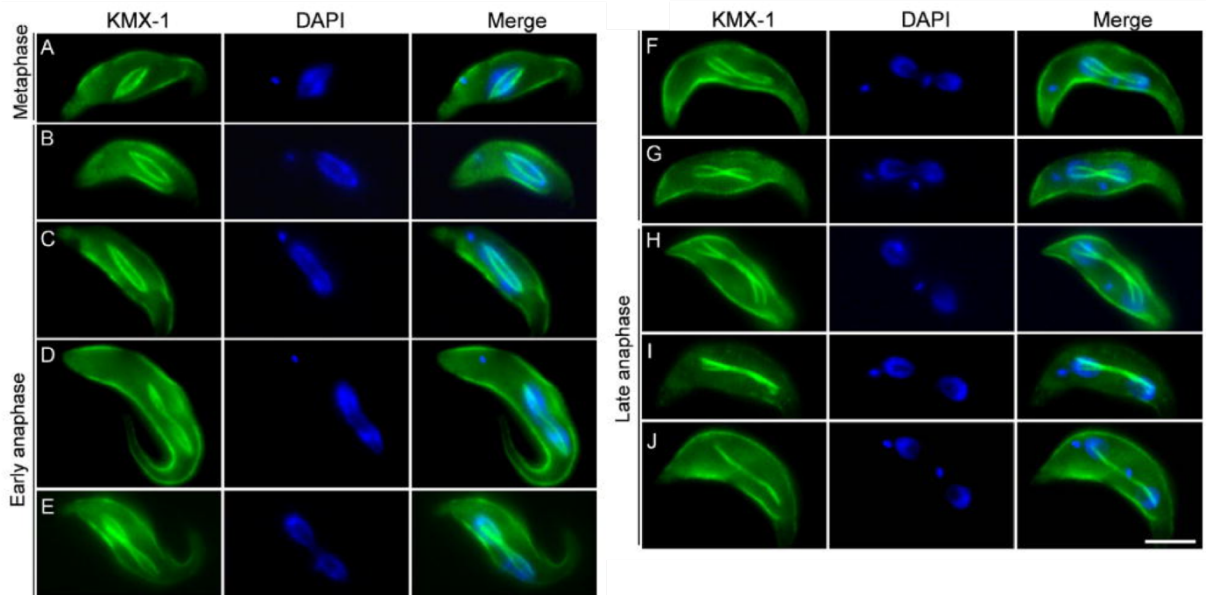

Figure 9 : The spindle during mitosis. Spindle recognised by the beta-tubulin specific KMX-1 antibody. DAPI stains the nucleus. Image modified from Zhou et al. 2014

The mitotic spindle

The spindle apparatus arises during mitosis and is responsible for the equal segregation of duplicated chromosomes. Chromosomes are fixated at their center to a specific set of MTs called the kinetochore MTs. Simultaneously, motor proteins are present where "polar" MTs are intertwined at the spindle's center. The activity of these motor protein between the tubules

slides the overlapping MTs to opposed sites which pushes the spindle poles into opposite directions. This in turn mediates segregation. Astral MTs are polymerized in the convergent direction of polar MTs and tether the spindle poles to the cell membrane. In many cells, the MT of the mitotic spindle arise from two opposing MTOCs that nucleate new MT towards the center where they attach the duplicated chromosomes.

The assembly of the spindle in trypanosomes is more enigmatic and MTOCs related to this process have not been described. A pathway for the assembly of spindle MTs guided by chromatin finds more support in the literature. Several genes commonly associated with chromatin-linked spindle assembly including Aurora-kinases and Kinesin-13 are indeed present in Trypanosomes. Nonetheless, the initiation of spindle assembly in this parasite remains under investigation (Chan and Ersfeld, 2010; Li and Wang, 2006; Tu and Wang, 2005; Zhou et al., 2014). Since the mitotic spindle apparatus is predominantly built from MTs it can be readily observed by antibodies recognizing tubulin. In the Trypanosome field the antibody most commonly used for this purpose is the beta-tubulin specific KMX-1 (Fig. 9) (Birkett et al., 1985). Unexpectedly, its alpha-tubulin counterpart TAT-1 does not stain the mitotic spindle well (Sasse and Gull, 1988; Woods et al., 1989). Several other antibodies that recognize different post-translational modifications (PTMs) of tubulin stain the mitotic spindle as well, however, some PTMs also seem to be absent.

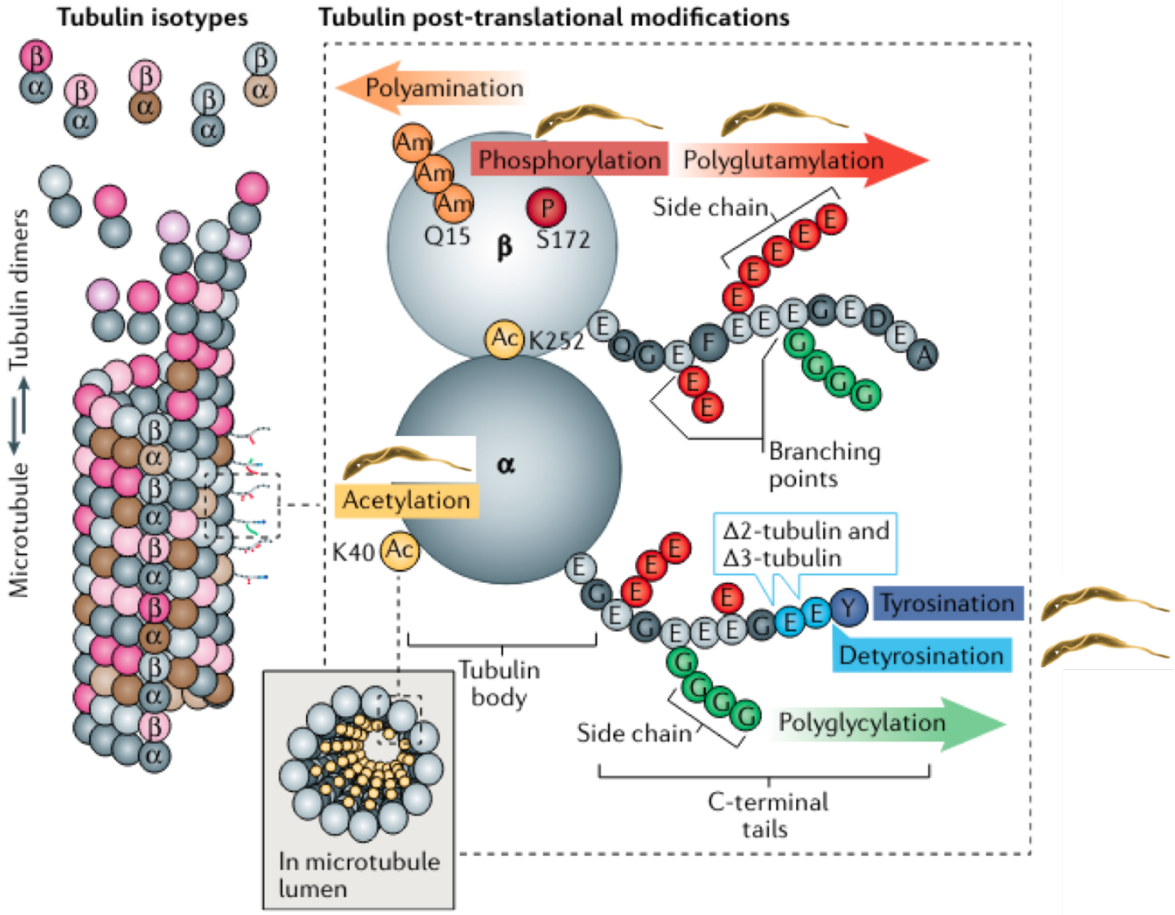

Figure 10: "The tubulin code" modified from Janke and Magiera 2020. The PTMs that are present in T.brucei are indicated with a trypanosome: Polyglutamylation occurs predominantly but not exclusively on the C-terminal tail of alpha and beta-tubulin (Schneider et al., 1997). Acetylation is found on one lysine at position 40 (K40 acetylation) on alpha-tubulin (Piperno and Fuller, 1985; Schneider et al., 1986). One tyrosine residue in the C-terminal tail of alpha and beta-tubulin is subject to detyrosination and retyrosination (Sherwin et al., 1987a). Phosphorylation has been described for multiple serine and lysine residues in beta-tubulin (Lee et al., 2023; Lee and Li, 2021). Alpha and beta-tubulin glycylation and polyglycylation is absent in T.brucei (Schneider et al., 1997) and polyamination has not been described.

Post-translational modifications (PTMs) of tubulin

The alteration, addition or deletion of amino acids after they are constructed into peptide-chains or proteins is commonly referred to as a post-translational modification (PTM). They are described for many proteins and are required for them to carry out specific functions, fine tune affinity for substrates or regulate incorporation of proteins into protein-complexes etc.

A concept that is useful to highlight the importance of PTMs in this context is the tubulin code: The combination of alpha and beta-tubulin isotypes, as well as the PTMs that are found on them can guide the structure of the tubules (e.g. number of protofilaments). It can mediate the interaction with microtubule associated proteins (MAP) and govern the construction, disassembly, longevity and stability of parts of MTs or even whole parts of the cytoskeleton. To further increase complexity nine isotypes of each alpha and beta-tubulins are for example found in humans (Janke and Magiera, 2020).

The list of individual PTMs of different tubulin isotypes in different species and their roles is very extensive even at a basic level. This chapter focuses mainly on the PTMs found on trypanosome tubulins, the known functions as well as the antibodies that recognize it. Only one gene each code for alpha and beta-tubulin (Berriman et al., 2005).

Acetylation:

This modification was initially described in the flagella of *Chlamydomonas* (L'hernault and Rosenbaum, 1983) and is found on one conserved lysine at position 40 of alpha-tubulin (referred to as K40 acetylation) (Fig. 10). This residue faces towards the lumen of the microtubule and is positioned on a structure that is referred to as the acetylation loop (Soppina et al., 2012). In most organisms, acetylated tubulin is associated with stability and often absent in more transient structures. In trypanosomes however, K40 acetylation is not only ubiquitous, it is found on all incorporated alpha-tubulin (Sasse and Gull, 1988; Schneider et al., 1986). This includes the sturdy microtubules of the subpellicular array, the new and old flagellum, as well as the mitotic spindle. Studies in trypanosomes have been carried out mainly with two distinct antibodies that recognize this modification: C3B9 and 6-11B-1 (Piperno and Fuller, 1985; Woods et al., 1989). Tubulin is acetylated during polymerization and remains modified while incorporated. A loss of tubulin-acetylation has not been studied for *T.brucei*. The ubiquitous presence of the modification on all incorporated tubulins might indicate that it is essential for survival.

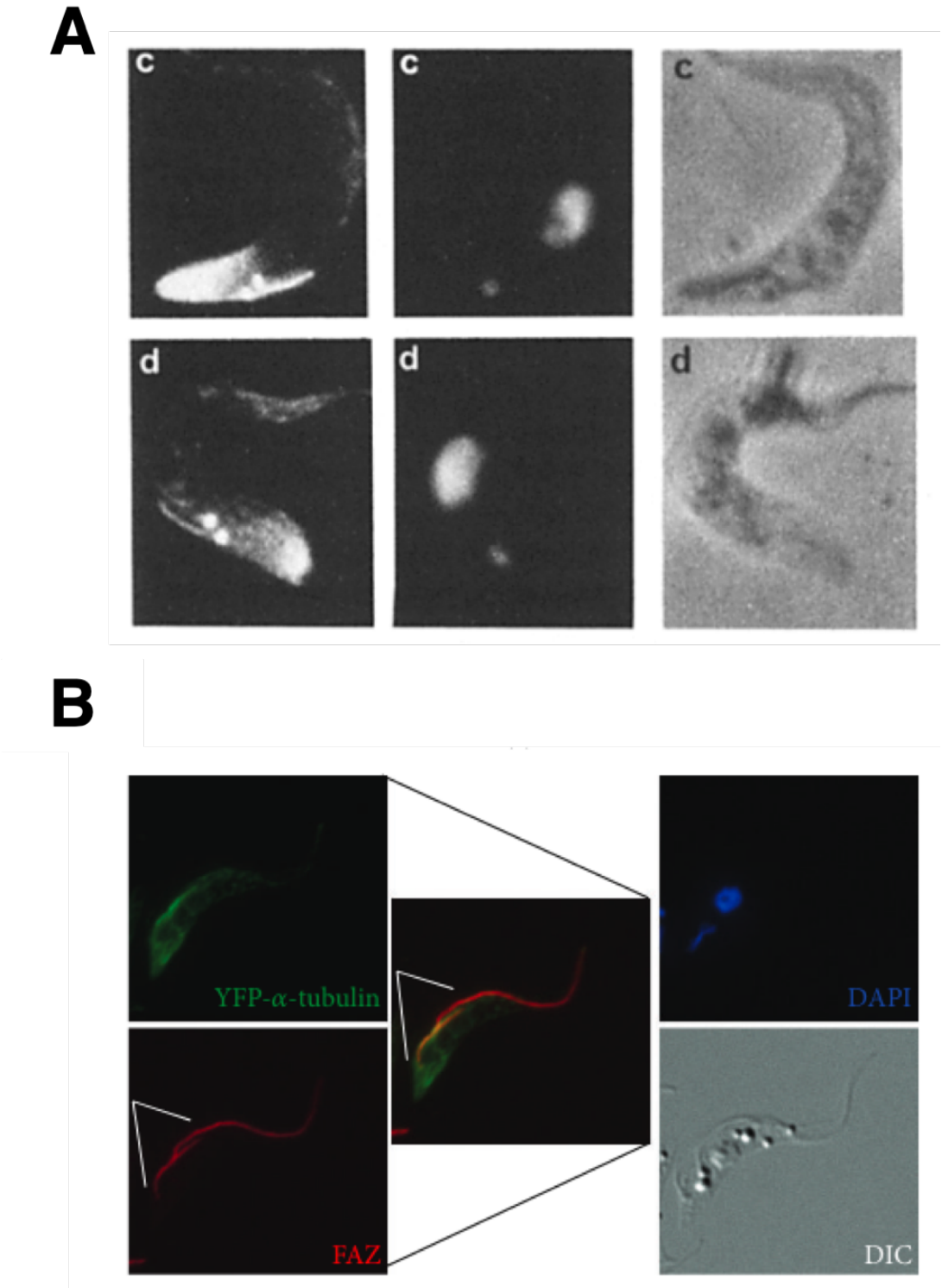

Figure 11 : Incorporation of new tubulin in the cytoskeleton of *T.brucei*. A: Cells stained with the YL1/2 antibody that recognises tyrosinated newly synthesized tubulin. Localisation is observed in the posterior MTs of the cell body as well as in the new flagellum. B: Inducible expression of YFP-tagged alpha tubulin. New tubulin is found in posterior cell body and in the region of the new flagellum FAZ.

Tyrosination / De-tyrosination:

In contrast to acetylation a major part of *T.brucei's* alpha-tubulin is de-tyrosinated. To achieve de-tyrosination, the residue is removed from the carboxy-terminus of alpha-tubulin during a reversible reaction (Sherwin et al., 1987). Tyrosinated tubulin can be recognised with the YL1/2 antibody and is observed mainly in the polymerizing microtubules of the posterior cell body as well as in the proximal part of the growing flagella (Kilmartin et al., 1971; Sherwin et al., 1987a; Woods et al., 1989, 1989) (Fig. 11A). Localization of tyrosinated tubulin in the trypanosome cytoskeleton was dissected by immunogold-staining and observed for single MTs of the subpellicular array. Shorter newly synthesized single tubules stained by YL1/2 can be spotted neatly intertwined between "older" MTs, not only at the posterior but throughout the whole cell body (Fig. 8A). These short "new" microtubules were more abundant in the early stages of the cell cycle and prove that some rearrangement of the subpellicular array is occurring cell wide and not only at the posterior. When compared to the subpellicular array, the mitotic spindle is certainly a more short-lived MT based structure. As it is disassembled during mitosis and resolves after nuclear division. Counterintuitively, it is not stained by YL1/2 that recognizes recently assembled tubulin. Upon knockout of *T.brucei* Vasohibin, a tyrosine carboxypeptidase that de-tyrosinates tubulin, the spindle is clearly positive for tyrosination again and the cells show severe defects in cell division and morphology (van der Laan et al., 2019). An example that highlights how unwanted absence (here absence as de-tyrosination is the modification) of a PTM can be detrimental for cell viability. Since tyrosination is predominant for newly synthesized / polymerizing microtubules and is removed relatively shortly after polymerization its presence is widely used for colocalization studies.

Glutamylation and Poly-glutamylation:

The addition of one or multiple glutamates to the existing glutamates in an amino acid chain is referred to as glutamylation. In the case of tubulin this modification is most present on but not exclusive to the C-terminal tails and very abundant in *T.brucei* (Schneider et al., 1997). Glutamates residues are negatively charged and responsible for the polar nature of tubulins C-terminal tail. Tubulin tyrosine ligase like (TTLL) enzymes catalyze the addition of glutamate residues to alpha and beta-tubulin. Nine of these TTLL enzymes have been identified in the Trypanosome genome, however, it is unclear if all of them possess glutamylase activity which is subject to current investigation.

TTLL6A as well as TTLL12B have been described as bona fide glutamylases. A knock down of these proteins results in reduction of glutamylation, which resulted in increased branching of MTs at cell posterior. This led to a general aberrance of morphology as well as defects in cell division and an increased number of cells without a nucleus (zoids). Intriguingly, tyrosinated tubulin picked up by the YL1/2 antibody was increased in these cells, potentially suggesting an overabundance of polymerizing tubulin (Casanova et al., 2015; Jentzsch et al., 2020; Nehlig et al., 2017). Together this implies a mis-regulation of tubulin incorporation into the posterior MTs. Similar phenotypes have been described and linked to the loss of beta-tubulin-phosphorylation. Indeed, the authors attributed this phenotype to an increase of incorporated material in the absence of a control mechanism that is governed by beta-tubulin phosphorylation (Lee et al., 2023; Lee and Li, 2021). Additionally, a significant increase in flagellar length and the length of the flagellar attachment zone (FAZ) was noted (Lee et al., 2023).

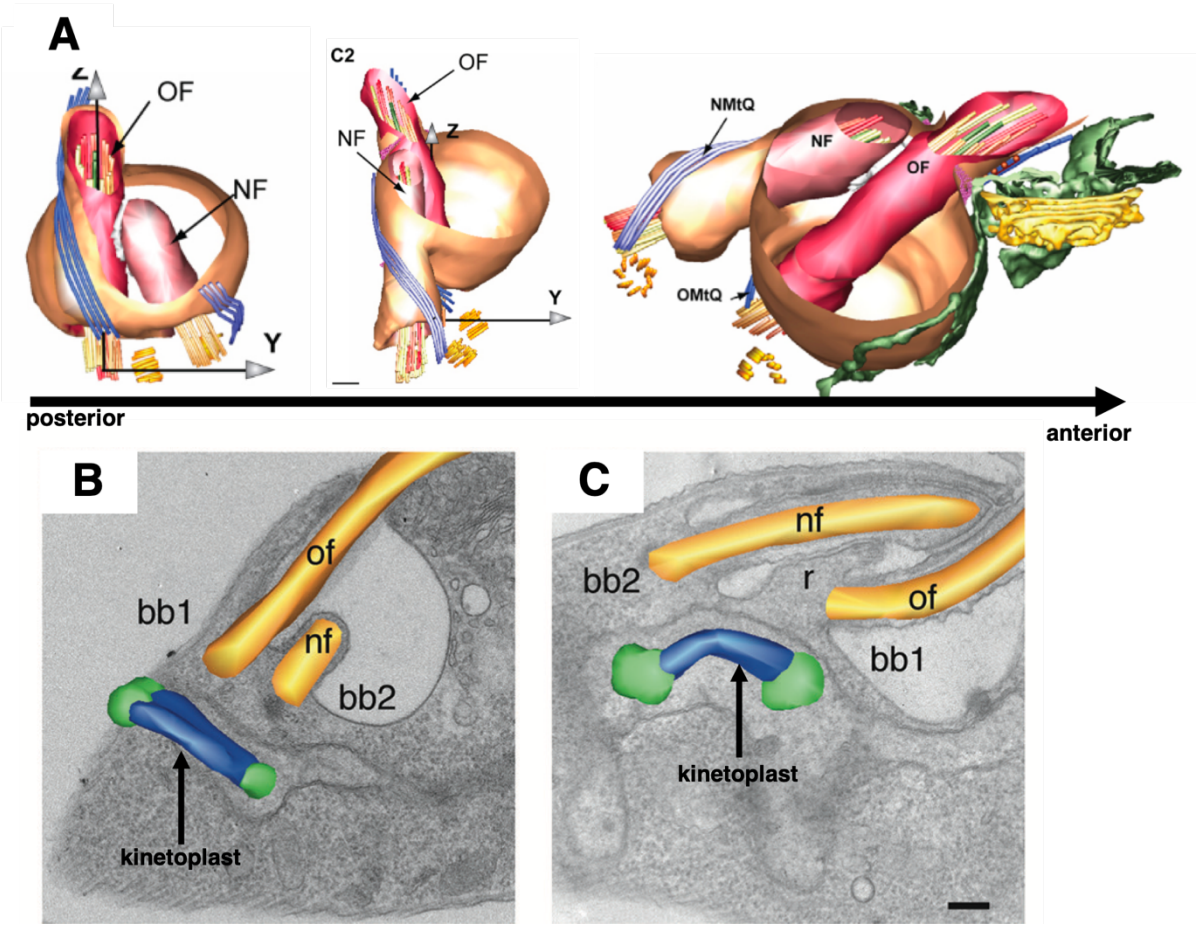

Figure 12 : A: Rotation of the NF around the OF from anterior to posterior inside the shared flagellar pocket. Blue indicates the MT quartets. In yellow are the BBs. B: longitudinal section by TEM with the NF anterior. C: NF is now posterior indicated in green and blue is the separating kinetoplast DNA. Images modified from Lacomble et al. 2010 and Vaughan and Gull 2010.

The cell cycle

In the previous sections we highlighted four important structures whose highly orchestrated assembly, duplication and division governs the cell cycle (Timeline of the cell cycle in Fig. 14B). It starts with a cell that possesses one kinetoplast, one nucleus and one flagelllum (1K1N1F), as well as, a mature BB (mBB) and a pro BB (pBB) that lies anterior to the mBB (Vaughan and Gull, 2016).

At the beginning, the genetic material of the kinetoplast is duplicated. Shortly after, the S-phase is initiated inside the nucleus as well. Almost at the same time the BBs are duplicated and are positioned anteriorly (Ploubidou et al., 1999; Sherwin and Gull, 1989; Vaughan and Gull, 2016). As the synthesis of a new genome is more difficult to image, the emergence of the new basal body is often referred to as the first traceable cell cycle event. The next cytoskeletal structure that arises is the MT quartet between the PBB and the mBB of the old flagellum (OF) (Lacomble et al., 2010, 2009). The pBB matures into the new mBB and gives rise to the transition zone and then the axoneme of the new flagellum (NF). At this stage the NF is still anterior of the old flagellum and they share the flagellar pocket (Lacomble et al., 2010; Sherwin and Gull, 1989). The next event has been resolved with tomograms as it cannot be observed in two dimensions. The new mBB that gave rise to the new flagellum starts to rotate around the MBB until it and its flagellum lie posterior to the mBB and the OF (Gluenz et al., 2011; Lacomble et al., 2010, 2009). The rotation of the short new flagellum from anterior to posterior around the OF inside the shared FP can be seen in Fig. 12.

As the NF axoneme elongates, a structure is formed at its tip. This structure is a layered transmembrane junction called the flagellar connector (FC), as it connects the NF tip to the OFs axoneme (Briggs et al., 2004). Coincidental with the emergence of the FC a membrane can be spotted, that extends into the space between the two axonemes inside the existing flagellar pocket (Lacomble et al., 2010). Progressively this membrane called the “ridge” will divide the shared FP into two separate ones (Fig. 12C, R=ridge). Meanwhile the NF

continuously elongates and the FC slides along the OF (Davidge et al., 2006). When the NF exits the cell body at the FP the addition of the PFR ensues. PFR components are then continuously added while the flagellum elongates (Bastin et al., 1999).

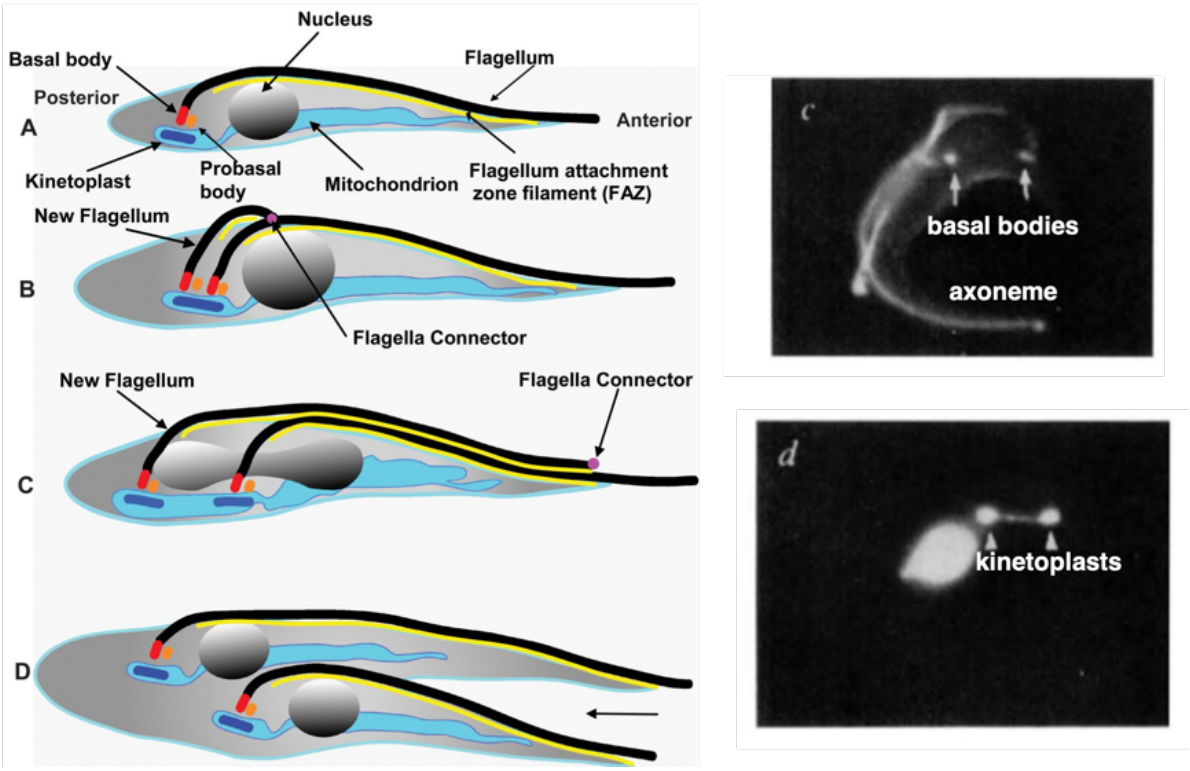

Figure 13 : Cell division highlighting the progressive separation of the BBs that drives division of kinetoplast and mitochondria, D indicates initiation of cleavage furrow ingression. Image modified from Vaughan and Gull 2016. B: The effect of teniposide on the separation of the kinetoplast. BB can still segregate but the kinetoplasts remain connected. Adapted from Robinson and Gull 1991.

The FAZ is made as well alongside the new flagellum and forms the connection between flagellar and cell membrane (Sunter and Gull, 2016). During new flagellum growth, replication of the genomic material of the kinetoplast is completed and migration of the two basal bodies begins. The NF BB migrates towards the cell posterior away from the OF BB. This segregation is aided by the elongation of the new flagellum and the FAZ that progressively power this process (Absalon et al., 2007; Gluenz et al., 2011; Kohl et al., 2003; Lacomble et al., 2010; Robinson and Gull, 1991) (Fig. 13A). Through a tri-layered structure that spans the

mitochondrial membrane, called the tripartite attachment complex, the BBs are attached to the kinetoplast DNA (Fig. 2, A + C) (Ogbadoyi et al., 2003). While the NF BB moves away from the MF BB it drags along half of the duplicated kinetoplast DNA inside the mitochondrion. BB migration is therefore responsible for the separation of the kinetoplasts (Robinson and Gull, 1991). Meanwhile, the FC slides along the length of the OF towards the distal tip. At first, the distance covered by the FC on the OF linearly correlates with the distance between the separating BBs. Around a point half way through the length of the OF, a stopping point occurs where the FC no longer continues to move anteriorly (Absalon et al., 2007; Briggs et al., 2004; Davidge et al., 2006). When the two BBs separated enough two divided kinetoplasts can be observed. In the meantime, the nucleus is expanding but not yet separated. This expansion is the consequence of a force that that slides the duplicated genetic material to opposite sides. This force is generated by the MTs of the mitotic spindle. Cells with that confirmation are referred to as 2K1N2F cells as they possess two kinetoplasts, one nucleus and two flagella (Fig. 14A). After mitosis is complete, all six copies of these structures can be clearly distinguished (2K2N2F). At this point the last remnants of the mitotic spindle are disappearing (Fig 9J), additionally, the connection between the NF and the OF has resolved (Briggs et al., 2004; Davidge et al., 2006). The cells are now ready to initiate cytokinesis at the cell anterior tip. The cleavage furrow ingresses unidirectional from the anterior to posterior along the trypanosomes longitudinal axis and intersects the two daughter cells between the two kinetoplasts, nuclei and mitochondria (Fig. 13A). After completion of cell division both daughter cells inherit one copy of each of these structures as well as a pro and mature BB. The daughter cell that had initially layed posterior inherits the NF which has reached roughly 80% of the length of the OF at that point (Fig. 14A) (Bertiaux et al., 2018).

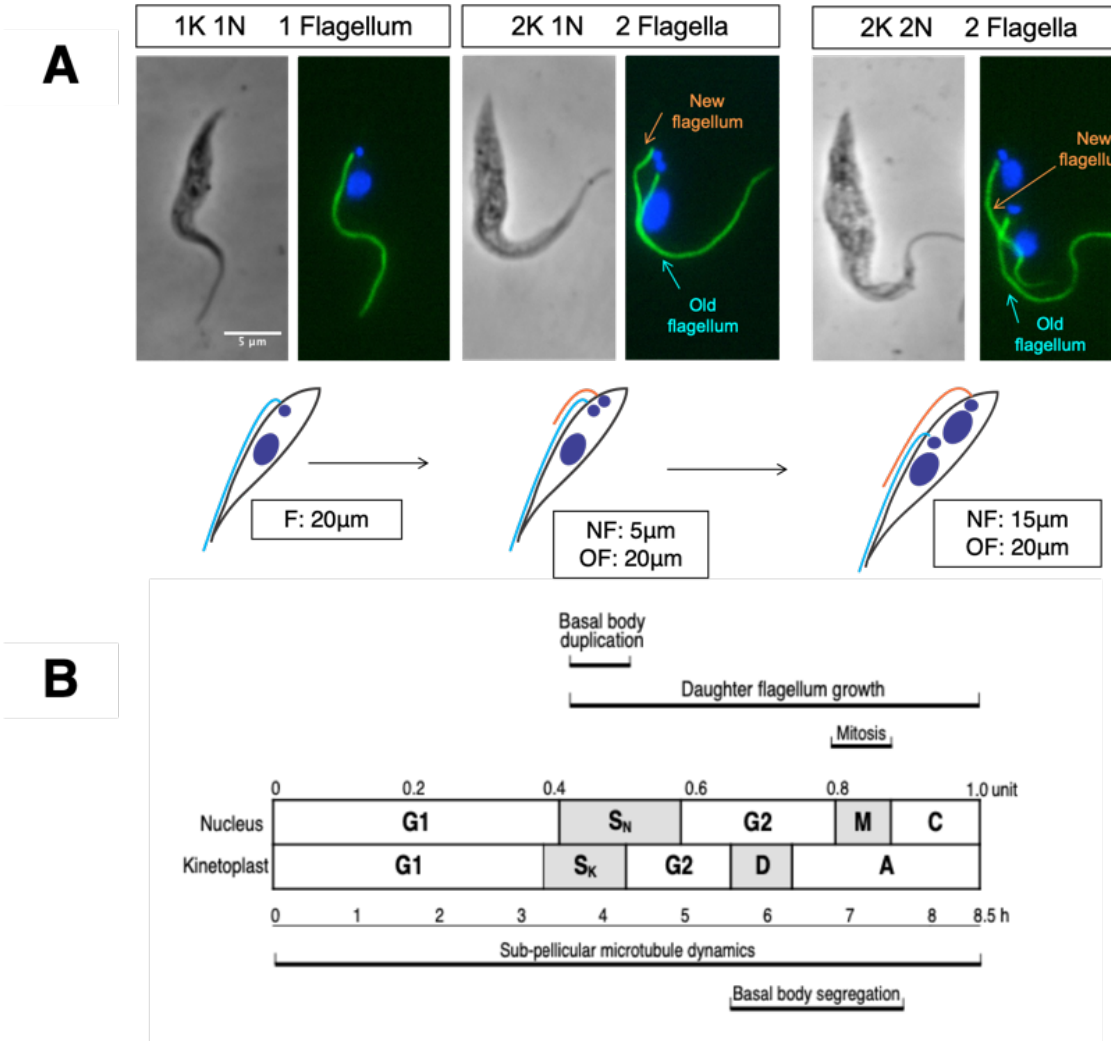

Figure 14 : Cell cycle progression with flagella kinetoplast and nucleus. Progressive elongation of the NF to ~80% of the length of the OF ahead of cell division. Addapted from Bertiaux et al. 2018. B: timescale of cell cycle progression indicating the formation of the BB and the NF. Adapted from Ploubidou et al. 1999.

Inhibiting cell division

As discussed above, kinetoplast segregation is mediated by the movement of the basal body, which is the structure that anchors the flagellum in the cells (Vickerman, 1985; Vickerman et al., 1988). After the two kinetoplasts migrated apart the duplicated nuclear DNA separates as well and the nuclei divide ahead of cytokinesis. This process can be blocked with an inhibitor of topoisomerase II called teniposide. This will prevent the concatenation/de-concatenation process that is necessary for faithfull segregation of the two kinetoplasts. After treatment with this drug the material of two kinetoplasts remains connected, hence preventing segregation. As kinetoplast separation needs to complete ahead of karyokinesis the division of the entire cell comes to a halt (Myler et al., 1993.; Robinson and Gull, 1991)(Fig. 13B). The application of teniposide has been used to study the timing of flagellar morphogenesis in the context of the cell cycle (Atkins et al., 2021; Bertiaux et al., 2018).

The cell corset during the cell cycle

During G1-phase one can observe the formation of new MTs at the posterior cell tip, forming the basis of the new daughter cells cytoskeleton. These MTs are positive for YL1/2, an antibody that recognizes tyrosinated (newly synthesized) tubulin. At the same time, YL1/2 stains the new tubulin at the distal tip of the assembling flagellum, as well as tubulins in the region of the newly forming FAZ adjacent to the new flagellum. A similar pattern is observed when tagged tubulin is ectopically expressed for short time periods (Fig. 11B). (Sheriff et al., 2014; Sherwin et al., 1987a; Sherwin and Gull', 1989). It is currently unknown if these new MTs in the proximity of the FAZ are part of the MT quartet or adjacent subpellicular MTs. It is conceivable that both have to undergo rearrangement during FAZ formation. The newly synthesized MTs of the posterior cell body and the FAZ region are asymmetrically inherited by the new flagellum daughter (Sheriff et al., 2014). The cell cycle can be traced in a timely manner through the lens of a microscope with the help of antibodies that recognize BB proteins and tubulin as well as fluorescent dyes that stain DNA such as DAPI or Hoechst (Fig. 14B).

As the formation of a new flagellum coincides well with the initiation of S-phase its elongation resembles a timescale on which a given cell divides. In that sense, the length of the new flagellum can be viewed as a time sensitive marker of the cell cycle.

What regulates flagellar length and why is it variable?

When studying the catalog of ciliated eukaryotes, the two most variable characteristics of flagella are their number and size. *T.brucei*, possesses one flagellum during G1-phase and then assembles a new flagellum in the same cell as it maintains the old one. At which point this makes them effectively a bi-flagellated cell. The number of flagella is intricate between all life cycle stages of *T.brucei*, however, their length is not.

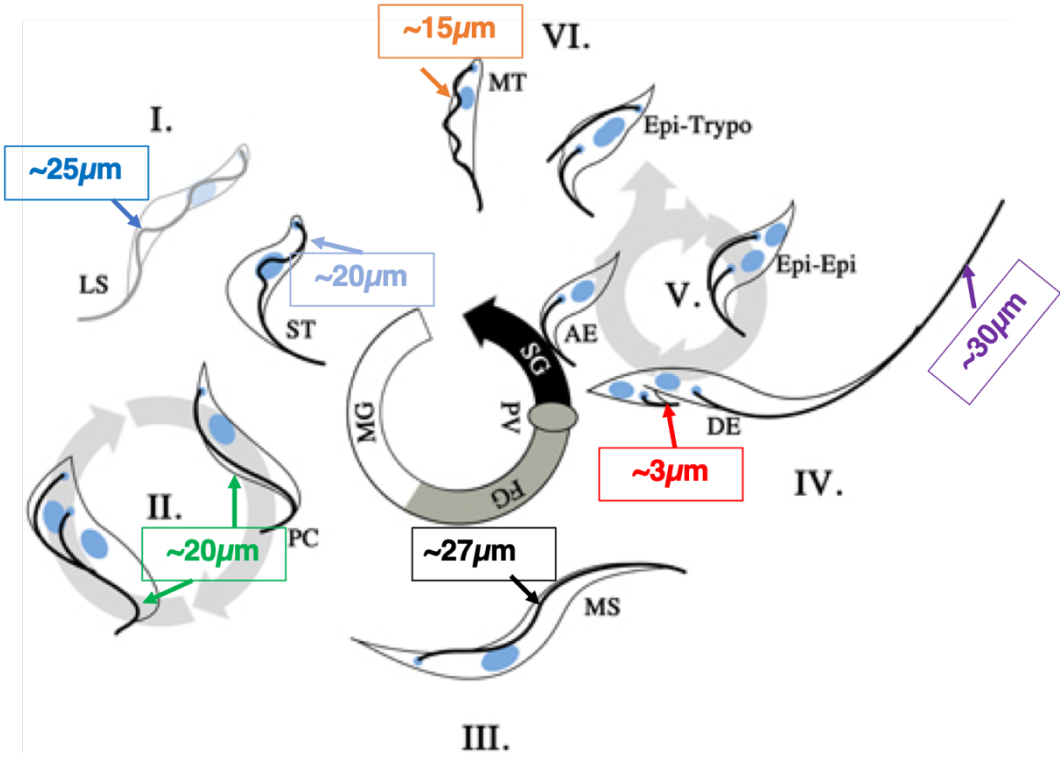

Figure 15 : The trypanosome life cycle indicating that most stages have flagella of different length . MG=midgut, FG=foregut, PV=proventriculus, SG=salivary glands. LS=long slender, ST=short stumpy, PC=procyclic, MS=mesocyclic, AE=adhering epimastigote, DE=dividing epimastigote, MT=metacyclics. Adapted from Ooi and Bastin 2013.

The flagellar life cycle of trypanosomes

The trypanosome life cycle is a complex endeavor that leads this parasite through two different hosts (Vickerman, 1985; Vickerman et al., 1988). In an infected mammal, trypanosomes are referred to as bloodstream forms (BSF), that live extracellularly in the bloodstream and some extravascular compartments, like the skin. Two stages of BSF trypanosomes are known. Slender BSF are motile swimmers and have a flagellum of ~25μm (Tyler et al., 2001)(Fig. 15, blue arrow). Motility is paramount to establish and maintain infection and properly beating flagella essential for their survival (Broadhead et al., 2006; Ralston and Hill, 2006; Shimogawa et al., 2018). Upon increasing parasitemia, slender BSF differentiate into stumpy BSF that are cell cycle arrested. This stage has a flagellum of ~20μm (Fig. 15, light blue arrow) and is metabolically pre-adapted to the insect vector. When the Tsetse fly takes a blood meal it will ingest slender and stumpy parasites. The meal including the trypanosomes passes through the fly crop into the midgut (Fig. 15, MG). In this compartment stumpy forms differentiate into procyclic forms. This dividing stage has a flagellum of ~20μm in length (Fig. 14, green arrow). Together procyclic trypanosomes and slender BSF are the most studied life cycle stage as they can be readily cultured in vitro and are amenable to genetic tinkering. How and when procyclic trypanosomes assemble their flagella is the main focus of the work presented here. The biology of the following stages is more enigmatic as they can only be studied in vivo (Vickerman et al., 1988). The stage found in the foregut (Fig. 15, FG) is called a mesocyclic trypomastigote. These cells are comparably longer and thinner than procyclic cells and carry a flagellum of 27μm. To reach the salivary glands (Fig. 15, SG), the trypanosomes have to cross the proventriculus (Fig. 15, PV) first. The stage that achieves this migration is the asymmetrically dividing epimastigote. While dividing, one daughter cell has a very short flagellum of 3μm (Fig. 15, red arrow) and the other one has a flagellum of roughly ten times that length (Fig. 15, magenta arrow). It is hypothesized that the long flagellum daughter propels the dividing cell into the salivary glands where the short daughter can then adhere to the

epithelium with its flagellum (Rotureau et al., 2012, 2011). The adherent epimastigotes differentiate into metacyclic trypomastigotes (Fig. 15, orange arrows) which are infectious for the mammalian host. Upon taking the next bloodmeal the tsetse fly will inject this stage that then turns into slender bloodstream forms again, therefore completing the life cycle (Vickerman, 1985). With every stage the trypanosomes pass during their journey through two different hosts the length of the flagellum changes. Throughout this process motility remains essential for life cycle completion (Broadhead et al., 2006, 2006; Shimogawa et al., 2018). It is very likely that trypanosomes need to adapt flagellar length to deal with the environmental changes when they pass from one organ to another (Lemos et al., 2020). Processes that involve the flagellum are, migration into different organs (Rotureau et al., 2014), the crossing of barriers between them (Rose et al., 2020; Shaw et al., 2019), sensing and signaling (Bachmaier et al., 2022; Shaw et al., 2022, 2019) and adherence to the epithelium in the salivary glands (Vickerman, 1985; Vickerman et al., 1988).

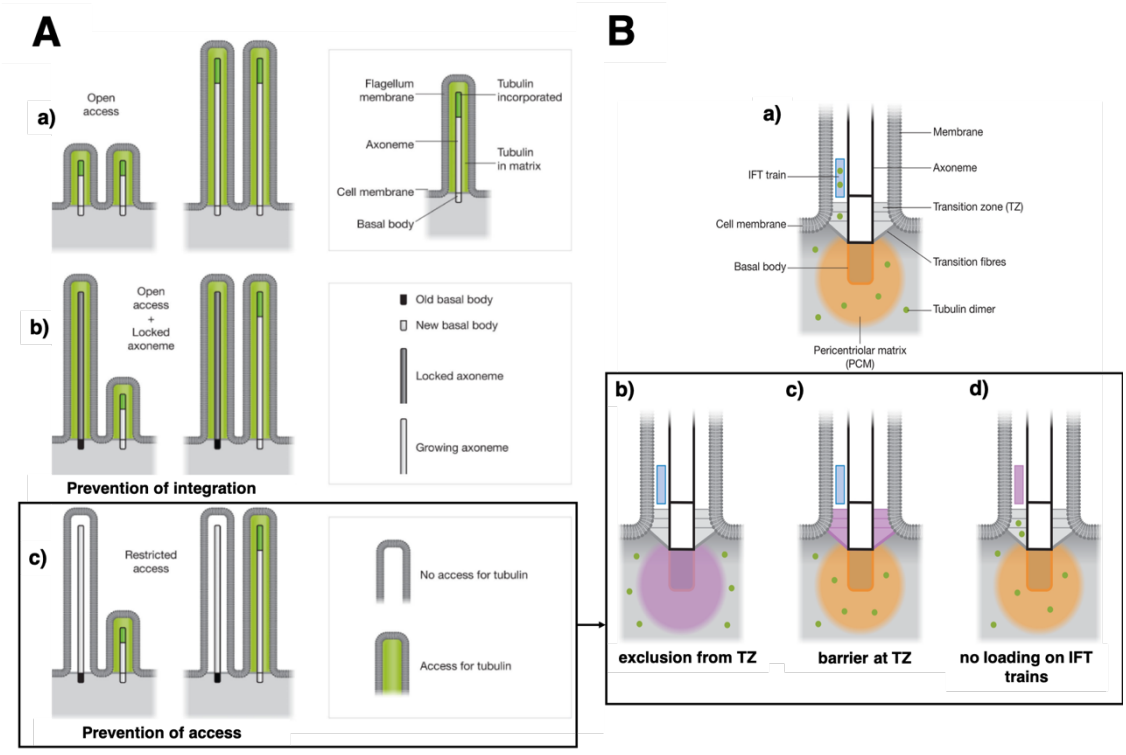

Figure 16: Two sets of cartoons indicating the possible control of assembly for cells with more than one flagellum. A: Three scenarios for the assembly of two flagella in the same cell are possible: a) Equal access of tubulin into the axoneme of both flagella. In this case simultaneous elongation can occur. b) Elongation is occurring in only one of the two flagella. In the other one tubulin can still enter the flagellum but integration is blocked at the level of the axoneme, which prevents elongation. c) Elongation is occurring in only one of the two flagella. In the other one, tubulin access to the flagellum is blocked at the flagellum base, preventing elongation. B: Three scenarios describing the possible mechanism that prevent flagellum entry of building blocks are highlighted. The cartoons (a-d) indicate how access to the flagellum could be blocked at the flagellum base. a) Cartoon of the flagellum base with the pericentriolar matrix (PCM) in orange surrounding the BB and tubulin in green. b) Access of tubulin is prevented by blocking the entry into the PM that surrounds the BB. c) Tubulin can still access the PM but its entry into the flagellum is prevented at the level of the TZ. d) Tubulin can freely access the TZ but loading on IFT trains is prevented, therefore transport into the axoneme is abolished. Figure adapted from Bertiaux and Bastin 2020.

How can cells control the length of the flagellum

In the previous section we highlighted how the length of the flagellum varies between different life cycle stages of trypanosomes, and why this might be necessary. To understand how trypanosomes, manage to control flagellar length it is important to understand, how cells can achieve this in general. Several models were proposed that explain the control of flagellar length. In essence, the control of flagellum length boils down to the balance between assembly and dis-assembly or the addition of new building block vs. their removal.

1) Balance-point: This model describes how, once a flagellum reaches its full length the ratio of assembly and dis-assembly is equal. In practice, the cells add as many new building blocks to the tip as they remove and the overall length does not change. This is how the green alga *Chlamydomonas reinhardti* maintains the length of its two flagella. In vivo this is a bit more complicated as dis-assembly is actually constant while the assembly-rate is variable. When the assembly rate is high Chlamydomonas elongates their flagellum. But they can also actively shorten their flagella by decreasing the assembly rate (Marshall and Rosenbaum, 2001).

2) The limiting pool model: A limited pool of available building blocks prevents the elongation of a flagellum after it reached a certain length. Essentially, this describes how the cells run out of material to make “more” flagellum. This is the case for the flagellum of *Naegleria fowleri* (Goehring and Hyman, 2012).

At the heart of the second model is the scarcity of material on the side of production. It is conceivable, however, that some organisms produce enough material but limit its availability for flagellar assembly by other means. New building blocks could for example be prevented from entering the flagellum altogether, effectively preventing elongation (limited access-model). This could happen by exclusion of material from the pericentriolar matrix that surrounds the basal body area (Fig. 16). Alternatively, a barrier at the transition zone could prevent the influx of new material into the flagellum (Fig. 16). Or the cells could inhibit the loading of cargo onto IFT trains who transport new building blocks to the flagellar tip for

incorporation (Bertiaux and Bastin, 2020), effectively preventing axonemal entry as well. Lastly, the incorporation of building blocks itself could be prevented at the site of incorporation, namely the axoneme. This would mean new material is still able to access the flagellum but cannot integrate. One way to facilitate this could be a cap that is present at the flagellar tip to seal access from new constituents (Bertiaux and Bastin, 2020).

Flagellar length control in procyclic trypanosomes

For procyclic trypanosomes a model was proposed in which a flagellum is grown and once it reaches full length, it gets locked. The lock would prevent further elongation or shortening, enabling procyclic cells to maintain a flagellum at full length of ~20μm. To gain this insight, the assembly process of flagella was slowed down by RNA interference (RNAi) mediated knock down that targeted proteins of the machinery which transports new building blocks required for flagella assembly into the flagellum (IFT). This resulted in cells constructing shorter flagella. After removal of RNAi the transport machinery was brought up to normal speed again, however, the old flagella did not increase in length. This showed that further elongation was not occurring anymore for the mature flagellum. Furthermore, the authors could show that when cell division is inhibited, new flagella were constructed to 100% of the length of mature one but did not exceed it. Suggesting that procyclic trypanosomes commit to locking their flagella before cell division. They called this mode of assembly the grow-and-lock model (Bertiaux et al., 2018). These findings opened the question how the trypanosomes facilitate the locking mechanism. An intriguing protein candidate, Cep164C, has been described that abides in establishing the lock at the base of the flagellum. Cep164C is found at the TF that connect the beginning of the TZ to the FP membrane. This localization is compatible with the establishment of a barrier at the flagellum base described in Fig. 16B, see C and D. Upon knockdown of Cep164C, old flagella of bi-flagellated cells are made to long while new flagella are made to short. A phenotype that is compatible with the removal of the locking mechanism.

The combination of relatively shorter new and longer old flagella suggested that the locking mechanism could be a strategy to avoid competition for building blocks between new and old flagella. Indeed, Cep164C is only found at the TF of the old but not the new flagellum and is absent in ~60% of mono-flagellated cells (G1-phase) (Atkins et al., 2021).

Taken together the work of Bertiaux, Atkins and their colleagues proposes a strategy how procyclic trypanosomes control the length of their flagellum: A cell initiates the assembly of a new flagellum, in the meantime Cep164C prevents access to the old flagellum possibly to avoid competition. The new flagellum then commits to the locking event before cell division and gets locked before it becomes and old flagellum itself for the first time. If other life cycle stages apart from procyclic forms regulate flagellar assembly in accordance with the grow and lock model remains under investigation.

Aim of the thesis:

What is known and what we are interested in

Flagella are cell protrusions found in many species of the eukaryotic lineage. Although the roles and appearance of these organelles may vary, the architecture, the building blocks and the assembly process share many similarities among species. The core of the flagellum which is called axoneme, is a microtubule-based structure that is anchored in the cell body by a microtubule organizing center. The Bastin lab has chosen African trypanosomes as a model organism to contribute to the investigation of how flagella are built and maintained and what their function may be in different life cycle stages. We study the subspecies *Trypanosoma brucei brucei*, a deadly parasite of livestock in eastern and western Africa that is closely related to the human pathogenic species Trypanosoma *brucei gambiense* and *rhodesiense.*

T.brucei is flagellated throughout the entire life cycle during which it shuttles between a mammalian host and the insect vector. Up to twelve stages can be distinguished when comparing cell morphology during an infectious cycle (Rotureau and Van Den Abbeele, 2013). The most distinguishable morphological feature of every trypanosome cell is the flagellum. Trypanosomes assemble a new flagellum in the same cell while maintaining an existing one. Over the life cycle, the length of these flagella can greatly vary. The most striking example for this is the case of asymmetrically dividing epimastigotes. Here, one daughter cell possesses a small 3 μm flagellum while the other one has a flagellum 10 times that size. The property of trypanosomes to construct flagella of different length is not unique to the epimastigote, but a phenomenon that is constantly observed throughout the life cycle of *T.brucei*. **The means by which trypanosomes manage to control the timing of flagellum assembly and its length is the main topic addressed in this work.**

We decided to investigate this first with the procyclic form, the first proliferating stage in the insect vector. Depending on the strain, this stage possesses a flagellum of roughly 18-22 μm length, that is longitudinally attached to the cell body, apart from a small portion at the very tip. Procyclic trypanosomes like all other dividing stages assemble a new flagellum (NF) while maintaining a mature one. Extension of the NF reaches ~16 μm (80% of the mature one) when the cell divides and assembly appears to be finished after the first division (Sherwin and Gull, 1989). However, a more precise timescale on when the new flagellum is finished needs to be determined and is one of the questions we addressed in this work.

Recently, our group proposed a model on how procyclic trypanosomes manage to maintain the length of the old flagellum while they extend a new one. In 2018, a paper was published proposing that mature flagella were locked after they were grown to full length (Bertiaux et al., 2018). In essence, this locking mechanism would prevent mature flagella from lengthening or shortening. In 2021 our collaborator Sue Vaughan in Oxford found a protein that plays a major role in the underlying mechanism. CEP164C is a protein that is localized to the transition fibers only of the old but not the new flagellum. In its absence, cells fail to properly apply the lock and old flagella are too long, while new ones appear too short. Intriguingly, CEP164C seems to be removed from the mature flagellum after cytokinesis and is therefore mainly present when the cells are bi-flagellated. This opens room for the hypothesis that the locking mechanism is established primarily to avoid competition for building blocks between the new and the old flagellum. Together, these findings are conclusively described with a model for flagellum assembly in trypanosomes in which the flagella are assembled to full length and then halt growth. It is possible that cells either prohibit entry of new building blocks into the flagellum entirely or prevent the incorporation of new building blocks into the axoneme (Bertiaux and Bastin, 2020). The precise nature of the locking mechanism however is unclear. Furthermore, it is not known if flagella of procyclic cells stay locked permanently or can be un-locked again.

Lastly, support for the grow and lock model has been obtained for procyclic trypanosomes but not for other stages.

Questions

We wish to address some of the outstanding questions by following the assembly dynamics of tubulin, the core component of the axoneme. Therefore, we need a system that allows us to track the incorporation of new building blocks into this structure with temporal resolution.

How can we trace axoneme assembly?

When do procyclic trypanosomes lock their flagella?

Is the locking system present in other stages?

Question 1: How can we observe axoneme assembly?

The first challenge is to generate a cell line in which we can monitor axoneme assembly. Tubulin is the main building block of the axoneme. It forms heterodimers that polymerize into the microtubules which organize into the axoneme. The axoneme is anchored in the cell by the basal body followed by the transition zone and then the axoneme, which is the stem of the flagellum that is built first. Proteins and structures that surround and decorate the axoneme are added after. In trypanosomes, a prominent accessory structure, the paraflagellar rod, is attached to the axoneme and has been used to describe assembly (Bastin et al., 1999). However, the PFR only emerges after the axoneme leaves the cell body and its assembly is therefore delayed. To monitor incorporation, we decided to use inducible expression of tagged tubulin under the regulation of a tetracycline operator. This should allow us to induce expression of tagged tubulin by the addition of tetracycline and follow its incorporation over time.

In the first part we will address the following questions:

1a.) Can tubulin be tagged in a way it gets incorporated into the flagellum?

Tubulin has been notoriously difficult to tag in a way it gets incorporated into flagella (Bastin et al., 1996; Sheriff et al., 2014), because it relies heavily on protein sequence integrity. Conventionally tagged (N or C-terminus) tubulin does not get incorporated into the axoneme. We therefore chose an approach that has been successfully carried out in yeast and mammalian cells, where a 6-Histidine tag or 17 random amino acids were introduced into a specific structure on the luminal side of the MT without disrupting tubulins function (Peter J Schatz et al., 1987; Sirajuddin et al., 2014). This structure called the acetylation loop is found around the acetylated lysine at position 40 (K40) and thought to be less visible for most of alpha-tubulins interacting partners (Piperno and Fuller, 1985; Soppina et al., 2012).

1b.) Is new tubulin added to the axoneme at the tip?

So far, we lack direct proof that new tubulin is added at the distal tip of growing flagella. There are however multiple factors that make this scenario very likely: First, the MT plus end, which is the growing end of MTs, is localized to the distal tip (Euteneuer and McIntosh, 1981). Secondly, addition of new material at the tip was shown for accessory building components such as the PFR (Bastin et al., 1999). Lastly, the tyrosinated form of alpha-tubulin localizes to the tip of growing new flagellum (NF). As tyrosination is a property of recently assembled or “new” tubulin, its presence at the flagellum tip indicates it that new tubulin is indeed added there. Nonetheless, trypanosomes are notorious for their unconventional cell biology and we were curious if this was the case for axoneme assembly as well.

Successfully tracking where new tubulin building blocks are added will also allow us to address the question if there is integration in the old flagellum (OF). A disassembly / reassembly process (or turn-over) has never been shown for the OF of trypanosomes.

1c.) Is incorporation coherent with the locking model and therefore exclusive to the new flagellum? (This would bring direct proof for the locking model for the axoneme)

In case axoneme assembly indeed follows a grow-and-lock pattern, incorporation should only be observed in the new but not the old flagellum.

1d.) What is the assembly rate of the axoneme?

Flagellar assembly is a rather diverse process when compared between different species and different types of flagella. The green alga Chlamydomonas is a popular model in which assembly rate of the flagellum is slow at first (lag phase) but then tremendously increases until it hits a plateau.

In trypanosomes the assembly rate has been measured by monitoring extra-axonemal PFR component PFR2. This protein is added at the tip at a linear rate of 3.6μm per hour (Bastin et al., 1999). Does the axoneme follow a linear assembly rate similar to this structure?

Question 2: When is the flagellum locked?

2a.) Are the dynamics of tubulin incorporation compatible with the locking model?

Following the dynamics of tubulin incorporation will allow us to determine which flagellum integrates new building blocks at what time. New, assembling flagella are of course expected to integrate tubulin but what is the situation in mature flagella that are considered locked?

2b.) When does the flagellum commit to the locking event?

Inducible expression of tubulin has the major advantage that we can directly observe addition of new material. This also allows us to pinpoint the time at which a flagellum stops the integration of new building blocks. In 2018, our group postulated that the flagellum commits to the locking event before cell division. It was shown that the length of the new flagellum never exceeded the one of the full-length old flagellum in cells where cell division was inhibited. This

meant, that the new flagellum must have committed to the lock ahead of division. We wish to see if we can monitor the cells commitment to the locking model directly.

2c.) When is a flagellum finished to full length?

Currently it is unclear at what time a flagellum becomes full length or if all old flagella in bi-flagellated cells are complete, as it is possible that maturation of the flagellum takes more than just one generation. In procyclic cells, the new flagellum is elongated to ~80% of the length of the old flagellum when the cells divide and one daughter cell inherits the new and the other one the old flagellum. The new flagellum is then finished after cell division. Can we trace this new flagellum after it had become an old flagellum for the first time? If yes, we can then compare its length to flagella that are older than one generation.

2d.) Is a flagellum locked forever?

Should a flagellum stay locked forever after it is constructed to full length, we would expect it to not incorporate tubulin post locking event at any point in time. To investigate this possibility, we will attempt to track old flagella over several cell cycles and observe their ability to integrate new tubulin.

To trace old flagella several generations after their emergence we designed a “pulse-chase” experiment in which we labelled initially new flagella with tagged tubulin and then chased them after the duration of multiple cell cycles. These experiments provided some insight but also raised the possibility that mature flagella are subject to change over several cell cycles.

Question 3: Is the locking system present in other stages?

We decided to introduce tagged tubulin under tetracycline regulated expression into bloodstream form trypanosomes (BSF). This is the stage that infects the mammalian host. Interestingly, assembly of the BSF flagellum differs in two important aspects from the procyclic form flagellum. First, BSF flagella are longer than the ones of procyclic cells. Secondly, the new flagellum is assembled to full length before cell division (Tyler et al., 2001). This means

assembly of a new BSF flagellum does not need completion after cell division as required for the new flagellum of procyclic forms. BSF can be differentiated into procyclic forms. First, they turn into a cell cycle arrested stage called stumpy BSF that is pre-adapted for its insect vector. Then, the stumpy BSF turn into procyclic forms. Both these differentiation steps can be synchronized, which allowed us to investigate:

3a.) Is the locking system present in BSF?

Based on the differences observed in assembly between BSF and procyclic forms we thought it is possible that BSF regulate flagellum length by other means and wanted to investigate if the locking mechanism was present in BSF as well.

3b.) Are flagella in Procyclic forms generated *de novo* or inherited from BSF?

Currently it is not known if the first generation of procyclic forms inherits a flagellum from a BSF and then adjusts it, or if a cell divides and gives rise to a cell with a proyclic specific flagellum.

We attempted to differentiate BSF into procyclic forms with different methods and then trace the incorporation of tagged tubulin.

Aim

Results

Introduction

Flagella are protrusions of the cell that are wrapped in a specialized membrane. The core of the flagellum is the microtubule based axoneme. In *T.brucei* the axoneme has a classical architecture of nine outer microtubule doublets and a pair of single microtubules in the center. The flagellum is anchored in the cell by the basal body (BB). At the flagellar pocket (FP) the flagellum leaves the cell body and at this point the axoneme is joined by an extra-axonemal structure called paraflagellar rod (PFR). To investigate the assembly of the axoneme we followed the incorporation of the main building block tubulin. Two isotypes (alpha and beta) form the heterodimers that make up the MTs found in the flagellum (axoneme), the cell body (subpellicular array), and the mitotic spindle. The presence and incorporation of tubulin in T.*brucei* has been mainly investigated with a variety of antibodies that recognize the protein and its various post-translational modifications (PTMs) (Schneider et al., 1986; Sherwin et al., 1987b; Sherwin and Gull', 1989; Woods et al., 1989). There are studies that follow tubulin-incorporation into the MTs of the subpellicular array (Sheriff et al., 2014; Sherwin and Gull', 1989), however, a time sensitive analysis of the assembly process for the axoneme is missing. The main reason for this experimental gap is the fact that conventional tagging-approaches have failed so far: N-or C-terminally tagged tubulin is not incorporated into the axoneme comparably to WT-type tubulin. Here, we provide a study that fills this gap. To achieve this, we chose to tag alpha-tubulin with an internal tag, using either one or two Ty-1-tags (Bastin et al., 1996) in a structure termed "acetylation loop" positioned in the microtubule lumen (Soppina et al., 2012), right after the threonine (T41) that follows the acetylated lysine (K40) (L'hernault and Rosenbaum, 1983)(Schneider et al., 1986). First, one and two Ty-1-tag(s) were introduced into alpha-tubulin at its endogenous locus. The exact position cannot be determined since *T.brucei* genome possesses around ~20 tandem copies of identical genes coding for alpha-

tubulin and beta-tubulin (Seebeck et al., 1983; Thomashow et al., 1983). Incorporation was then observed in most of the described MT-based structures. Secondly, the Ty1-tagged tubulin was placed under the control of a tetracycline operator and the incorporation into the flagellum and cell corset was monitored over time. The following chapters describe how the assembly of the axoneme with newly synthesized tubulin takes place over short as well as extended periods of time. We found that the axoneme is assembled at a linear rate and that incorporation is exclusive to the new flagellum in bi-flagellated cells as proposed by the grow-and-lock model (Bertiaux et al., 2018). We describe evidence that the tip of old flagella is subject to change even after multiple cell cycles, most likely in the G1-phase of the cell cycle. Furthermore, we could highlight the exceptional stability of the trypanosomes MTs and lastly, describe how the locking model holds true for BSF trypanosomes as well.

Ty-1-tagged tubulin is incorporated into microtubules of the subpellicular array, mitotic spindle and the flagellum

Endogenous tagging with Ty-1-tubulin p2675

Due to the difficulty of tagging tubulin at the amino or carboxy-terminus, we chose to place a 10 amino acid short Ty-1-tag inside the open reading frame of alpha-tubulin. The goal was for the cells to express the tag inside the acetylation loop, a structure that faces the MT lumen, where the tag would be less likely to interfere with protein-protein interaction. According to the literature, up to 17 amino acids have been successfully introduced into the acetylation loop of tubulin without disrupting its localization or function. This was done by BamHI-linker guided mutagenesis and 17AA the maximal insertion in frame (Schatz et al., 1987). It is therefore possible that more AA can be introduced. Since multiple copies of epitope tags can increase the likelihood of detection, we choose to attempt to insert into the loop one of two copies of the

Ty-1-tag (10AA). Other groups have inserted a 6-histidine tag into this loop that allowed the detection of tagged tubulin without impairing its function (Sirajuddin et al., 2014). This was carried out in yeast cells and we wanted to investigate if a similar approach is valid in trypanosomes. The UTR flanking a transcript can greatly impact when, where and how much protein trypanosomes express (Clayton, 2016). Untimely expression of a tightly regulated housekeeping gene like tubulin could affect its incorporation. To rule out artifacts related to mRNA-regulation, tubulin was first *in situ* tagged in one of the ~40 gene copies. For that matter, a construct was selected that introduced the first 500bp of alpha-tubulin containing the epitope tag. The antibiotic resistance was placed on the 5' end followed by the alpha-beta-tubulin intergenic region, which was in turn followed by the first 500bp of the alpha-tubulin ORF containing one or two copies coding for the Ty-1-tag. After recombination, the tagged tubulin is flanked by its endogenous UTRs and expression is expected to be comparable to wild type alpha-tubulin (see methods figure 1).

Selection and screening of 1xTy-1 and 2xTy-1 tagged cells shows heterogeneity between wells.

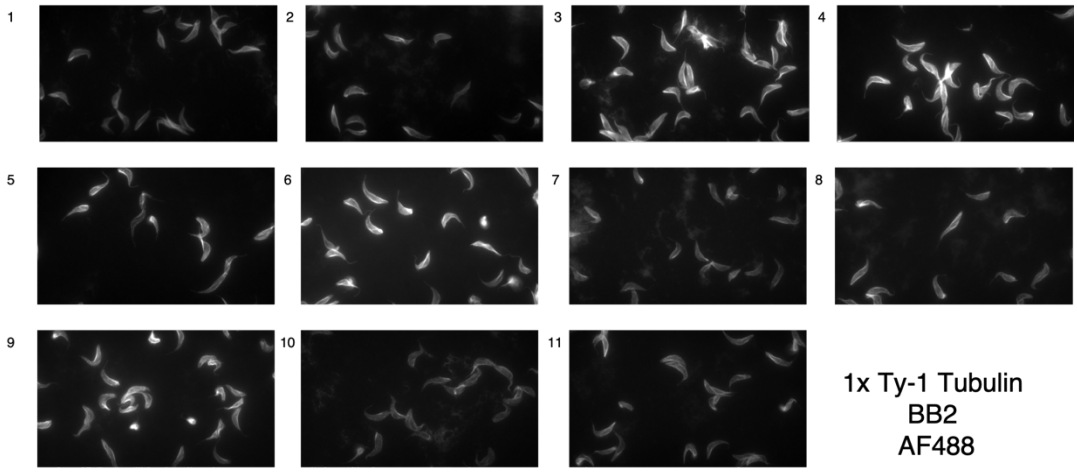

Figure 1 : IFA with whole cells that were transfected with p2675 1xTy-1-tub. Each field represents one well. Cells were stained with BB2, the antibody recognizing the Ty-1-tag. Intensity was normalized between the different fields with ImageJ *(*Schindelin et al., 2012).

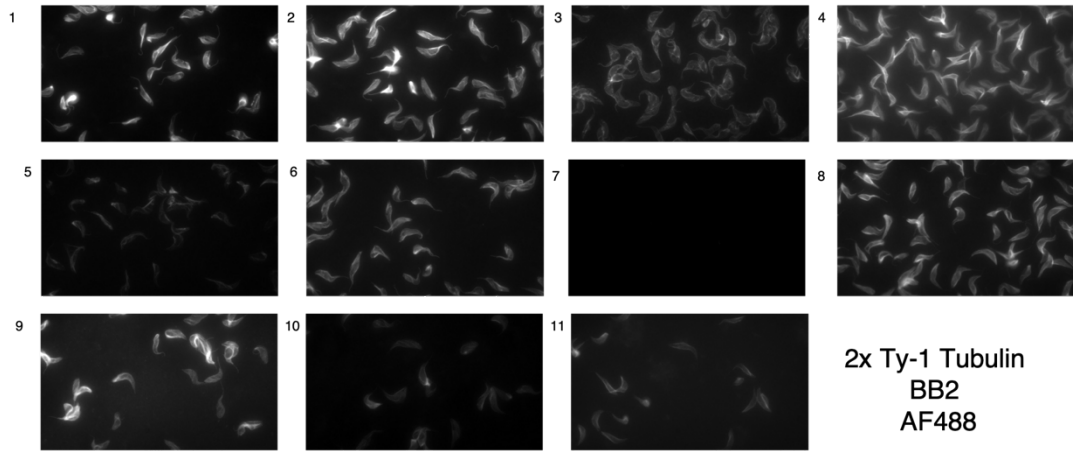

Figure *2* : IFA with whole cells that were transfected with p2675 2xTy-1-tub. Each field represents one well. Cells were stained with BB2, the antibody recognizing the Ty-1-tag. Intensity was normalized between the different fields with ImageJ (Schindelin et al., 2012).

After linearization, the vectors were transfected according to protocol and the cells selected for 10 days with puromycin. A high transfection efficiency was expected for two reasons. First, the construct can recombine into ~40 loci in the trypanosome genome. Second, the beta-alpha-intergenic region that is adjacent to the tagged alpha-tubulin sequence. As this is alpha-tubulins endogenous 3'UTR, it adds to the fragment that can recombine within the genome. These factors enhance the chances for integration of multiple copies of the tagged tubulin construct into the genome.

Indeed, the transfection was efficient and almost all wells had growing cells after 10 days. There was no difference in transfection efficiency between cells transfected with plasmids for the expression of one or two Ty-1-tags.

After the initial selection, the wells were picked and screened by IFA with the Ty-1-tag specific BB2 antibody (Bastin et al., 1996). Figure 1 (1xTy-1) and 2 (2xTy-1) depict fields of eleven different wells per transfection. Here, only the BB2 channel is shown, to highlight the heterogeneity of signal intensity across different wells but also inside the fields. The increased fluorescence intensity when individual cells were compared to others could be a consequence of integration into multiple genes. No remarkable difference in fluorescence intensity was observed when cells transfected with 1xTy-1tubulin were compared to the ones transfected with 2xTy-1-tubulin. Of importance was the detection of tagged tubulin in the flagellum. Based on this analysis, the wells with the most uniform signal were picked and then subjected to clonal selection. The upcoming cells were then further analyzed.

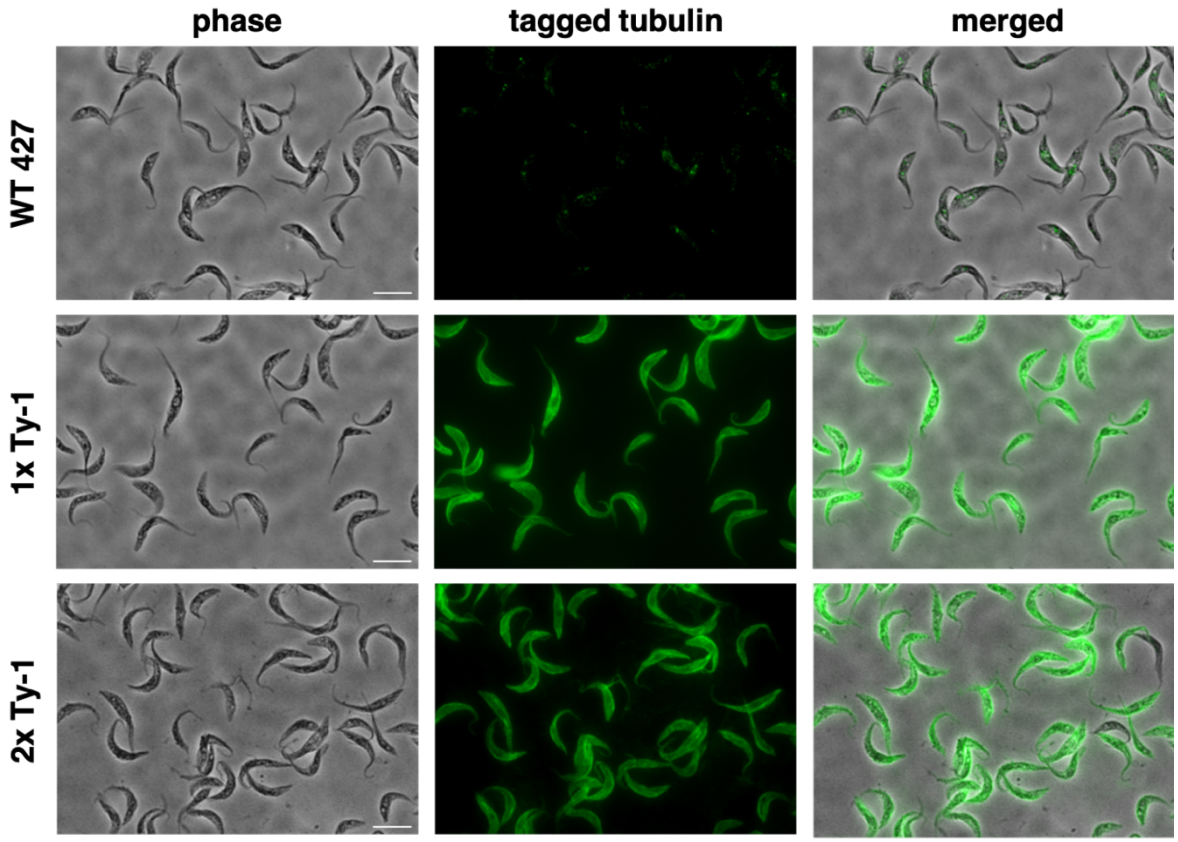

Figure *3* : IFA with whole cells from a WT 427 procyclic strain and from cells where alpha-tubulin was tagged with 1xTy-1 (middle) or 2xTy-1 tags (bottom). The slides were stained with the BB2 antibody that recognizes the Ty-1 epitope.

Whole cells were harvested for IFA and stained with the BB2 antibody (tagged tubulin). Figure 3 shows fields of whole cells from the parental wild type (WT) cell line as well as one clone for the 1xTy-1 and the 2xTy1 cell line after clonal selection. The signal between the individual cells was relatively uniform, in contrast to the non-clonal wells depicted in figures 1 and 2. For the WT sample, no signal is detected by the BB2 antibody apart from occasional weak spots that are likely background. In the 1xTy-1 as well as the 2xTy-1 tubulin cell lines, the tagged protein was observed in the cell body, but also in the old as well as the new flagellum. The observed localization of the tagged protein is coherent with what is expected for tubulin. Nonetheless, we had to further analyze if the tagged protein is indeed associated to the cytoskeleton and how well it co-localizes with a marker for alpha-tubulin.

Ty-1-tagged alpha-tubulin is cytoskeleton-associated and co-localizes with alpha-tubulin

To dissect the localization of tagged tubulin in more detail, cells from selected wells were harvested and subjected to extraction by detergent. After the addition of 1% NP-40 all soluble proteins are extracted, leaving only the cytoskeletons and tightly associated proteins. The tagged tubulin cell lines were subjected to this treatment and the slides then co-stained with the BB2 antibody that recognizes tagged tubulin as well as TAT-1 that recognizes all alpha-tubulin (TAT-1) (Woods et al., 1989).

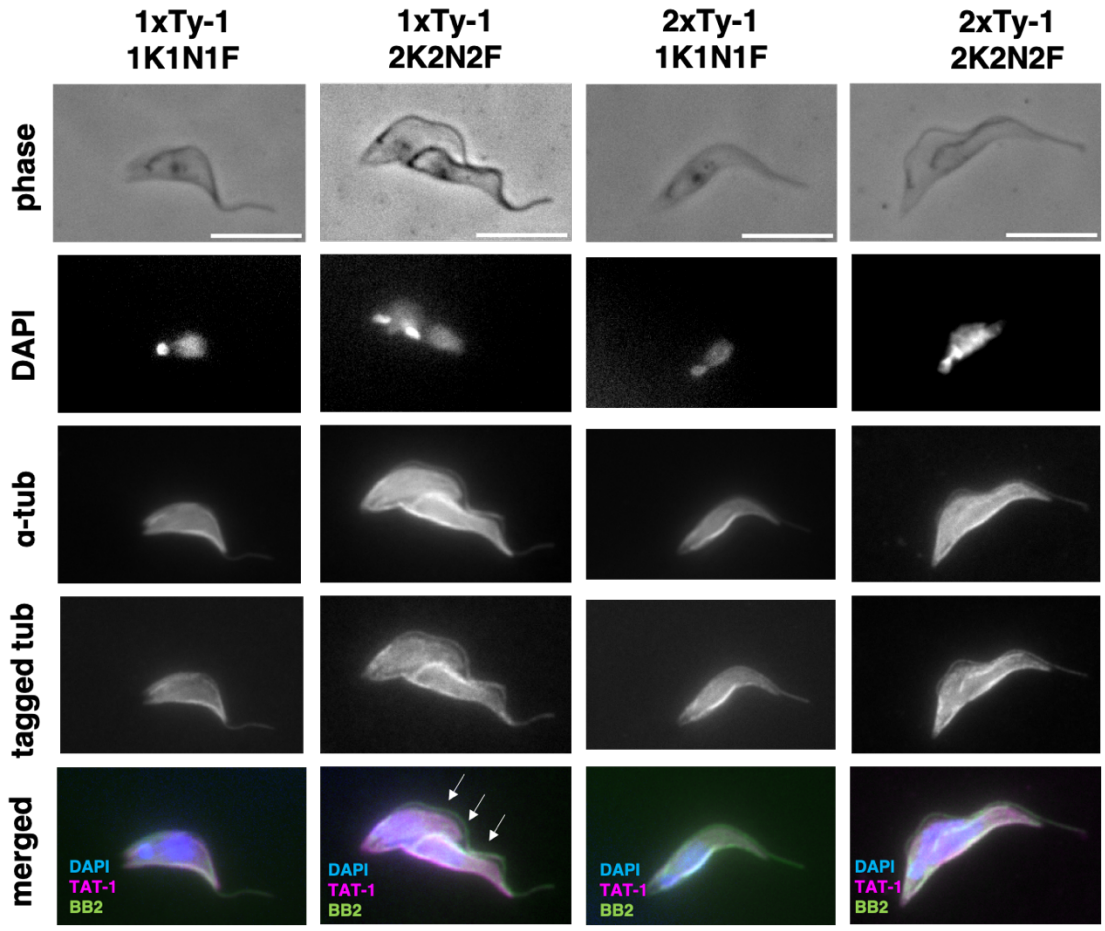

Figure 4 : Cytoskeletal extracts of cells expressing tagged tubulin (1x or 2x Ty-1-tags). Cells were detergent extracted with 1%NP-40 in PEM buffer and then fixed with methanol. The cells were stained with antibodies: TAT-1 (Woods et al., 1989) that recognizes alpha-tubulin, BB2 which detects the Ty-1-tagged alpha-tubulin and DAPI to stain DNA in the nucleus and the kinetoplast. The arrows indicate a flagellum.

This experiment provided two crucial details. In Fig. 4, one can observe cytoskeletons of cells in G1 phase with one kinetoplast, one nucleus and one flagellum (1K1N1F, Fig. 4 panel 1+3) as well as cells before division (2K2N2F, Fig. 4 panel 2+4). Staining with the BB2 antibody revealed that tagged tubulin was present inside the cytoskeleton as well as the flagellum of 1K1N1F and both flagella 2K2N2F cells. The localization was virtually identical to the one observed with the TAT-1 antibody that recognizes all alpha-tubulin. Since these cells were detergent extracted, this is formal evidence that tagged tubulin must have integrated into the microtubules. The co-localization with TAT-1 showed that there is no particular sub-cellular exclusion of tagged tubulin. Therefore, it localizes like wild type tubulin to the MTs of the subpellicular array (cell body) and the flagella. Intriguingly, there seemed to be relatively higher intensity in the flagellum vs. the cell body with the BB2 antibody when compared to TAT-1 (Fig. 4 merged panel). One explanation for this observation could lie in the difference in accessibility of the epitope. In the case of TAT-1, the antibody recognizes an epitope towards the C-terminus that is positioned on the outside of the MT, while the Ty-1 epitope faces the MT lumen. When compared to the singlet MTs in the cell body and the busy surface of axonemal MTs, the TAT-1 epitope could be less exposed to the antibody. This might result in a weaker signal in the flagellum relative to the cell body. On the other hand, the antibody that binds to the Ty-1 epitope faces the theoretically less busy MT lumen. Here the difference of MTs between the axoneme (9+2 architecture) and cell body (MT singlets) might not have been as relevant and the signal therefore more uniform.

Ty-1-tagged alpha-tubulin tubulin can be distinguished from endogenous alpha-tubulin on Western blots

As a next step, western blots (WB) were performed to formally prove that the protein detected with the Ty-tag specific antibody BB2 is indeed alpha-tubulin. Therefore, separate membranes were probed with antibodies recognizing the Ty-1-epitope as well as alpha-tubulin.

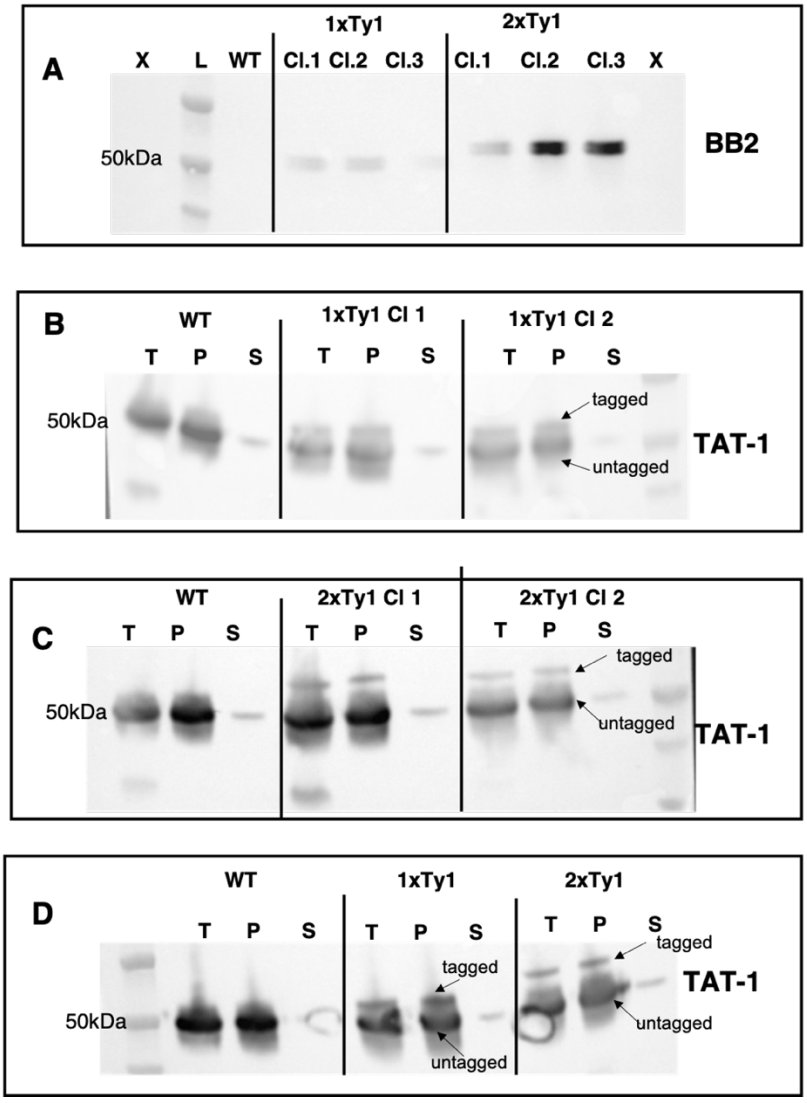

Figure *5* : Western blots with a WT cell line, the 1xTy-1 and 2xTy-1 cell lines. A: Whole cell lysates of WT and three clones for each tagged cell line. Membrane was stained with the BB2 antibody (tagged tubulin). B-D: Membranes were incubated with the TAT-1 antibody that recognizes all alpha-tubulin. B: Extracts from WT and 2 clones of the 1xTy-1 cell line. C: Extracts of a WT sample and 2 clones of the 2xTy-1 cell line. Membrane was stained with TAT-1 (alpha-tubulin). D: Extracts of WT, 1xTy as and 2xTy-tagged-tubulin cell lines. T: whole cell lysates, P: cytoskeletal fraction, S: soluble proteins.

T.brucei alpha-tubulin has a size of ~49.8 kDa (TriTrypDB.org) and migrates to the expected position in an SDS-PAGE gel (Fig. 5). Each copy of the Ty-1-tag is expected to add ~1.2 kDa in size when added to alpha-tubulin. The tagged protein was therefore not expected to migrate at a notably different size when compared to WT-alpha-tubulin. In Fig.5A three clones of each cell line (1xTy-1 Cl. 1-3; 2xTy-1 Cl. 1-3) can be observed. In addition, a WT sample was used as a negative control. In the latter no band was visible as expected. In contrast, one band is visible that migrates slightly above the 50 kDa of the marker in all samples of the Ty-1-tubulin cell line (Fig. 5A 1xTy-1, 2xTy-1 Cl. 1-3). The bands of the three clones tagged with 2xTy-1 epitopes (Fig. 5A, 2xTy-1 Cl. 1-3) migrated higher when compared to their single epitope-tagged counterparts (Fig. 5A, 1xTy-1 Cl. 1-3). Since the size difference of 1xTy-1-tag (10AA, 1.2 kDa) was enough for a notable shift it was possible that tagged tubulin could be separated from untagged tubulin as well.

To test if tagged tubulin can be distinguished from endogenous tubulin by WB, membranes from protein isolates were stained with the TAT-1 antibody. In addition to whole cell lysates, detergent extraction was performed to separate cytoskeletal proteins in the pellet from the soluble proteins in the supernatant.

Since microcopy showed that tagged tubulin is detergent resistant and had an almost identical localization as WT-tubulin, we expected the WB to reflect that. Fig.5B and C depict WBs with protein isolates from whole cells (T), cytoskeletons (P), and soluble proteins (S). For each cell line, isolates of two clones are shown for the 1xTy-1 cell line, Fig.5B) and 2xTy-1 cell line (Fig.5C). For all fractions in all cell lines a band is observed that migrates around the 50 kDa marker. The bands of whole cell isolate and cytoskeleton have similar intensities while the band of the soluble fraction is considerably fainter in comparison. The reason for this is that the soluble pool of tubulin in *T.brucei* is known to be low and most tubulin is in fact incorporated into MTs (Schneider et al., 1986; Sherwin et al., 1987a).

In the WT cell line, only one band is visible for all the isolates. However, in the cell lines where alpha-tubulin was tagged with one or two Ty-1-tags, an additional band is visible that migrated a little bit further up. These bands are clearly separated and observed even higher up in the cell lines tagged with two epitopes (comparison of tagged bands in Fig. 5B to tagged bands Fig. 5C). This size shift (highlighted in Fig. 5D, 1xTy vs 2xTy) confirmed the results described in Fig. 5A. Therefore, Ty-1-tubulin indeed migrates at a higher size compared to untagged alpha-tubulin.

Based on the number of added AA a size shift of that magnitude was not expected. However, epitope tagged proteins have been shown to migrate substantially different in patterns that are not explicable by just the added size. Such an observation was made for example with Ty-1-tagged PFR-A/PFR2 where a similar size shift occurred (Bastin et al., 1999). It is possible that this size difference reflects different detergent binding properties of Ty-1-tagged proteins (Rath et al., 2009).

As in the WT sample, the intensities of the tagged tubulin bands between the total and the pellet fraction are comparable. A band for the soluble pool was not visible potentially because it was below detection limit. A quantification of the bands labelled with TAT-1 was done with the Cytiva ImageQuantL software. These measurements showed that the upper bands (tagged tubulin) represent about ~3% of the lower band (endogenous tubulin). Such a ratio is expected when only one out of the 40 gene copies of alpha-tubulin is tagged. The complete absence of a tagged tubulin band in the soluble fraction is a hint that there is no substantial amount of Ty-1-tubulin retained in the soluble pool. In contrast to what was observed for terminally-tagged tubulin by our group and others (Sheriff et al., 2014), where a majority of tagged tubulin is not incorporated into MTs and found in the soluble fraction.

Furthermore, quantification of the ratio of total to cytoskeletal fractions for the untagged and tagged bands showed that they were nearly identical. In conclusion, Ty-1-tubulin can be distinguished on WB from untagged proteins. It is incorporated in nearly identical quantities into the cytoskeletal fraction and a relatively substantial soluble pool like in previous tagging-

attempts is not observed. This is the first time that tagged *T.brucei* alpha-tubulin is succesfully incorporated in MTs of the cell body and the flagellum similar to endogenous alpha-tubulin.

Inducible expressed Ty-1-tubulin incorporates into MTs similar to WT alpha-tubulin

From the results obtained with the *in situ*-tagged cell lines, we concluded that tagging alpha-tubulin in the acetylation loop is indeed a viable strategy. As a next step we wanted to see if tubulin tagged with this approach can be expressed from an ectopic locus (For construct see MM Fig. 2). A construct was generated in which the whole ORF of alpha-tubulin with one copy of the Ty-1-tag was cloned downstream of a procyclin promoter containing two tetracycline operators (Ty-1-tub-pHD430) (Wirtz and Clayton, 1995) (see Fig. 2 methods). First, this construct was transfected into a WT cell line. This allowed the cells to express tagged tubulin from an ectopic location independently of tetracycline addition. This way, we tested if ectopically expressed Ty-1-tagged tubulin could be incorporated similar to *in situ* tagged tubulin. After that, we subjected these cell lines to clonal dilutions and transfected them with a construct for the expression of the tetracycline repressor. The repressor should bind to the operators that are present in the procyclin promoter and prevent the transcription of the tagged tubulin gene. After tetracycline is added, it should bind to the Tet-repressor and inhibit its binding to the operators. Therefore, transcription of tagged tubulin can ensue and the cells should produce the protein. In the field, the addition of tetracycline to the medium, is commonly referred to as induction. In continuation, we will call the Ty-1-tagged alpha tubulin whose expression is induced after the addition of tetracycline tagged tubulin. Incorporation of tagged tubulin can then be monitored over different points of time.

Ectopically expressed Ty-1-tubulin is incorporated into MTs

After transfection with the 1xTy-1-tubulin-pHD430-construct, cells underwent an initial IFA screen with the BB2 antibody. The most uniform clones were picked and subjected to clonal dilutions. In Fig. 6, whole cells of one clone are shown co-stained with the BB2 antibody that recognises the tag and DAPI, staining DNA in the nucleus and the kinetoplast. In the WT sample (Fig. 6, top, tagged tubulin), there is almost no signal apart from green spots that is likely background. For the tagged cell line (lower panel) signal is present in >90% of cells in the cell body as well as in flagella. Signal intensity between individual cells was fairly uniform.

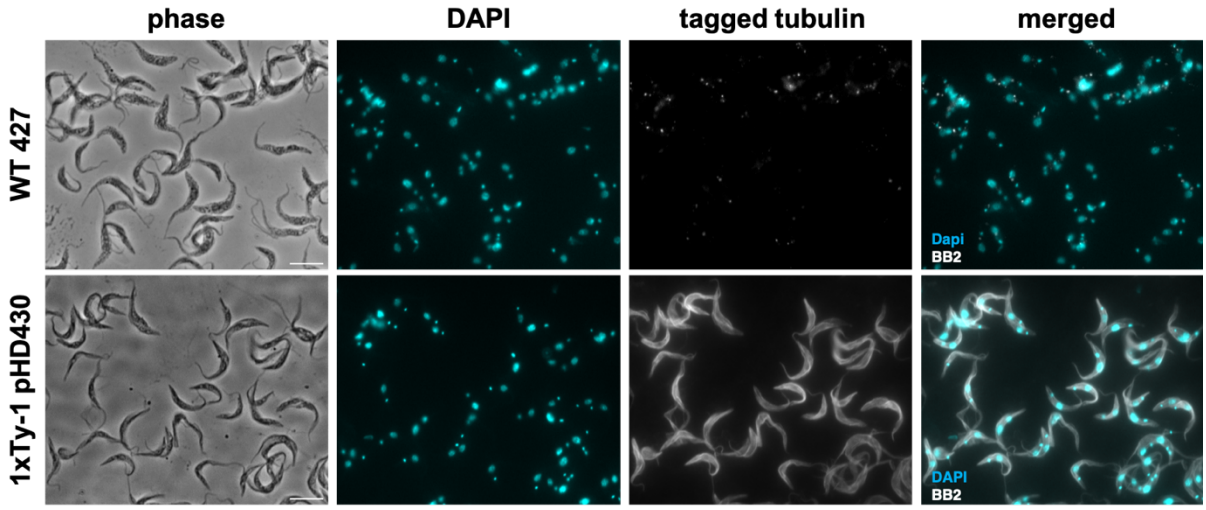

Figure *6* : IFA with whole cells of a WT cell line (top) as well as the 1xTy-1 pHD430 cell line (bottom) in which an ectopic copy of intragenic Ty-1-tagged alpha-tubulin was introduced. Samples were stained with the BB2 antibody (tagged tubulin) and DAPI (DNA).

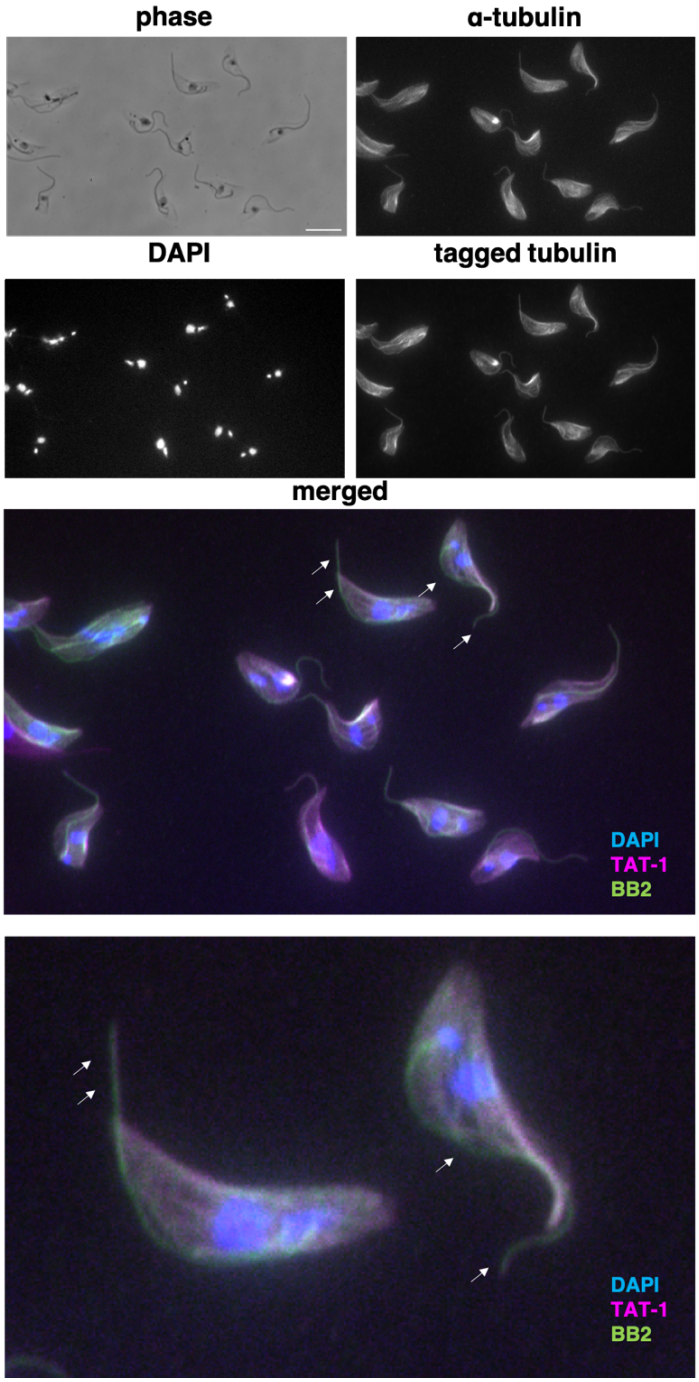

Figure 7 IFA with detergent extracted cytoskeletons of the 1xTy-1 pHD430 cell line (bottom) in which an ectopic copy of intragenic Ty-1-tagged alpha-tubulin was introduced. Samples were stained with the BB2 antibody (green, tagged tubulin), TAT-1 (magenta, alpha-tubulin) and DAPI (blue, DNA). Arrows indicate flagella

Next, we subjected these cell lines to detergent extraction to test if ectopically expressed Ty-1-tagged tubulin is incorporated into MT. Fig. 7 depicts cytoskeletal extracts of the Ty-1-tub pHD430 cell line co-stained with BB2 (tagged tubulin), TAT-1 (all alpha-tubulin) and DAPI (DNA). Here in green, the tagged tubulin was observed in the cell body as well as in flagella. Since these are detergent extracts, we can infer that ectopically expressed Ty-1-tubulin is indeed incorporated into the MTs of the cell body and the axoneme inside the flagellum (Fig. 7, tagged tubulin). Additionally, the tagged protein co-localizes very well with the alpha-tubulin recognized by the TAT-1 antibody (Fig. 7, α-tubulin). In the merged panel (Fig. 7, arrows) we observed that the intensity from flagella to cell body was again higher in flagella with the tagged protein, as was observed for the *in situ* tagged protein (Fig. 4 lowest panel, arrows in 1xTy, 2K2N2F cell).

Since ectopically expressed Ty-1 tubulin was incorporated into MTs and co-localised with WT-alpha-tubulin, the next step consisted in introducing the tetracycline repressor, to render expression tetracycline dependent.

Expression of tagged tubulin is repressed by the tetracycline repressor and can be induced.

The clonal cell line Ty-1-tubulin pHD430 was transfected with the pHD360 plasmid to introduce the tetracycline-repressor. When this protein is expressed, it should bind to the tet-operators on the promoter and silence the expression of tagged tubulin. Selection was carried out with hygromycin, which is the resistance marker present on the pHD360. Phleomycin, the marker that was used to select for the pHD430 construct was not added in this selection. The reasoning for that is that expression phleomycin resistance and tagged tubulin on the pHD430 1xTy-tubulin are not independent but both mediated by the procyclin promoter. Therefore, the introduction of the tet-repressor with the pHD360 construct should also silence the expression of phleomycin. After ~10 days, of hygromycin selection, the upcoming wells were picked and tested by IFA. Every well was tested after the addition of tetracycline (overnight induction) and without. Wells that showed expression of tagged tubulin only under the tetracycline induced conditions were chosen and further selected by clonal dilution. After this, the wells were screened for the presence of tagged tubulin in induced and non-induced conditions again, and one clone was chosen for further experiments.

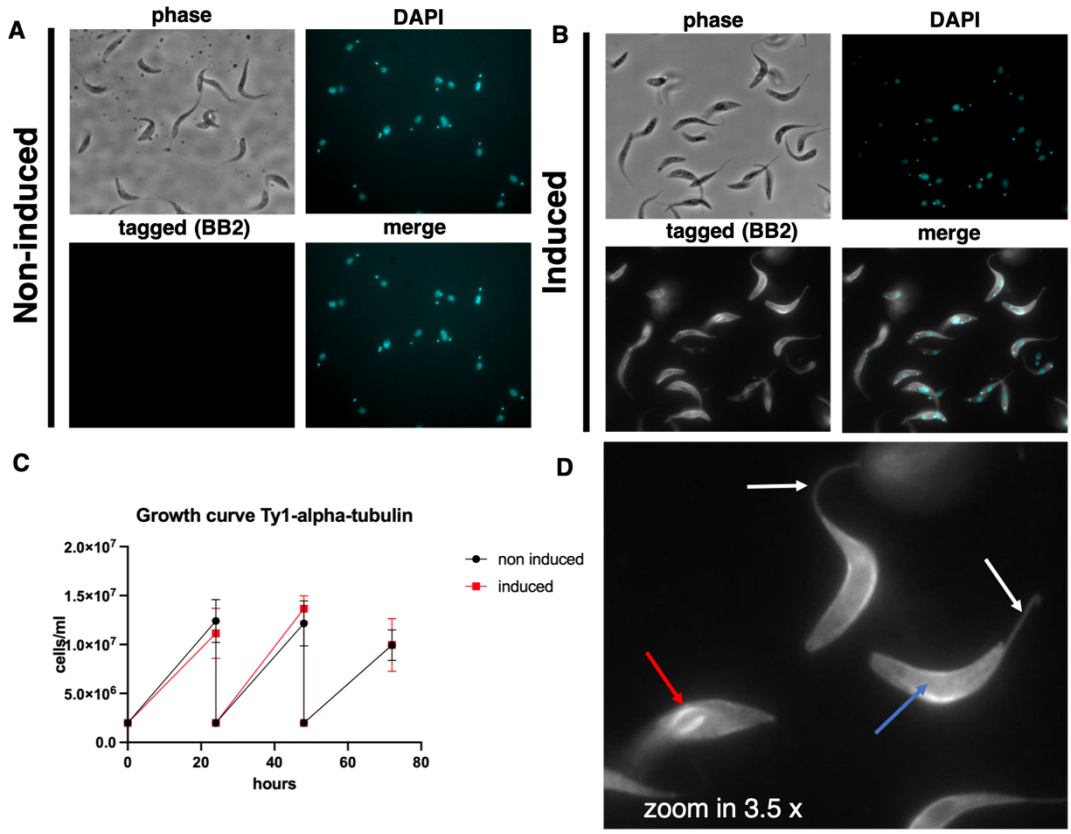

Figure *8* : IFA with whole cells of the inducible 1xTy-1-tubulin cell line. Non-induced (left panel) and after Ty-1-tubulin expression was induced 24h with 1μg/ml of tetracycline. Samples were stained with the BB2 antibody (white, tagged tubulin) and DAPI (Cyan, DNA). Arrows indicate flagella (white), MTs of the cell body (blue), the mitotic spindle (red). C: Growth curve with cells from the tagged tubulin cell line induced (black) and non-induced (red). Cells were diluted every 24h to 2x10^6 cells/ml. D: zoom in of the tagged tubulin channel highlighting the different MT based structures.

In Fig. 8 one can observe whole cells of the inducible tagged tubulin cell line under non-induced conditions (no tetracycline, Fig. 8A) and when cells were induced for 24 hours (+ 1μg/ml tetracycline, Fig. 8B). Without the addition of tetracycline, tagged tubulin is not detected (Fig. 8A). On the contrary, when tetracycline was added to the culture, signal is observed in the cell body, in the old and new flagellum and the mitotic spindle (Fig. 8B). The latter was clearly visible as dense MT based structures that engulfed the nucleus of cells with two kinetoplasts. Since the TAT-1 antibody which recognizes alpha-tubulin does not stain the spindle very well, the fact that we could clearly distinguish the mitotic spindle with tagged-tubulin was a surprise. This structure can be stained with antibodies that recognize acetylated alpha-tubulin (C3B9 or 6-11B-1(Piperno and Fuller, 1985; Sasse and Gull, 1988; Woods et al., 1989). The epitope to which these acetylated-tubulin specific antibodies bind is in the immediate proximity of where the Ty-1-epitope was introduced. Therefore, these three antibodies C3B9, 611B-1 and BB2 (tagged tubulin) are binding at an almost identical position in the lumen of the microtubule. The explanation why TAT-1 does not recognize the spindle might again be the limited accessibility on the surface of the microtubule, similar to what was discussed for Fig. 3 and 4.

Additionally, we quantified that ~90% of cells had incorporated tubulin after 24 hours of induction. To assess if tagged tubulin can be observed in cells where no tetracycline was added we screened fields of non-induced cells in the eyepieces of the microscope. Roughly 1 in 200 – 300 cells showed incorporation with an intensity comparable to an overnight induction. We concluded that this little amount of “leakiness” should not affect quantification of experimental procedures in a meaningful way.

In summary, expression of tagged tubulin was suppressed by the presence of the tetracycline-repressor and could be induced with the addition of tetracycline. The expressed protein is visible in the cell body, old and new flagella, as well as the mitotic spindle of whole cells. A large majority of cells responded well to induction, while without the addition of tetracycline, expression of tagged tubulin is rare and could be neglected.

Assembly dynamics of tagged tubulin can be traced in extracted flagella and the subpellicular MTs.

We then tested for the presence of ectopically expressed tagged tubulin in detergent extracted cytoskeletons as well as flagella after high salt extraction. Tagged tubulin expression was induced for 48 hours and the cytoskeletons extracted with detergent, slides were then stained with BB2 (tagged tubulin), Mab25 (an axonemal marker), anti-FTZC (transition zone) (Bringaud et al., 2000) and DAPI (DNA). FTZC is a marker for the transition zone and represents the start of the axoneme. Mab25 (*T.brucei* SAXO protein) is a well-known marker commonly used for the axoneme (Dacheux et al., 2012).

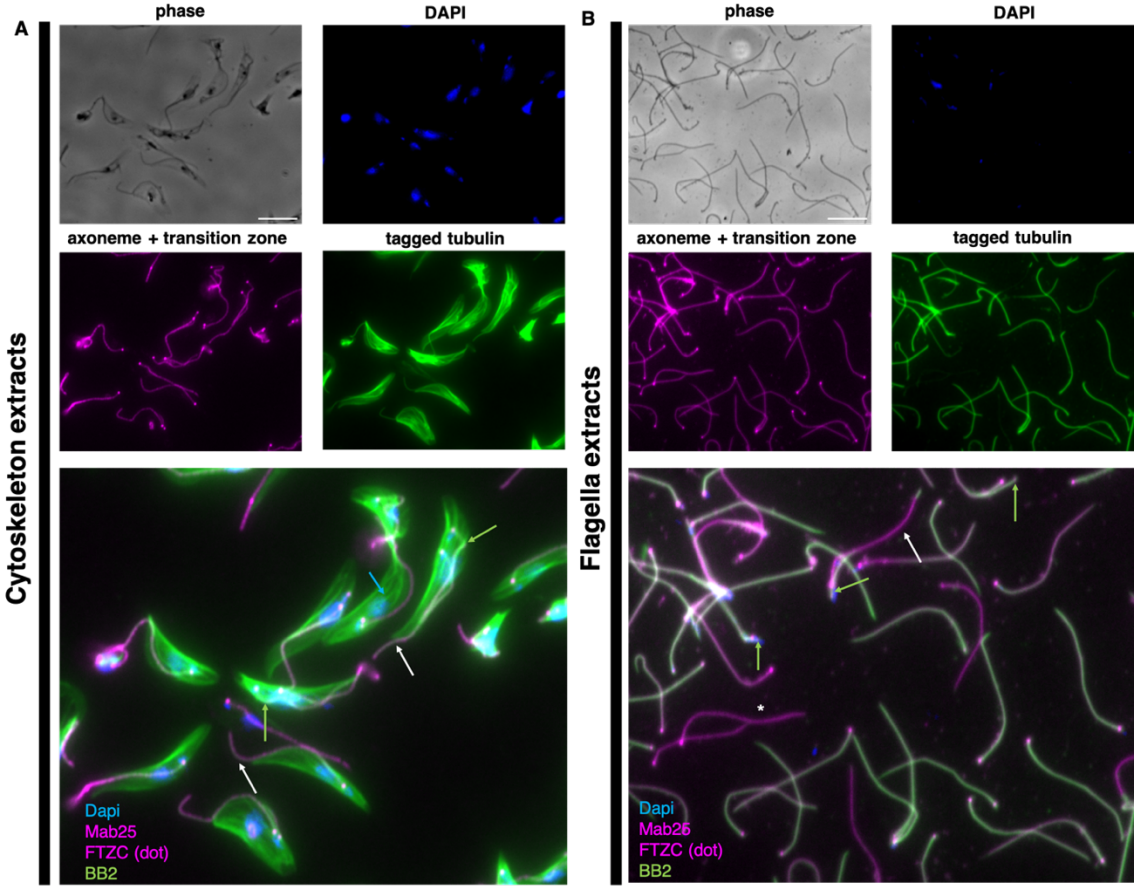

Figure *9* : IFA with samples from 1xTy-1-tubulin cell line after 48 hours of induction. Left panel: Detergent extracted cytoskeletons, right panel: high salt extracted flagella. Samples were stained with the BB2 antibody (green, tagged tubulin), Mab25 (magenta, axoneme), anti-FTZC (magenta (dot), transition zone) and DAPI (blue, DNA). Arrows: white=old flagellum, green=new flagellum, blue=cell body. ✷=cell that did not respond to induction.

We then tested for the presence of ectopically expressed tagged tubulin in detergent extracted cytoskeletons as well as flagella after high salt extraction. Tagged tubulin expression was induced for 48 hours and the cytoskeletons extracted with detergent, slides were then stained with BB2 (tagged tubulin), Mab25 (an axonemal marker), anti-FTZC (transition zone) (Bringaud et al., 2000) and DAPI (DNA). FTZC is a marker for the transition zone and represents the start of the axoneme. Mab25 (*T.brucei* SAXO protein) is a well-known marker commonly used for the axoneme (Dacheux et al., 2012).

One goal of this experiment was to prove that inducible expressed Ty-tubulin is incorporated into MTs. The second goal was to get an idea which extracts provide the most feasible way of tracing incorporation into the new and old axoneme. Fig. 9 provides two panels with cells that were induced for 48h. Both fractions depicted are from the same induction experiment. In the cytoskeleton fraction (left panel), incorporation of Ty-1-tubulin is clearly visible in the MT of the cell body (blue arrows) as well as in new (green arrows) and old (white arrows) flagella.

It was noticed that flagella are sometimes hard to track along their entire length when some of the portions overlap with the cell body, even with the presence of an axonemal marker. In general, the signal intensity in the subpellicular array is very high when compared to the MTs of the axoneme. This is expected and simply owed to the fact that the MTs of the cell body are much more numerous than the twenty MTs in the flagellum. The most MT dense section of subpellicular array is in the region of the nucleus where it amounts to ~100 MT singlets (Meyer and De Souza, 1976; Sinclair et al., 2021).

Detergent extracted cytoskeletons can be further treated with a high salt solution (1.1M NaCl) which will extract the MTs of the subpellicular array and only leaves the flagellum on the slide. In Fig. 9B, flagella extracted in this manner are shown. They are from the same induction-experiment co-stained with the same antibodies that were used for the cytoskeleton extracts. Tagged tubulin (green) clearly integrates into the axoneme along its entire length (Fig. 9B).

Unless the flagella overlap each other, incorporation of Ty-1-tubulin can be easily traced along the whole axoneme. The new flagellum can be distinguished from the old one even at early

stages when its length is short. The biflagellate cell marked with a star, did most likely not respond to the tetracycline induction (Fig. 9B).

Overall, incorporation of tagged tubulin could be observed after induction in cytoskeletons and flagella. Its incorporation into the axoneme was traceable with both extraction methods. However, incorporation into extracted flagella was easier to analyze because the signal in the axoneme is not overshadowed by the subpellicular MTs. Even after prolonged induction time (48h), the cells show neither aberrant morphology nor doubling time (Fig. 8C), which show that integration of tagged tubulin after induction does not interfere with cell viability. This begs the question on how substantial the proportion of tagged tubulin is when compared to untagged tubulin.

Tagged tubulin is incorporated as efficiently as endogenous alpha-tubulin

The procyclin promoter under which tagged tubulin is expressed is a very strong promoter (Sherman et al., 1991). It was therefore conceivable that it results in overexpression. During the experiments that were performed so far, the cells were not struggling after the addition of tetracycline. Therefore, we wanted to assess how efficiently tagged tubulin is incorporated into MTs. To quantify this, a culture was induced with tetracycline for 16h. WBs were then performed with extracted cytoskeletons and the soluble fraction as well as whole cells (similar to the experiments described in Fig.5).

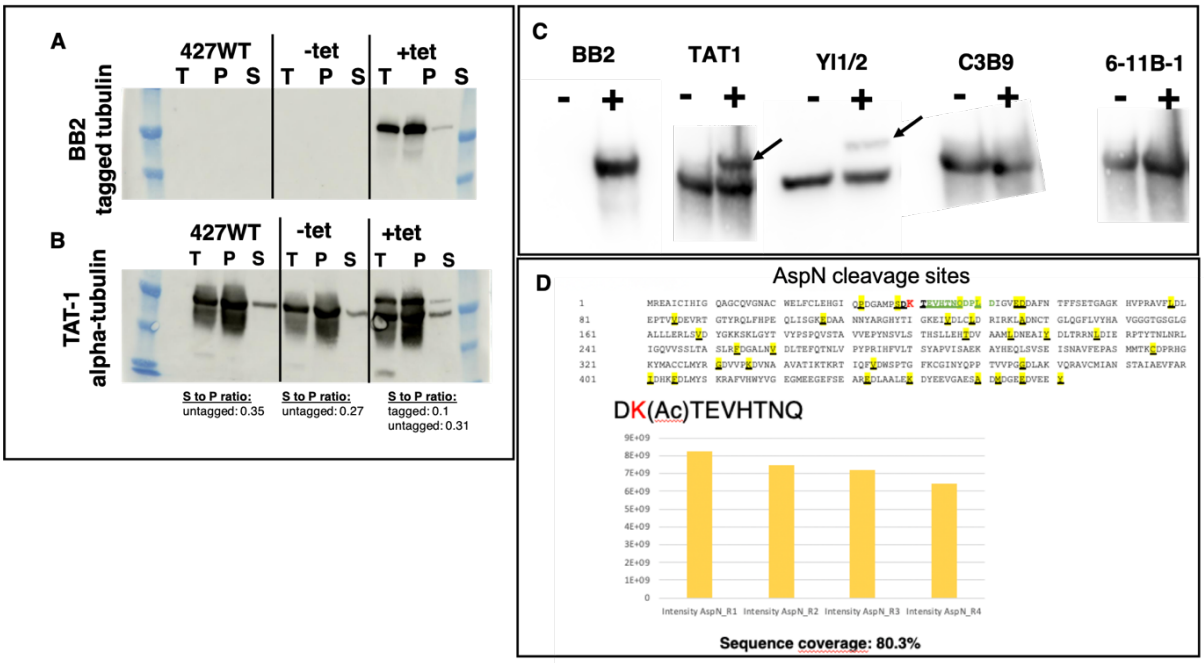

Figure *10* : Western blots of extracts from a WT sample as well as the inducible 1-Ty-1-tubulin cell line before and after induction. A: Extracts from WT (left), non-induced 1xTy-1-tubulin cell line (middle), overnight induced 1xTy-1-tubulin cell line (right). Membranes was stained with the BB2 antibody (tagged tubulin). B: Membrane was stained with the TAT-1 antibody (alpha tubulin). T: whole cell lysates, P: cytoskeletal fraction, S: soluble proteins. S to P ratio marks the ratio quantified by ImageQuantL between the cytoskeleton (P) and the soluble fraction (S). C: Membranes were stained with antibodies that recognise different PTMs on alpha-tubulin. Yl1/2 recognises tyrosinated tubulin, C3B9 and 6-11B-1 recognise acetylated tubulin. Arrows indicate the tagged tubulin band. An additional band that corresponds to tagged tubulin was not visible with the two antibodies that recognise acetylated tubulin. D: Mass spectrometry analysis of extracted flagella, cleavage with Asp N revealed that tubulin with the Ty-1-epitope (green) is indeed acetylated.

Extracts of three samples were prepared, one where Ty-1-tubulin expression was induced for 16h (Fig. 10, +tet), a non-induced sample (-tet) and the WT cell line (427WT). Whole cells (T), cytoskeletal fraction (P) and soluble proteins (S) were loaded on two gels and then transferred onto separate membranes. One was stained with the BB2 antibody (tagged alpha-tubulin, Fig. 10A) and the other one with the TAT-1 antibody (alpha-tubulin, Fig. 10B). Based on the results obtained by IFA we expected to detect tagged tubulin only in the samples where tetracycline was added (Fig. 10, +tet). Similar to Fig. 5, total and cytoskeleton fractions should be at similar intensities while the soluble fraction should have a notably fainter band. On the blot that was incubated with BB2 (tagged tubulin, Fig. 10A), no bands were visible neither for the WT sample nor for the non-induced control. On the blot that was stained with TAT-1 (all alpha-tubulin, Fig. 10B), the band of untagged tubulin around 50kDa is present for all three fractions: two bands of similar intensity were present for the whole cell fraction (T) and the cytoskeleton fraction (P). In comparison, the band of the soluble fraction (S) is fainter. The smear below and above the T and P band might correspond to alpha-tubulin with different posttranslational modifications (PTMs) as it is also visible in non-induced conditions and the WT sample. A likely candidate for such a PTM is poly-glutamylation, as it is abundant on tubulin and can be present with many glutamate residues, which would account for the range of the smear (Schneider et al., 1997).

On the membrane stained with BB2, the induced samples (+tet) had one band in each fraction: These were of high intensity in whole cells and cytoskeleton fraction, while much fainter for the soluble pool. This indicated that a majority of tagged tubulin is incorporated into the cytoskeleton and only little retained in the soluble pool. On the blot stained with TAT-1 (Fig. 10B, +tet) an additional band that corresponds to Ty-1tagged tubulin is visible above the endogenous alpha-tubulin band. When compared to the lower band of untagged tubulin, which also serves as a loading control, these share a similar pattern of intensity between the three

fractions. Intriguingly our quantifications suggest that the ratio between soluble tubulin and the cytoskeletal fraction was ~two-fold lower for tagged tubulin when compared to untagged tubulin (Fig. 10B, S to P ratio).

To conclude, Ty-1-tubulin could be observed on WBs after induction. Signal in non-induced samples was below detection limit and the samples not distinguishable from WT. Therefore, leakiness of expression in the absence of tetracycline was not observed on WBs. The soluble pool of Ty-1- tubulin was lower compared to untagged tubulin. Taken together this strongly suggests that tagged tubulin is readily expressed and then incorporated into MTs as efficiently as untagged tubulin.

Next we tested if known PTMs of alpha-tubulin could be detected on tagged tubulin as well. Western blots were performed with whole cells lysates of non-induced and overnight induced cells from the tagged tubulin cell line. Membranes were then stained with BB2 (tagged tubulin), TAT-1 (alpha-tubulin), Yl1/2 (tyrosinated alpha-tubulin) (Sherwin et al., 1987a), C3B9 (acetylated alpha-tubulin) (Woods et al., 1989) and 6-11B-1 (acetylated alpha-tubulin) (Piperno and Fuller, 1985). An additional band that corresponds to tagged tubulin is visible on the blots stained with BB2, TAT-1 as expected, as well as, on the membrane stained with Yl1/2 which revealed that tagged tubulin is also tyrosinated. In contrast, the blots stained with the antibodies that recognise acetylated tubulin (C3B9, 6-11B-1) did not reveal an additional band (Fig. 10C). This was unexpected as, according to literature, all alpha tubulin is expected to be acetylated (Schneider et al., 1986). We hypothesized that the insertion of the tag just 1 AA after the acetylated lysine (K40) (Piperno and Fuller, 1985; Soppina et al., 2012) might have changed the epitope to which C3B9 and 6-11B-1 bind and rendered it unrecognizable for these two antibodies. We therefore induced the tagged tubulin cell line for 1 week to enrich the tagged ectopic copy vs. endogenous tubulin as much as possible. Flagella of these cells were then extracted and subjected to LC-MS/MS analysis by our collaborators at the MS-platform of Institut Pasteur. Samples were cleaved with the Asp-N enzyme and the Ty-1-tag specific sequence was analysed for the presence of acetylation. These experiments revealed that

tagged alpha-tubulin is indeed acetylated. We concluded that the absence of an additional band on the membranes (Fig. 10C) stained with acetylated alpha-tubulin specific antibodies is because, C3B9 and 6-11B-1 lost affinity for the acetylated epitope due to the tag.

Tagged tubulin is suitable to track assembly dynamics of MTs

In the previously described experiments, expression of Ty-1-tubulin was induced over 48 hours (or 4-6 cell cycles). From these experiments, we concluded that tagged tubulin can be expressed from an ectopic locus after the addition of tetracycline. Furthermore, the tagged protein is incorporated into MTs as efficiently as endogenous alpha-tubulin. As a next step, we wanted to trace tubulin incorporation over shorter periods of time.

Ty-1-tubulin expression is detectable after ~1-1.5 hours of induction on WBs

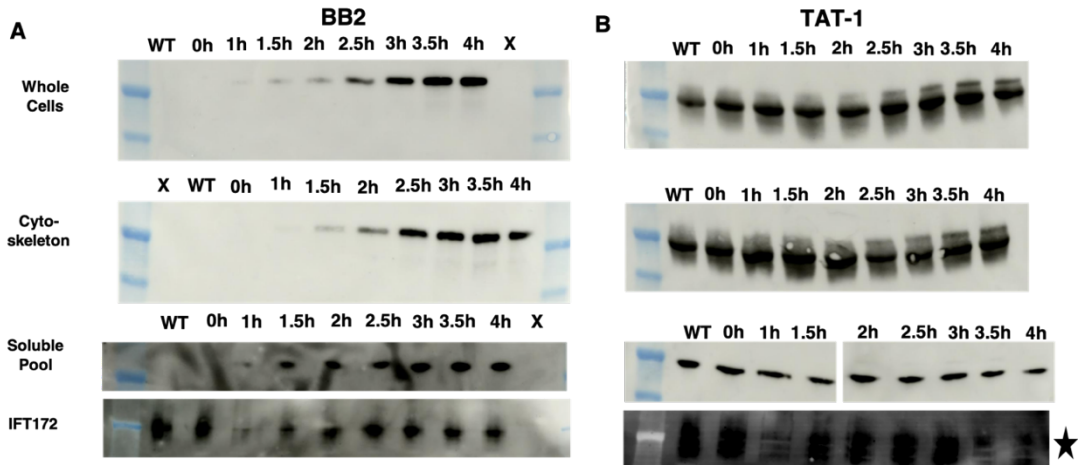

Figure 11 : WBs with extracts of WT cells and cells from the inducible 1xTy1-tubulin cell line that was incubated with tetracycline for 0 – 4 hours at 30 minute-intervals. Two blots are shown per fraction: Left panel: blots that were incubated with the BB2 antibody (tagged tubulin). Right panel: blots that were incubated with the TAT-1 antibody (alpha-tubulin). IFT172 was used as a loading control for the soluble pool. WT=427 WT cell line, 0h=non-induced, X=empty lane. Star: blot was overexposed.

Western blots were performed to assess how long it takes for tagged tubulin to be expressed after the addition of tetracycline. Cells were induced with tetracycline and then harvested after one hour and in thirty-minute intervals thereafter up to a total of four hours. Protein samples of whole cells, cytoskeleton and soluble fraction were then prepared as above. Two gels were run per fraction and then transferred to individual membranes, either incubated with the BB2 antibody that recognizes tagged tubulin (Fig. 11A) or with the TAT-1 antibody, which recognizes alpha-tubulin (Fig. 11B). The intraflagellar transport protein IFT172 was used as a loading control for the soluble fraction.

On the membrane treated with BB2 (Fig. 11A), no signal is visible for the WT cell line as well as the non-induced Ty-1-tubulin cells (0h). Bands then started to appear with increasing intensity during induction time in all three fractions. A very faint band is visible already after one-hour post induction in all three fractions including in the soluble pool. The signal of the soluble pool is weak as expected.

On the blots that were stained with TAT-1 (Fig. 11B) one band per lane is visible for endogenous tubulin as expected. A second band above the untagged tubulin band is detected around 1.5 hours after induction in whole cells and the cytoskeleton fraction. In the soluble fraction, the upper bands are not visible possibly because they were beyond detection limit.

The relative intensity of the Ty-1tubulin band compared to the untagged was quantified and after four hours it had reached a ratio of ~0.31 (~25% of total tubulin).

Ultimately, Ty-1-tubulin is detectable as early as 1 - 1.5h after induction with WBs similar to what is observed by IFA. The level of tagged protein increases to approximately 25% of total alpha-tubulin around 4h. In previous experiments (Fig. 11B) where we calculated the ratio between soluble and cytoskeleton fraction after overnight induction, we also quantified the ratio between untagged and tagged bands and saw that this ratio can go as high as 40% of total alpha-tubulin after an overnight induction.

Incorporation of tagged tubulin can be monitored in 30-minute intervals.

An average cell cycle takes ~9 hours to complete (Ploubidou, et al., 1999; Sherwin and Gull, 1989). Most trypanosomes spend approximately 3h of the cell cycle in a mono-flagellated state. At this stage they start to elongate MTs in the posterior of the cells. The cells then initiate the assembly of a new flagellum which is present for the rest of the cell cycle (6 hours) before the cells divide. Based on the previous WBs, we determined that the expression of tagged tubulin after induction is feasible to track the dynamics of MT assembly by IFA. Cells were induced for maximally four hours in thirty-minute intervals. After every interval, samples were harvested. Whole cells, cytoskeleton and flagella extracts were prepared and the slides stained with BB2 (tagged tubulin), Mab25/α-FTZC (axoneme and transition zone) and DAPI.

From staining with the YL1/2 antibody (tyrosinated, new tubulin) it was known that newly synthesized tubulin is incorporated at the posterior cell tip of the cell body as well as the new flagellum (Fig. 10 introduction, Sherwin and Gull, 1989). Additionally, a study has strengthened this evidence for the cell body but not the flagellum (Sheriff et al., 2014). The authors could show that YFP-tubulin was incorporated first at the posterior cell body after short induction times (Fig. 10 introduction).

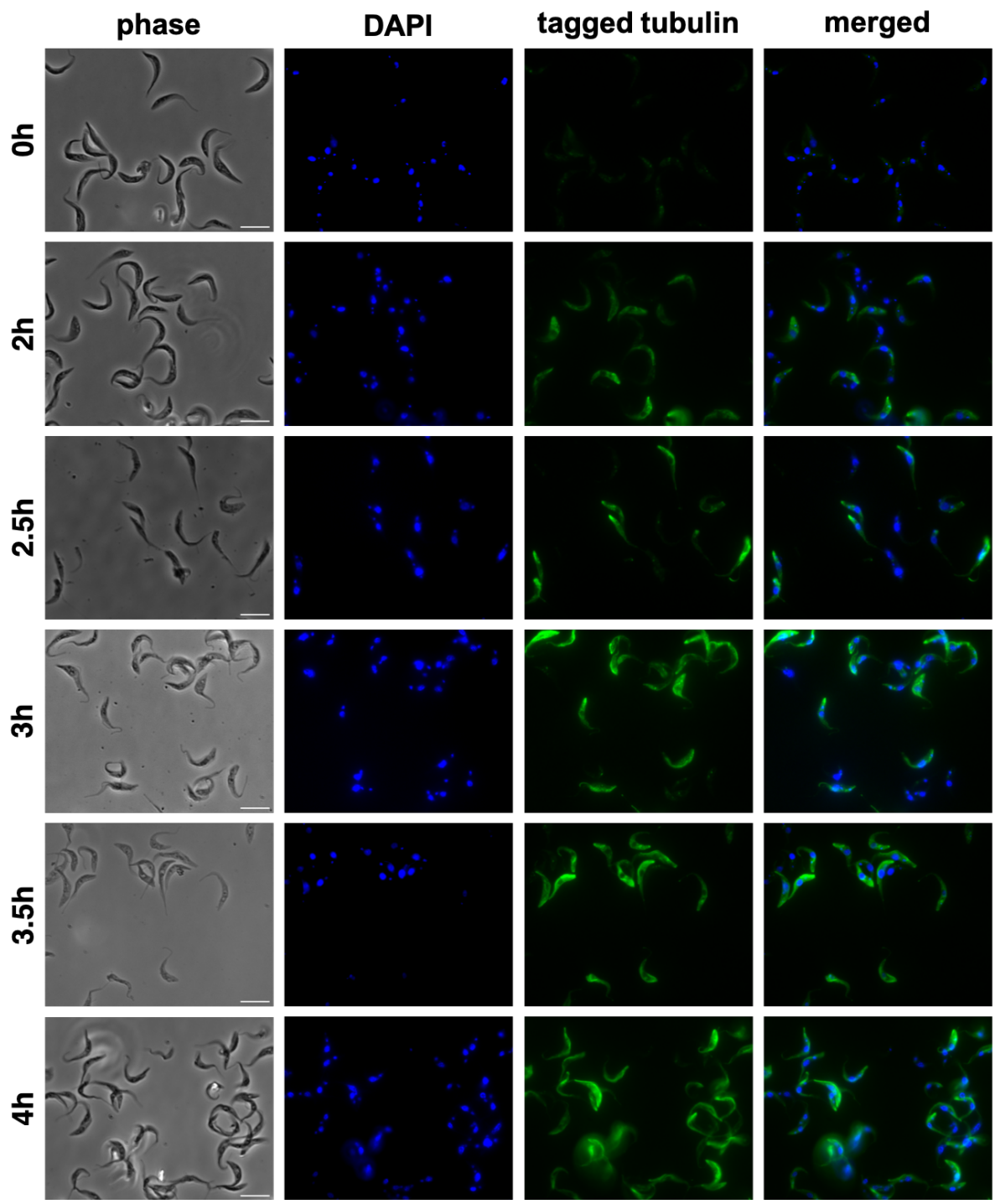

Figure 12 : IFA of whole cells that were incubated with tetracycline for 2 – 4 hours in 30 minute-intervals. Samples were incubated with the BB2 antibody (green, tagged tubulin) and DAPI (DNA).

Fig. 12 shows whole cells where tagged tubulin expression was induced for 2 – 4 hours. The samples were co-stained with BB2 (tagged tubulin) and DAPI. A general trend is observed that the signal intensity increases over time (Fig. 12, tagged tubulin in green). A majority of cells are seen to incorporate tubulin in the posterior cell tip. With increased incubation time, the signal extends towards the anterior. These observations are coherent with what is known from YL1/2 staining and what was reported for inducible expression of YFP-tubulin (Sheriff et al., 2014). The mitotic spindle is visible already as early at 2 - 2.5h. Incorporation in new and old flagella is visible as well, and discussed in more detail in Fig. 14, where the flagella extracts are shown. Occasionally, fully stained cells are observed even in non-induced conditions (<1%), these cells were very rare and discarded from analysis.

4-hour time course with cytoskeletal extracts

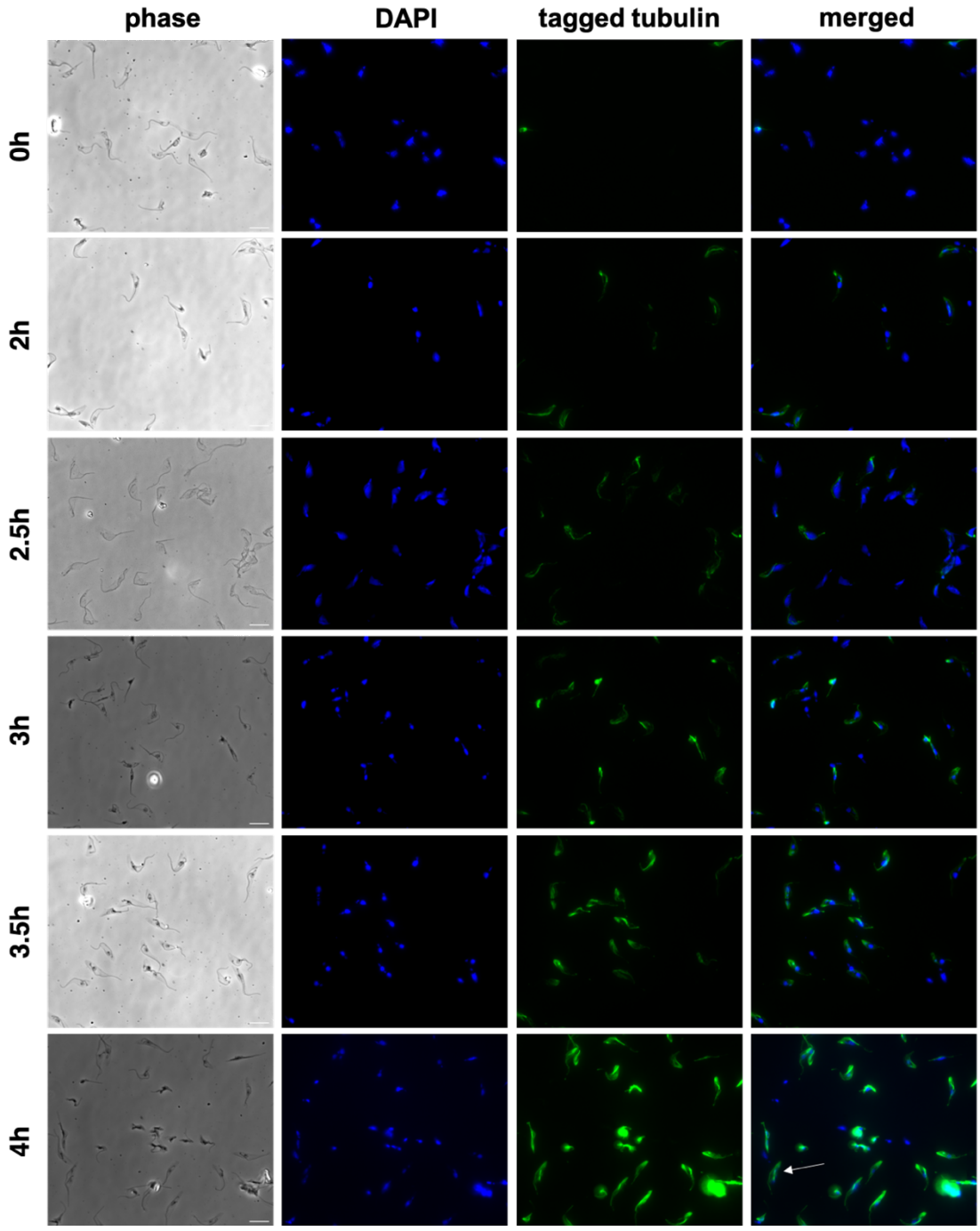

Figure 13 : IFA of detergent-extracted cytoskeletons that were incubated with tetracycline for 2 – 4 hours at 30 minute-intervals. Samples were incubated with the BB2 antibody (green, tagged tubulin) and DAPI (DNA). The white arrow in the 4-hour timepoint indicates a cell that is highlighted in Fig. 15.

The cells used in the experiment described in the previous Fig. 12 also underwent detergent extraction and were stained with BB2 (tagged tubulin) and DAPI. Representative fields are shown in Fig. 13. A similar trend was observed for cytoskeletons when compared to whole cells. Ty-tagged tubulin is first incorporated into MTs at the posterior cell body. The staining then expands towards the anterior of the cell at later timepoints. The stained portion in new flagella gets increasingly longer with prolonged induction, and is sometimes observed along the entire length of the new flagellum. We noted that old flagella of mono and bi-flagellated cells have integrated tubulin at the tip but have never incorporated tubulin across their entire length. Although the MTs of the mitotic spindle are sometimes regarded as less resistant to detergent extraction, this structure could be observed in cytoskeleton extracts. To summarise the time course experiments with whole cells and cytoskeletons, a zoom in of a representative cell is shown in Fig. 14. The zoomed in cell is highlighted with a white arrow in Fig. 13, in the tagged tubulin panel at 4h. This cell (Fig. 14) has two nuclei (✣), two kinetoplasts (✷), and both the old (white arrows, OF) and new (white arrows, NF) flagellum as well as the mitotic spindle (★). Tagged tubulin (green) is clearly incorporated at the posterior but not the anterior part of the cell body as well as in the new but not the old flagellum. Due to the overlap of new flagella and the MT of the subpellicular array it is sometimes difficult to determine if the new flagellum incorporated tagged tubulin along its entire length. We therefore decided to track axoneme assembly in high salt extracted flagella.

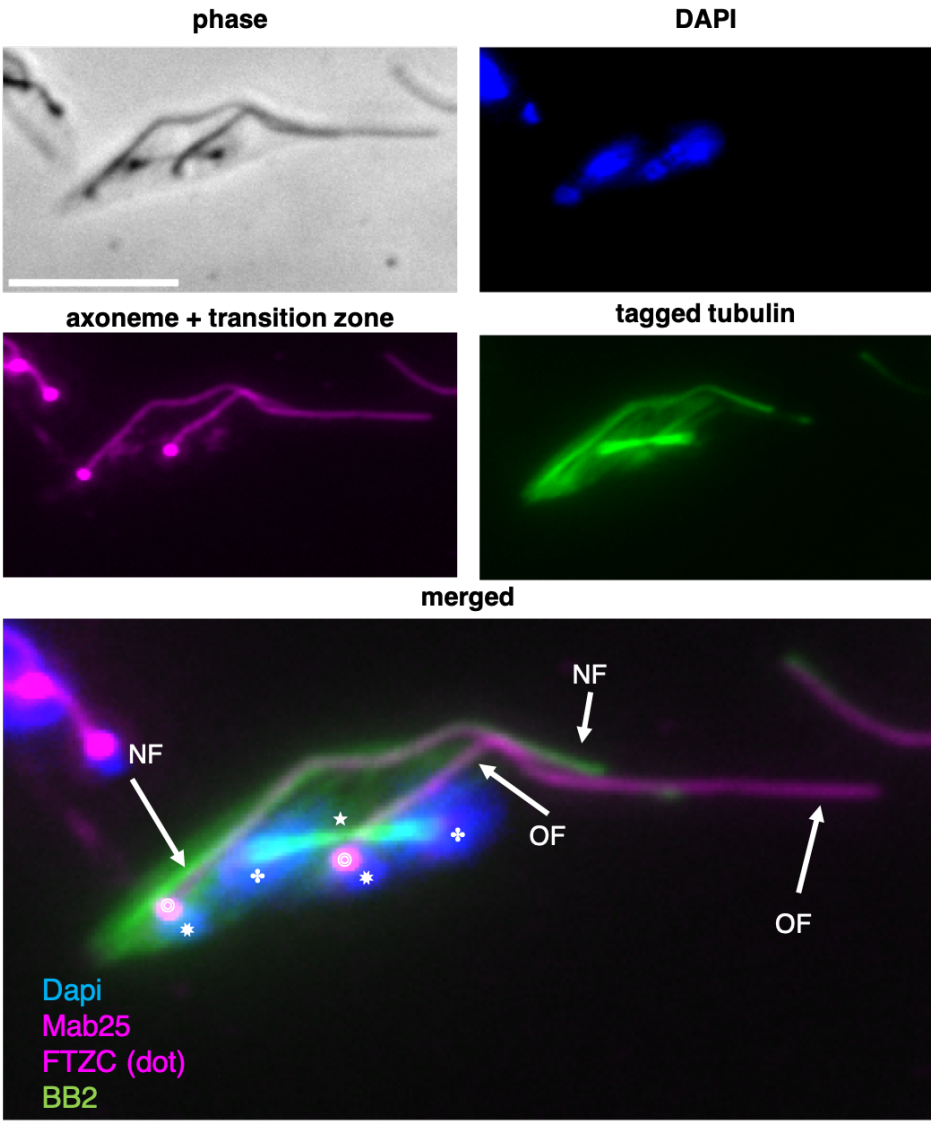

Figure 14: Zoom-in of a single detergent-extracted cell in 2K2N2F stage (zoom-in of Fig. 13, white arrow, tagged tubulin panel) 4 hours after the addition of tetracycyline from the experiment described in Fig. 13. Samples were incubated with the BB2 antibody (green, tagged tubulin), Mab25 (magenta, axoneme) and (anti-FTZC, magenta (dot)). ✷=kinetoplast, ◎=transition zone, ✤=nucleus, ★=mitotic spindle.

4-hour time course with flagella extracts

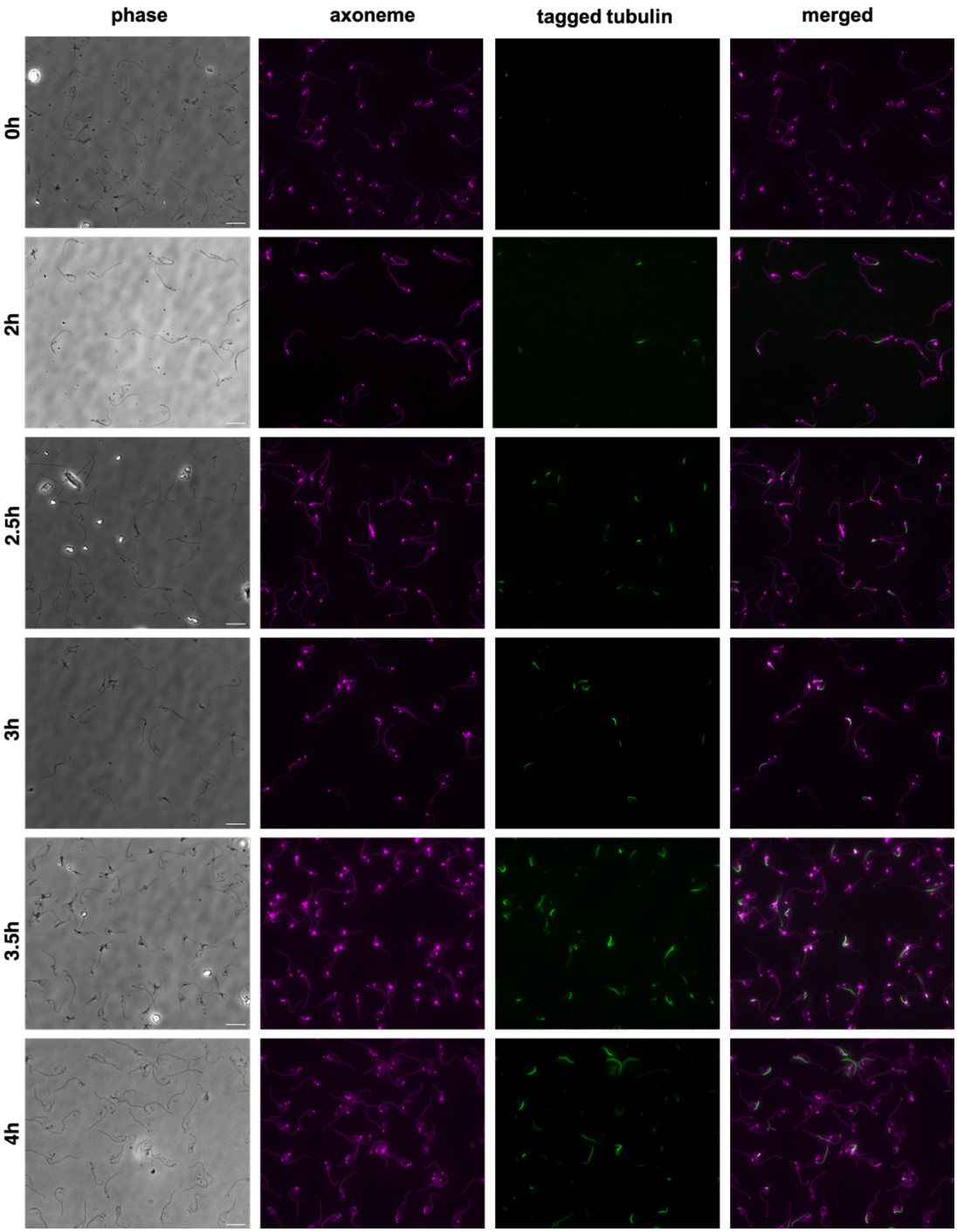

Figure 15 : IFA of high salt extracted flagella that were incubated with tetracycline for 2 – 4 hours in 30 minute-intervals. Samples were incubated with the BB2 antibody (green, tagged tubulin), Mab25 (magenta, axoneme) and (magenta (dot), anti-FTZC).

In previous experiments, we noticed that observing the incorporation of Ty-1-tubulin into MTs of the axoneme is easiest in high salt extracted flagella (Fig. 9B). We therefore analyzed these extracts in more detail to visualize how tagged tubulin is assembled into the flagellum. Fig. 15 shows six panels with extracted flagella stained with BB2 (tagged tubulin), Mab25 (axoneme) and α-FTZC (transition zone) (Bringaud et al., 2000). The new flagellum is attached to the old one via a dedicated structure called flagellar connector (Briggs et al., 2004; Davidge et al., 2006). This structure is resistant to high salt treatment and still present in flagella extracts. Since the connection between NF and OF resolves before cell division (Davidge et al., 2006; Varga et al., 2017), it is possible that the connector in cells with very long new flagella is less stable than in the ones with shorter new flagella. This trend was observed in some extracts, where relatively longer new flagella tended to detach a bit more. Sometimes, new flagella were observed isolated even when they were not fully elongated. For coherent analysis, we focused measurements and interpretation on cells in which the new flagellum was clearly connected to the old one (bi-flagellated cells).

Based on the observations made in Fig. 9, 13 and 14 we expected to find tagged tubulin in high salt extracted flagella. Indeed, tagged tubulin is incorporated in the axoneme as early as 2 hours post induction (Fig. 15, tagged tubulin at 2h). A clear tendency was noted, that the length of the flagellum where tagged tubulin is incorporated increases after every thirty minutes of induction. To simplify, we called the part of the flagellum that was stained by the BB2 antibody the “green portion”. After two hours, the green portion can be easily observed, predominantly in new flagella. At earlier timepoints the green portion is mainly observed in the distal region of the new flagellum. Based on the unstained portion at the distal region, these flagella most likely started assembly of the new flagellum before induction in the absence of tagged tubulin. This means that new tubulin is indeed incorporated at the tip of growing flagella. The only fully green flagella that were observed were short new ones. Over time the number of fully stained new flagella increases and longer green flagella are present. During the first three hours of induction, incorporation of tagged tubulin as also observed in flagella mono-

flagellated cells but very rarely in OF. Lastly, the range of the green portion's length became more heterogenous at later timepoints. In summary, Ty-tagged tubulin is incorporated into high-salt extracted axonemes of predominantly new flagella as short as 2 hours after expression was induced. The green portion is more present in new flagella and its length increased over the time course. In cells where NF assembly has started before induction, new tubulin building blocks are added at the flagellar tip. In theory, these partially green new flagella were elongating during the entire induction, therefore we chose to measure the assembly rate with this type of flagella.

Assembly rate of the axoneme is linear

The assembly rate of the flagellum has previously been estimated by monitoring inducible expression of a PFR component. According to these experiments, the growth rate was linear at a speed of ~3.6 μm per hour (Bastin et al., 1999). The PFR is attached to the axoneme only after it leaves the flagellar pocket, and its assembly is therefore delayed. To get an estimate on how fast the axoneme itself is assembled, we measured the length the portion that had integrated tagged tubulin after induction. For greater accuracy, the estimate of the assembly rate was measured with new flagella that had a proximal portion where only untagged tubulin had integrated and a distal portion where tagged tubulin was present. These flagella had emerged before tetracycline was added and must have been in the assembly process during the entire induction, as they were still a NF attached to an OF when harvested for IFA. For fully green NF the estimate would have been less accurate as it is not possible to tell how much time they spent in G1-phase during induction, before assembly of a NF.

Cells were induced for 2 to 4 hours at 30-minute intervals. Flagella from each timepoint were extracted and stained with the antibodies BB2 (tagged tubulin), anti-FTZC (transition zone) and Mab25 (axoneme). Merged images were then analyzed and the green portion in the BB2 channel was measured in ImageJ.

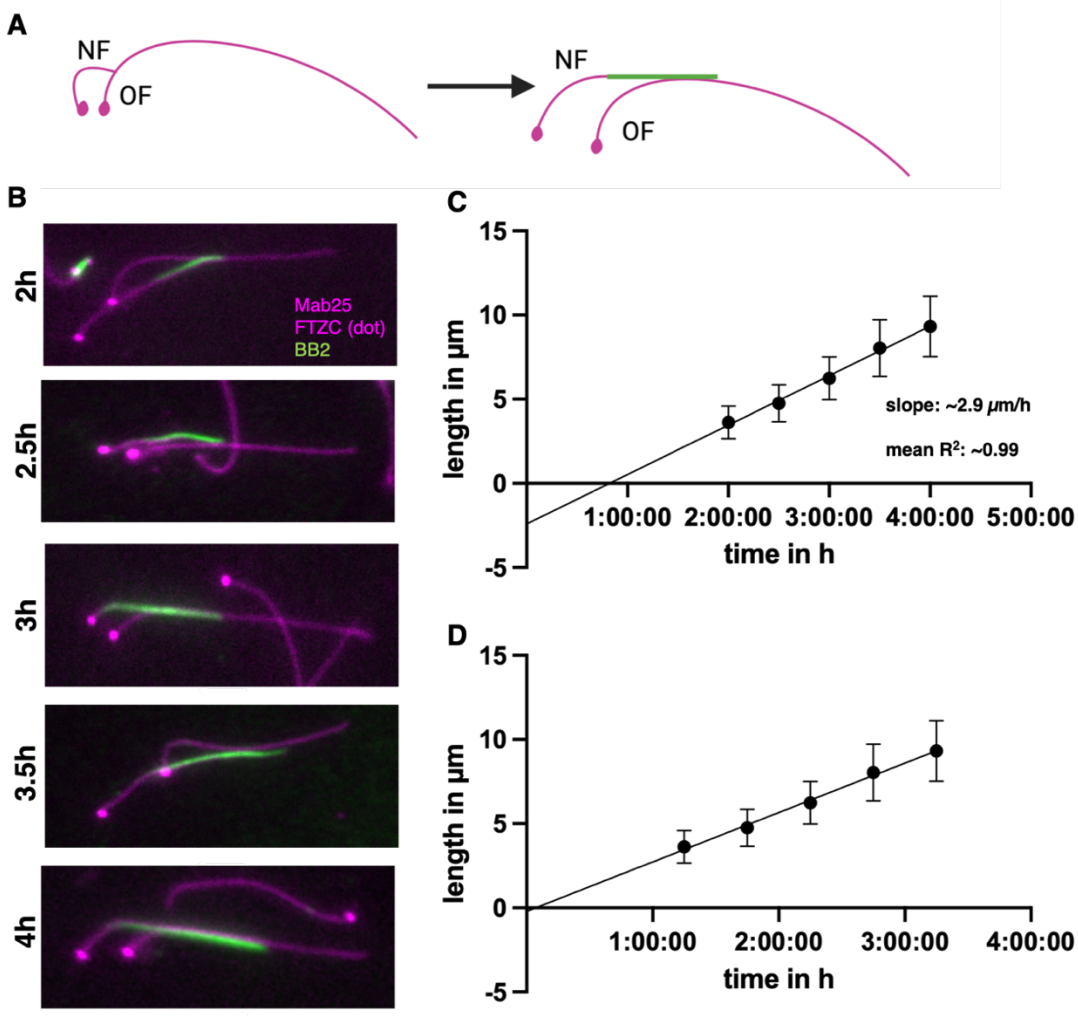

Figure 16 : A: The figure indicates that this flagellum had already started assembly at the time of induction. The second cartoon shows a bi-flagellated cell with a partially green new flagellum. The length of new flagella was measured to assess the assembly rate of the axoneme. B: IFA of high salt extracted flagella from cells that were incubated with tetracycline for 2 – 4 hours at 30 minute-intervals. Samples were incubated with the BB2 antibody (green, tagged tubulin), Mab25 (magenta, axoneme) and anti-FTZC (magenta (dot). Images show a example of partially green new flagella at various time points. C: Measurements of the green portion these flagella. Data of three independent experiments were pooled for each timepoint. Means of the length measurements with standard deviations are shown for each 30-minute-timepoint. Simple linear regression of the mean was performed with Prism V10. D: Timescale was (X-axis) corrected by subtracting the estimated time that the cells need to respond to tetracycline before expression of protein (~45 min) from each timepoint. Example: 2h – 45min = 1.25h.

In three independent experiments, roughly a hundred partially green new flagella were measured per timepoint and experiment (~1500 flagella in total). As noted in previous experiments the green portion increased in length over longer periods of induction, indicating that this approach was valid to measure the assembly rate. For each timepoint, the length measurements from the three individual experiments were pooled and plotted against time (Fig. 16B).

The average length of the green portion for the timepoints are 2h: ~3.6 μm (± 1), 2.5h: ~4.8 μm (± 1), 3h: ~6.2 μm (± 1.3), 3.5h: ~8.0 μm (± 1.7), 4h: ~9.3 μm (± 1.8). A simple linear regression analysis of the means was performed and revealed a slope of 2.9 μm/hour with a mean R^2 of 0.99. When the regression line was forced through Y=0 it intersects the time-axis at ~0.83 hours (50 min). This is most likely the average time it takes a cell to respond to the presence of tetracycline with protein expression. Response rates to tetracycline of 0.5 – 1hour have been reported regularly (Bastin et al., 1999; Wirtz and Clayton, 1995). Fig. 16C shows an adjusted curve where 45 minutes was subtracted from every timepoint to correct for the tetracycline response time. The regression line then intersects close to the (0/0) point of the axis.

We concluded that Ty-1-tubulin is incorporated at the distal tip of the axoneme at a linear rate of 2.9 μm per hour, similar to what is observed for the PFR (3.6 μm/h) (Bastin et al., 1999).

Integration of tagged tubulin in bi-flagellated cells follows the grow and lock model

Next, we were curious if tagged tubulin is incorporated in a way that is coherent with the locking model by focusing on new and old flagella in bi-flagellated cells. The grow-and-lock model describes how old flagella are locked after they are constructed to full length, which prevents them from extending in length or shortening any further (Bertiaux et al., 2018). According to this model, old flagella of bi-flagellated cells should therefore not incorporate tagged tubulin because they are locked. Fig. 17A shows a model of how incorporation could take place in new as well as old flagella. On the top is the case of a new flagellum that did not start assembly before induction (Fig. 17 Type 1). It therefore constructed its new flagellum exclusively in the presence of tagged tubulin (Fig.17A top). Based on that, it is expected to incorporate tagged tubulin along the entire length. For old flagella we were curious if they also incorporate tagged tubulin at the distal tip (Fig. 17 A, type 1a) or not (Fig. 17A, type 1b case of the grow and lock model). For a cell in which assembly of the new flagellum had started before induction when only untagged tubulin was available (Fig. 17A, type 2) two scenarios are possible. Type 2 a shows a cell where both flagella are partially green, if tagged tubulin integrates at the same time into the new and the old flagellum. Type 2a shows a cell that had started assembly before induction and is now incorporating tagged tubulin at the distal end of the new flagellum but not the old one.

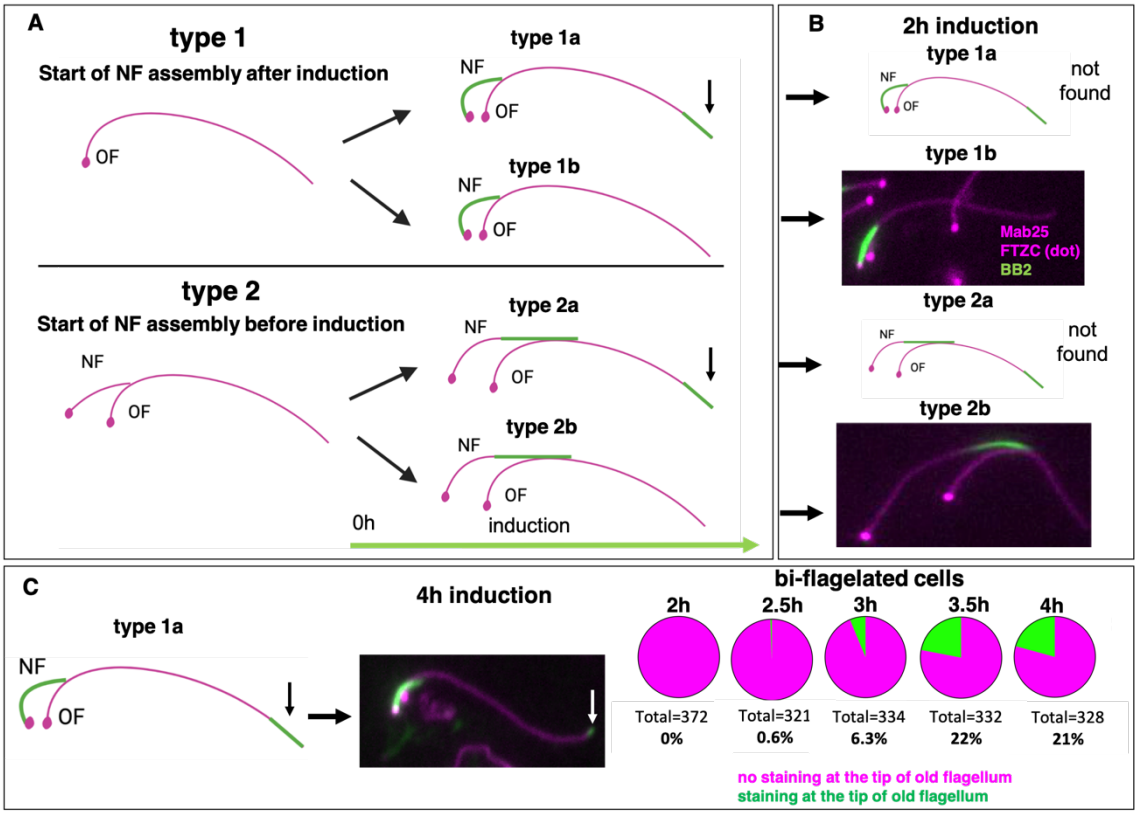

Figure 17: A: A model depicting how tubulin could be incorporated into the new flagellum and potentially in the old flagellum. Type 1: NF has emerged after induction. Incorporation is expected along the entire length of the new flagella in cells where assembly had started after expression of tagged tubulin was induced. The arrows indicate integration at the tip of old flagella. Type 1a: Both new and old flagellum incorporated tagged tubulin. Type 1b: Only the new flagellum incorporates tubulin (case of the grow and lock model). Type 2: NF has emerged before induction. Type 2a: Simultaneous integration into new and old flagella. Type 2b: Incorporation only into the new flagellum. B: Representative images from an IFA of high salt extracted flagella from cells that were incubated with tetracycline for 2 hours. Samples were incubated with the BB2 antibody (green, tagged tubulin), Mab25 (magenta, axoneme) and (magenta (dot), anti-FTZC). In bi-flagellated cells, incorporation of tagged tubulin was only observed in the new but not the old flagellum after 2 hours of induction. C: Representative image of a bi-flagellated type that was only found at later timepoints. It represents the cells described in type 1a flagella. The Pie-charts indicate the proportion of these cells among all bi-flagellated cells that had incorporated tagged tubulin along the entire length of the new flagellum. In green are the cells that had also incorporated tagged tubulin at the tip of old flagella. Type 2a (partially green new and old flagellum) was never observed.

Old axonemes are locked in bi-flagellated cells

To test if tagged tubulin incorporates in accordance with the grow and lock model, we analyzed in which flagella the green portion was present after expression of tagged tubulin was induced. Three independent experiments of 4-hour time courses were performed. 15-20 fields per 30-minute interval were acquired and merges of BB2 (tagged tubulin), anti-FTZC (transition zone) and Mab25 (axoneme) were analyzed.

We scored how many old flagella of bi-flagellated cells had incorporated tubulin in the individual timepoints. To exclude cells that did not respond to tetracycline induction, only cells in which the new flagellum had incorporated tagged tubulin were scored for the presence of green staining in the old flagellum.

Two main observations were made during these experiments: First, it was noticed that Ty-1-tubulin is incorporated along the entire length of relatively short new flagella (Fig. 17A+B type 1, Fig. 17C, type 1a) and at the distal portion of relatively long new flagella (Fig. 17A type 2b). This further confirms that new tubulin building blocks are indeed added at the distal tip.

Second, since untagged tubulin is always available, assembly of partially green new flagella must have started before the addition of tetracycline. Only simultaneous integration into new and old flagella, would allow both flagella to be partially green. At none of the five timepoints was a cell observed that has a partially green new flagellum and a partially green old flagellum (Fig. 17A+B type 2b). We did however observe cells with short fully green new flagella that had a green portion at the tip of the old flagellum as well (Fig. 17C). The proportion of these cells among all bi-flagellated cells was scored. Two hours after induction we could not find a single cell with this pattern. Over time however, it increased to ~20% of the bi-flagellated cell population (Fig. 17C).

These were possibly cells that finished construction of the old flagellum after expression of tagged tubulin was induced. During the induction, these cells then went through the G1-phase and started to assemble a new flagellum. Unless assembly of new and old flagella was

simultaneous, this could only happen at later timepoints. Coherently, new flagella of cells with this pattern were very short and therefore have not been in construction for very long.

To sum up, after expression was induced, tagged tubulin had incorporated at the tip of the axoneme in predominantly new flagella. Incorporation into old flagella was only observed when the new flagellum was fully green. These cells became more common with time.

Cells commit to locking their flagella before cell division

We previously proposed that old flagella are locked after they are constructed to full length (Bertiaux et al., 2018). This lock would prevent them from elongating further and cells commit to the underlying mechanism before cell division is concluded. To prove this, cell division was blocked and the length of old and new flagella measured. Trypanosome cell division can be prohibited by treatment with teniposide, a drug that prevents the kinetoplast from segregating. Under these conditions cell division is inhibited as well (described in introduction) (Robinson & Gull, 1991).

In untreated cells, the new flagellum grows to ~80% of the old flagellums length before the cells divide. However, when cells were treated with teniposide, the new flagellum grows to ~100% of the length of old flagella but does not extend any further. The circumstance that they did not extend beyond the old flagellum's length, supported the fact that they committed to locking the new flagellum before cell division. However, one could consider that the new flagellum is assembled as proposed by the balance-point model and, therefore is subject to constant turnover.

Naturally, we wanted to test if the experiments that determined the timing of the locking event could be reproduced with the inducible system. An experiment was set up in which cells were treated with teniposide for 15 hours. At this point, both flagella should be constructed to full length. If cells indeed commit to locking their flagella before cell division both flagella should be locked as well. Therefore, after 15 hours of teniposide treatment a culture is expected to only contain locked flagella while an untreated culture is a mixture of old and new flagella. When tetracycline is then added to teniposide treated cells to induce the expression of tagged tubulin, no incorporation of tagged tubulin is expected. After 6 hours of induction, trypanosomes were harvested and subjected to detergent extraction. Cytoskeleton extracts were used to test if the cells were still able to express and incorporate tagged tubulin into the subpellicular MTs of the cell body after teniposide treatment. As a control, a regular 6-hour

induction without teniposide was performed. The samples were stained with the antibodies BB2 (tagged tubulin), anti-FTZC (transition zone) and Mab25 (axoneme).

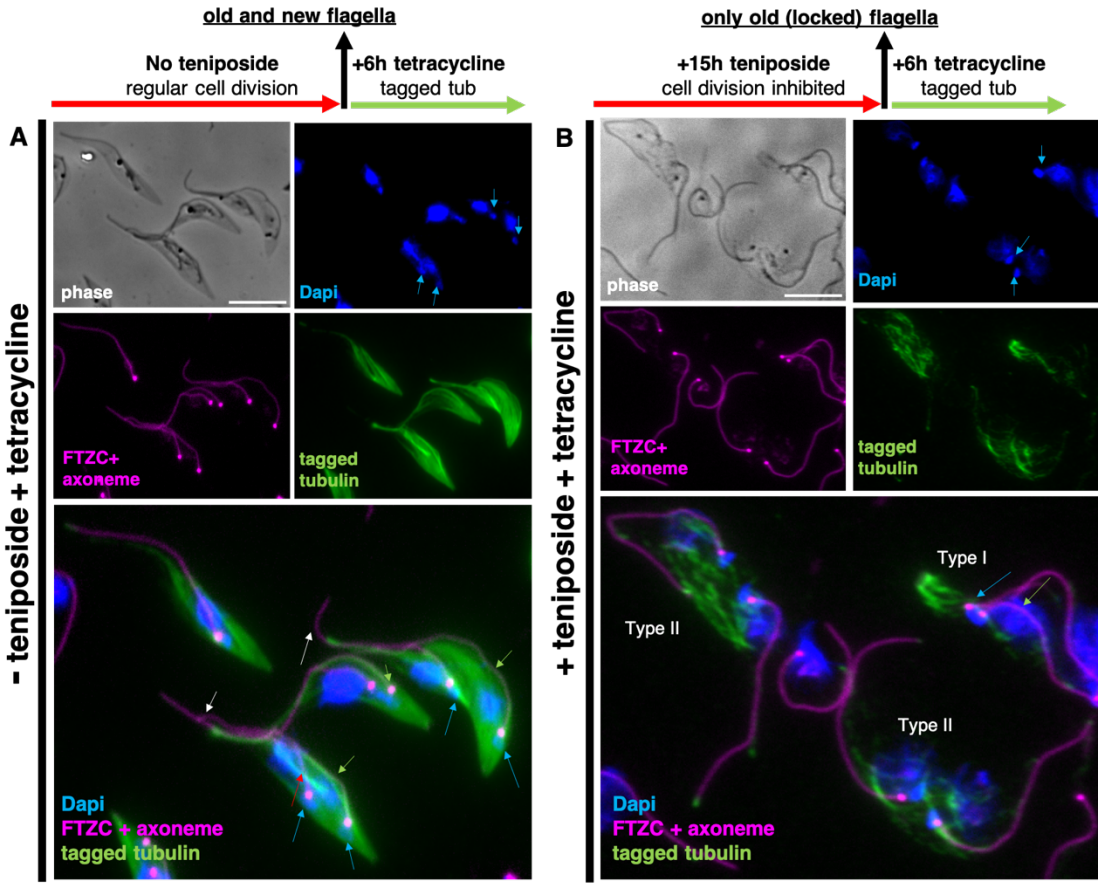

Figure 18 : IFA with detergent extracted cytoskeletons of Ty-1-tubulin cells in which Ty-1-tubulin expression was induced for 6 hours with tetracycline. A: Detergent extracted cells that were not treated with teniposide, Incorporation of tagged tubulin is seen in the cell body as well as in NF but not OF. B: Detergent extracted cells that were treated with teniposide for 15 hours ahead of tetracycline induction. Incorporation of tagged tubulin is seen in the cell body but no elongated portion with the presence of tagged tubulin was seen in the flagellum. Samples were stained with BB2 (green, tagged tubulin), Mab25 (magenta, axoneme), anti-FTZC (magenta (dot), transition zone) and DAPI (blue, DNA).

Fig. 18A shows cytoskeleton extracts of cells where tagged tubulin expression was induced for 6 hours that were not treated with teniposide and could still divide normally. Two 2K2N2F cells are visible, the nucleus has divided and the kinetoplasts (indicated by blue arrows) are posterior to their respective nucleus as expected. Tagged tubulin was incorporated into the MTs of the posterior part of the cell body as well as the mitotic spindle (red arrow). The new flagella can be distinguished emerging clearly posterior to the old ones as it is reported in the literature. Additionally, the new flagellum is still connected by its tip to the old axoneme as visible in the FTZC/axoneme channel (Fig. 18A). New flagella of the three bi-flagellated cells are fully green (green arrows). Meanwhile staining is absent in the old flagella (white arrows), coherent with the grow and lock model. All observations are in line with what was previously described for integration of tagged tubulin post tetracycline induction.

The cells visible in the right panel (Fig. 18B) were treated with teniposide for 15 hours and then induced with tetracycline for 6 hours, before being extracted with detergent and stained with the same antibodies mentioned above.

In this experiment, two main types of bi-flagellated cells could be distinguished. First, cells like the one seen on the top right (called Type I). The kinetoplasts are still connected despite the new flagellum being very long and the two nuclei being separated. Here the new flagellum can be clearly distinguished from the old one by its anterior position (Fig. 18B).

In the second type, represented by the other two cells (Type II), the kinetoplasts are (at least visibly) segregated, however, their positioning implied that the cells were unable to complete division. The two flagella were no longer connected and had approximately the same length. This made it virtually impossible to distinguish which one is the new and which one is the old flagellum.

In most teniposide-treated cells, we observed tagged tubulin in the cell body, although notably less when compared to untreated cells. It is conceivable that cells that are stuck before cell division do not produce and integrate as much tubulin since they cannot divide and give rise to new cytoskeletal material needed for new daughter cells. Nonetheless, they were still

capable of producing tagged tubulin and able to incorporate it into MTs of the subpellicular array to a certain extent.

On the other hand, integration into the flagellum was absent apart from a tiny portion at the very tip where little tagged tubulin had integrated. It was noticed that this green portion was present in old and new flagella and in many cases extended beyond the Mab25 co-staining.

However, notable extension of several μms or fully stained flagella, as present in untreated cells after a 6-hour induction, was never observed after teniposide treatment.

To conclude, cells that were treated with teniposide before tetracycline induction did not extend neither their old flagella nor their new flagella with tagged tubulin by lengths characteristic for a 6-hour induction.

Flagella extracts of teniposide treated cells

The teniposide experiments described in the previous section were then repeated with high salt extracted flagella. Samples were stained with BB2 (tagged tubulin) and Mab25 (axoneme) (Fig. 19).

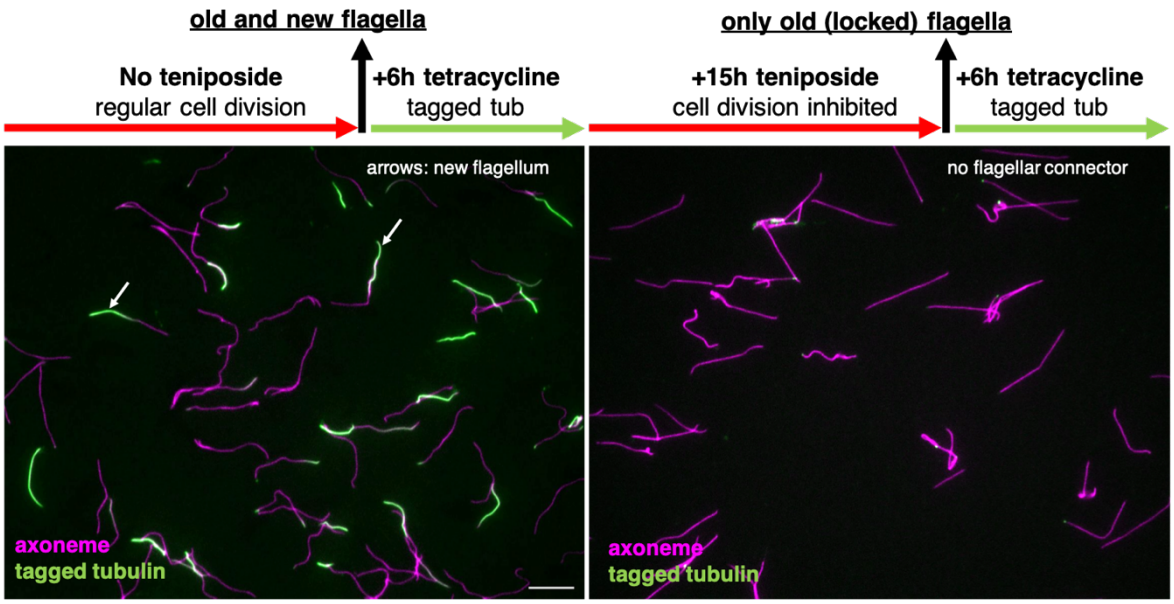

Figure 19 : Top panel: IFA with detergent extracted cytoskeletons of Ty-1-tubulin cells in which Ty-1-tubulin expression was induced for 6 hours with tetracycline. Cell in the left panel were not treated with teniposide, the cells in the right panel were treated with teniposide for 15 hours ahead of tetracycline induction. Samples were stained with BB2 (green, tagged tubulin), Mab25 (magenta, axoneme), anti-FTZC (magenta (dot), transition zone) and DAPI (blue, DNA). Lower panel: IFA with high salt extracted flagella of Ty-1-tubulin cells in which Ty-1-tubulin expression was induced for 6 hours with tetracycline. Samples were stained with BB2 (green, tagged tubulin), Mab25 (magenta, axoneme). White arrows in the left panel indicate integration of tagged tubulin into new flagella in the left panel. In the right panel the flagella are not connected via FC anymore.

The two pictures show flagella extracts of cells where tagged tubulin expression was induced for 6 hours. Flagella on the left belonged to cells not treated with teniposide. New flagella have integrated tubulin and are attached to the old flagellum at their tip via the flagellar connector. Cells on the right were treated with teniposide for 15 hours before the addition of tetracycline. Flagella were no longer connected to each other due to the absence of the connector, which resolves ahead of cytokinesis further indicating that cell division was indeed blocked in these cells. Integration of tagged tubulin is not observed apart from a very small portion at the tip, exactly as seen in cytoskeleton extracts (Fig. 18A, Fig. 19 top panel). In summary, the lack of tagged tubulin incorporation can be observed easily when comparing flagella that were treated with teniposide before induction (Fig. 19, lower panel).

Longer induction reveals novel aspects of assembly in old flagella

Taken together, the above experiments further demonstrate that the incorporation of recently assembled tagged tubulin after induction follows patterns that are consistent with the grow and lock model. We could show that integration is happening only in the new flagellum in bi-flagellated cells and happens at a linear rate. Additionally, there was no extension in cells where cell division was arrested, which verified that cells commit to locking their flagella before cell division. Next, we wanted to dissect the timing of flagellar assembly over the duration of a whole cell cycle. Therefore, cells were induced for 9 hours (one cell cycle) and then harvested for IFA. Slides with whole cells, cytoskeleton extracts and flagellar extracts were performed and stained with BB2 (tagged tubulin), α-FTZC (transition zone), Mab25 (axoneme) and DAPI (DNA). It is important to keep in mind that trypanosomes divide asynchronously.

Assembly of old and new flagellum is sequential and not simultaneous

First, we wanted to evaluate flagella assembly dynamics over an entire cell cycle. We noticed that with longer induction times resulted in the presence of bi-flagellated cells, that had integrated tagged tubulin at the tip of both flagella. We thought this to be the consequence of cells that finished assembly of their flagellum after the addition of tetracycline, then passed the mono-flagellated state and started the assembly of a new flagellum. This hypothesis was strengthened by the fact that in short inductions, old flagella never had integration at the tip.

Cells after 9 hours must have passed one entire cycle and therefore went through at least one G1-phase. New flagella at the start of the 9-hour induction would therefore turn into old flagella at the end of induction. Coherently, integration of tagged tubulin was expected in both new and old flagella of some bi-flagellated cells. According to our model the new flagellum should finish its construction, then gets locked and turns into an old flagellum.

In these experiments, we took advantage that these new OF ("1st-generation-old flagella") could be traced easily, hence providing a great temporal marker. Old flagella that were only

partially green, must have started assembly before induction (unstained portion in magenta) but finished assembly during the induction.

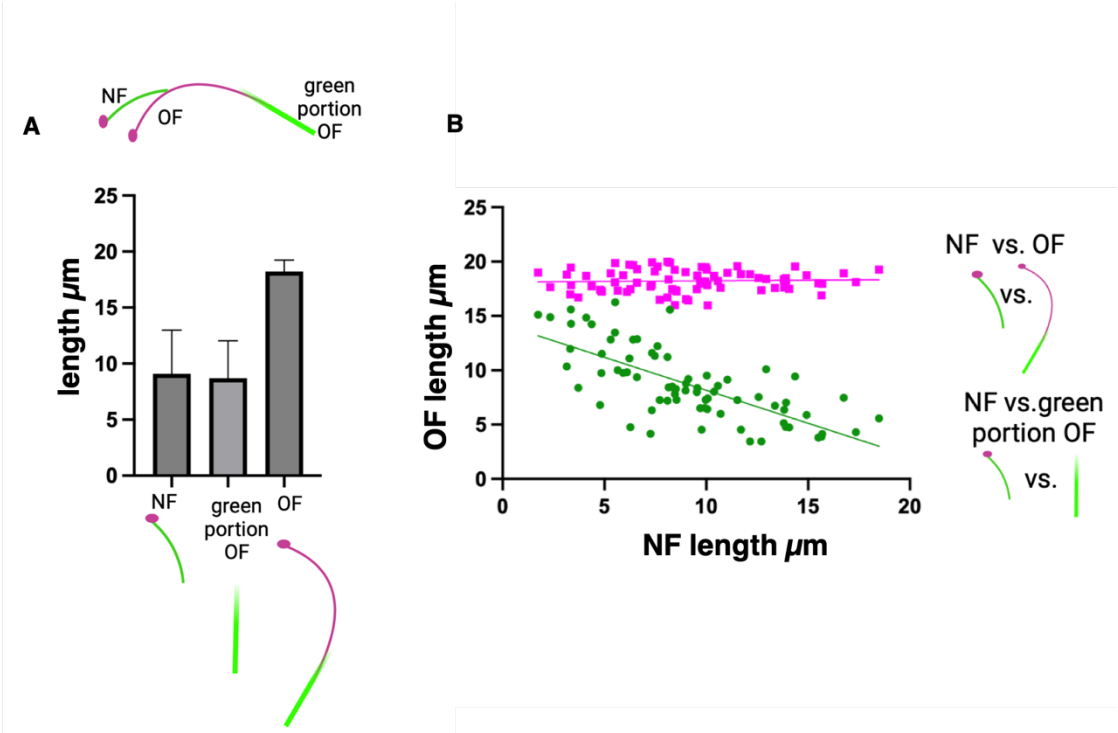

Figure 20 : Measurements from bi-flagellated cells with a partially green old and a fully green new flagella. When induction started the OF was a new flagellum that emerged before induction but was finished during induction (untagged proximal, tagged distal portion). It is therefore a "new" OF (or 1st generation OF). Length measurements of different portions of flagella: NF: Length of fully green new flagella in bi-flagellated cells. green portion OF: is the length of only the green distal portion of partially green old flagella in bi-flagellated cells, OF: is the entire length of the partially green mature flagella in bi-flagellated cells including the proximal untagged part. Left panel shows the average measurements of the individual portions. Right panel: Green dots: Each dot represents length of fully green new flagella (NF, X) plotted against the length of the green portion of partially green mature flagella (green portion OF, Y) from the same cell. The negative correlation indicates that new OF (partially green) were finished before the NF emerged in the same cell. Magenta dots: Each dot represents Length of fully green new flagella (NF, X) plotted against the full length of partially green mature flagella (OF, Y) from the same cell. This indicates that total length of new OF does not correlate with the length of the NF.

First, we focused on the 1st-generation old flagella in the bi-flagellated state and measured their entire length, the length of the green portion and the length of the new flagellum (Fig 20A.) If assembly of new and old flagella was indeed sequential and did not happen at the same time a trend was expected between the length of the green portion in the old flagellum and the length of the green new flagellum.

In Fig. 20B (green dots) a clear negative correlation is visible between the length of the new flagellum and the length of the green portion of the old flagellum. A correlation between the entire length of the old flagellum and the new flagellum is not observed (Fig 23B, magenta dots). These findings further strengthen the validity of the grow and lock model.

Three different kinds of old flagella?

In previous sections, we mentioned the presence of 1st-generation old flagella. These could be clearly distinguished because they were only partially stained and assembly had therefore started before Ty-1-tubulin expression was induced. This means we can address the long-standing question of when the elongation of new flagella finishes after cell division. We decided to measure the length of these first-generation old flagella in the bi-flagellated state to determine if they reached full length before the assembly of a new flagellum had started.

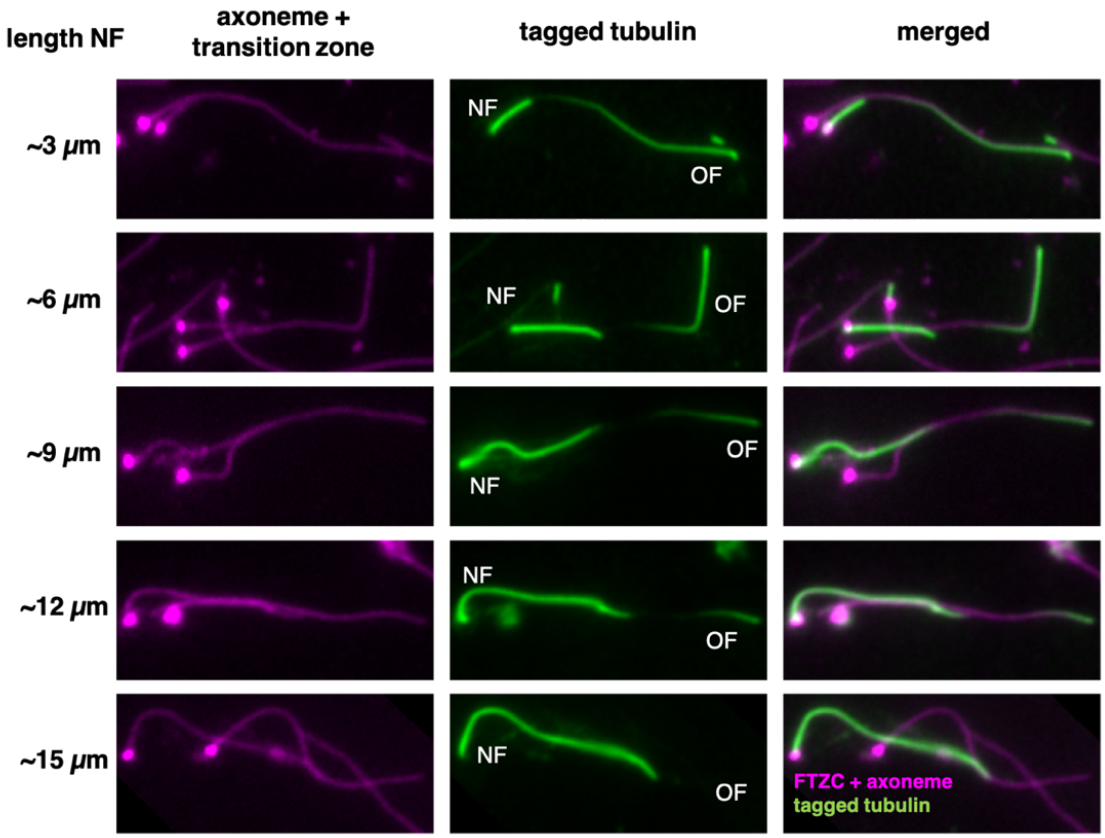

Figure 21： IFA of high salt extracted flagella from cells that were incubated with tetracycline for 9 hours. Samples were incubated with the BB2 antibody (green, tagged tubulin), Mab25 (magenta, axoneme) and (magenta (dot), anti-FTZC). Panels are sorted from top to bottom by the descending length of the new flagellum.

In Fig. 21, five examples of these partially green old flagella are shown, ordered by the length of the associated new flagellum. As described above, the length of the green portion in the old flagellum correlated negatively with the length of the new flagellum (Fig 20B, green dots). When we observed the green portion in the old flagellum, we also noticed that there was a clear gradient in which the signal intensity increased towards the flagellum tip (Fig. 22, type 3). This could be easily explained by the proportion of tagged tubulin vs. untagged tubulin, which increases in favor of tagged tubulin with longer induction time. To determine if these old flagella had reached their maximum length, we measured them and compared them to the other types of old flagella that were present.

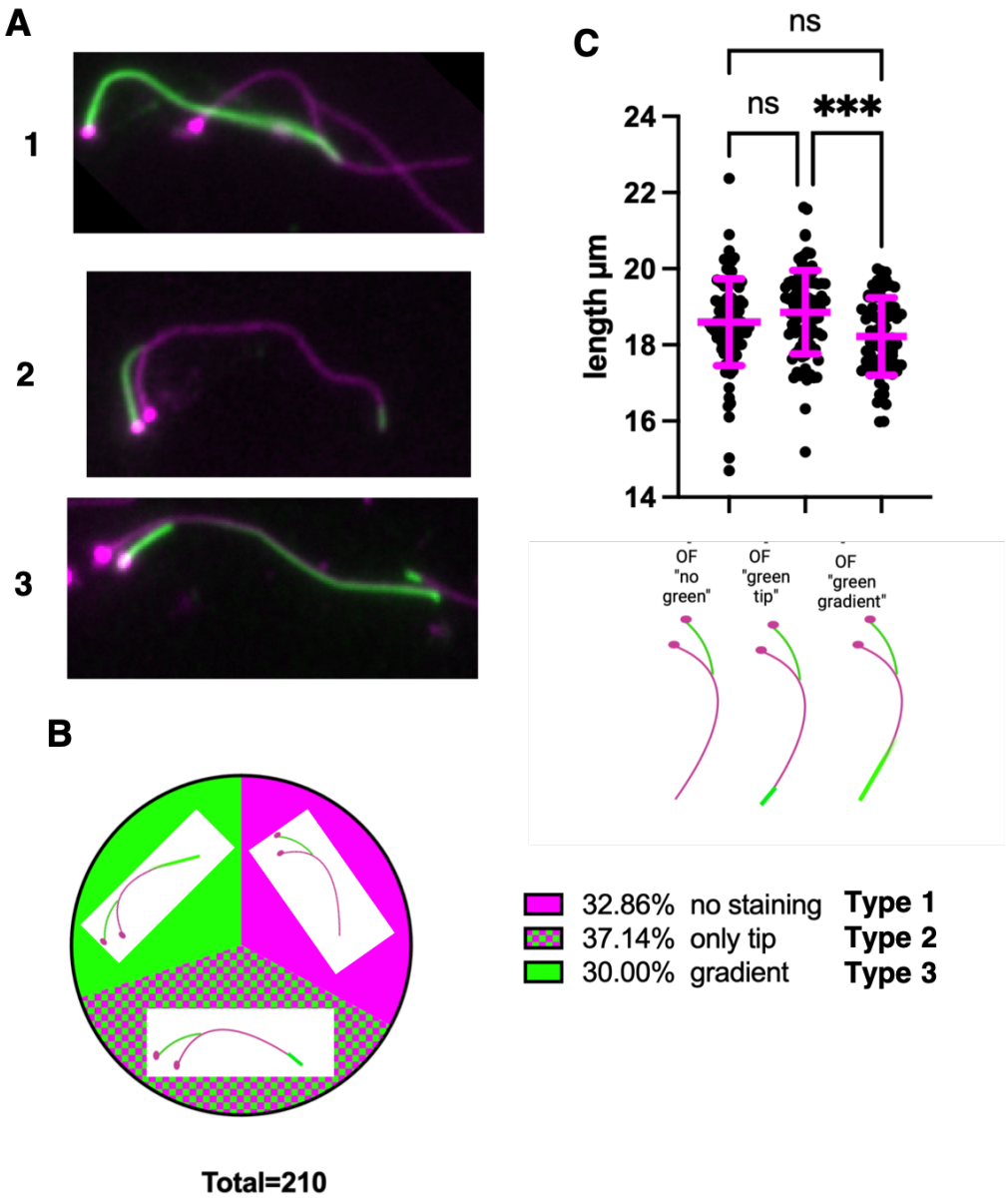

Figure 22 : A: IFA of high salt extracted flagella from cells that were incubated with tetracycline in for 9 hours. Samples were incubated with the BB2 antibody (green, tagged tubulin), Mab25 (magenta, axoneme) and (magenta (dot), α-FTZC). These are representative images of bi-flagellated cells with different types of old flagella: 1: no tagged tubulin incorporated in the old flagellum, 2: tagged tubulin incorporated only at the tip of the old flagellum. 3: tagged tubulin incorporated along longer portion of the old flagellum, starting with a gradient. B: The pie-chart shows the abundance of each type of old flagellum as part of all bi-flagellated cells that had incorporated tagged tubulin along the entire length of the new flagellum. C: Individual measurements of the entire length of the different types of old flagella. Significance was determined by ordinary one-way ANOVA test.

Apart from first generation new flagella (type 1), two more types of old flagella could be distinguished. First, there were the ones that had not incorporated any tagged tubulin at their tip (Fig. 22, type 1). The third and slightly more abundant type of old flagella were the ones in which Ty-1-tubulin had incorporated only at the very tip (~1μm) (Fig. 22 A, type 2). Two main characteristics separated them from the flagella with a gradient (1st gen old, Fig. 22A, type 3). First, the green portion had a sharp cut off and no gradient. Second, the length of the corresponding new flagella was independent (discussed in the next section). The three types of old flagella and their distribution as well as the length measurements are depicted in Fig. 22A. On average, the presumably 1st gen old flagella were with 18.2μm the shortest while the old flagella with staining only at the tip with 18.9μm the longest. This difference, although small, was statistically significant (determined by ordinary one-way ANOVA). The mean length of the green tip was ~0.9μm. From the literature we know that new flagella are assembled to ~80% (16μm) of the length of old flagellum before the cells divide. Since first generation old flagella are ~18.2μm in length, our results suggest that there is further elongation before cells complete another G1-phase and start to assemble a new flagellum. Nonetheless, these flagella are on average shorter than other OF types and it is possible that another elongation step takes place (~1μm) in subsequent cell cycles.

Is absence of staining at the tip of old flagella based on cell cycle progression?

As flagellum assembly is intrinsically linked to the cell cycle, the length of the new flagellum is a sensitive indicator of the cell cycle progression. To understand the origin of the different types of old flagella, we decided to measure the length of their respective new flagellum (Fig. 23A).

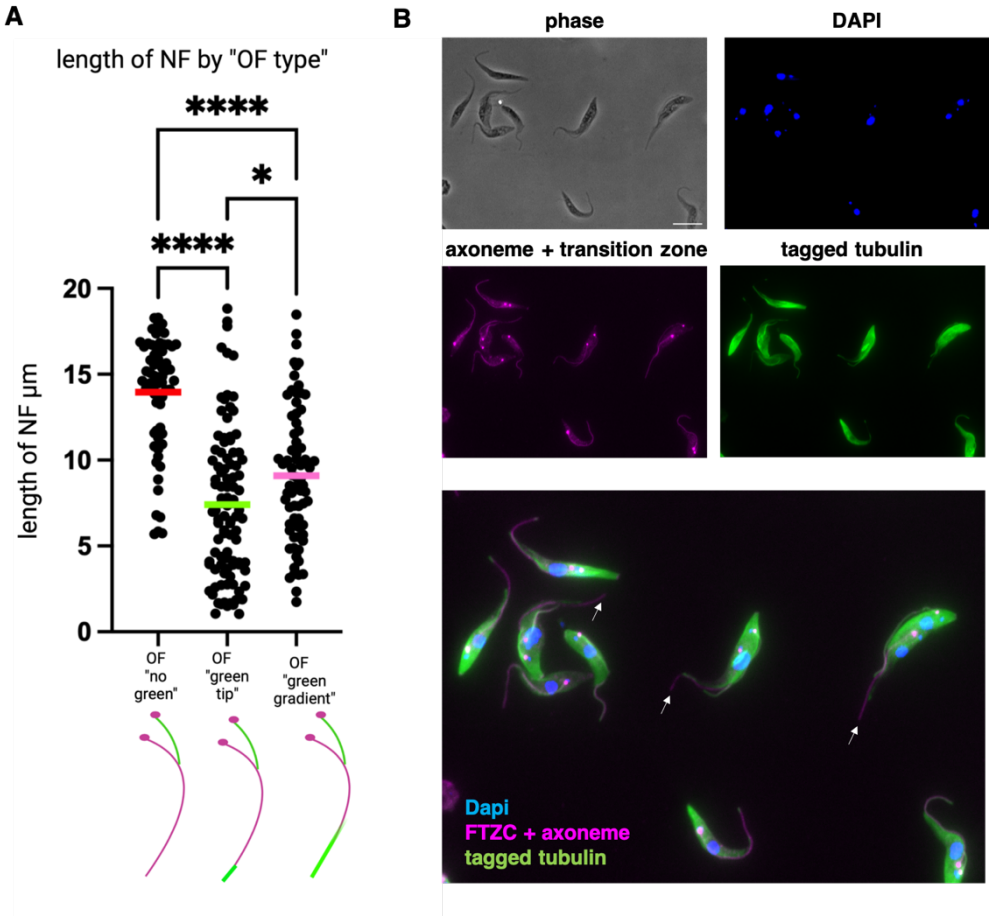

Figure 23 : IFA of whole cells that were incubated with tetracycline in for 9 hours. Samples were incubated with the BB2 antibody (green, tagged tubulin), Mab25 (magenta, axoneme) and (magenta (dot), anti-FTZC) and DAPI (blue, DNA). A: Measurements of the length of new flagella grouped by the different types of mature flagella. B: IFA with whole cells from the same induction experiment as in A. Arrows highlight the OF tip of cells that are advanced in the cell cycle (2K2N2F, or cells where the mitotic spindle is present). No tagged tubulin is visible at the OF distal tip in these cells. Significance was determined by ordinary one-way ANOVA test.

In cells where no staining was present in the old flagellum, new flagella were very long. Most of the measurements cluster around ~14μm and these new flagella were therefore close to the length at which cells usually divide. For the other two types, the distribution of new flagellum length is fairly homogenous and the average length significantly shorter. To investigate if the absence of staining at the tip could be related to cell cycle progression, we looked at whole cells from the same induction. Indeed, bi-flagellated cells that had no staining at the tip of the OF were usually very advanced in their cell cycle based on the configuration of nucleus and kinetoplast, in coherence with the above average length of the new flagellum (Fig. 23B). In many cases the mitotic spindle could be observed or the nuclei had already divided.

One explanation is that these flagella were issued from new flagella that had finished assembly of the new flagellum just before tagged tubulin expression was induced and therefore "missed" the staining at the tip (Fig. 21 bottom panel, ~15μm new flagellum). However, if old flagella stay indeed locked at least 50% of flagella (9h for a full cell cycle) without staining at the tip should carry new flagella of average length.

Taken together, we observed three different types of old flagella in bi-flagellated cells during a full cell cycle induction. One of them could be clearly identified as old flagella that had started out as new flagellum at the beginning of induction (gradient, 1st-generation old). These are on average the shortest old flagellum type. The origin of the other two cannot be timed clearly. Old flagella in which no tubulin was incorporated had above average length new flagella, which raised the question if absence of staining was cell cycle specific. The old flagella that had incorporation only at the very tip were the most abundant species. The length of their new flagella was homogenously distributed. These findings opened the possibility that old flagella are subject to integration even after several cell cycles had passed since they were new flagella, presumably when cells harboring them were in the G1-phase.

Are flagella locked forever?

In previous sections, we corroborated the presence of a locking event that prevents mature flagella from incorporating tubulin while a new flagellum is assembled. The inducible expression of tagged tubulin proved a robust tool to measure assembly dynamics during short induction times (2-9h) that do not exceed the duration of one cell cycle. The nature of this system however, has three limitations when following the integration of tagged tubulin over longer induction times of more than one cell cycle.

1) Trypanosomes do not divide synchronously. The only flagella in which we can definitely trace the time of emergence are fully green new flagella at early induction times as well as flagella that have proximal portions, where they only incorporated untagged material and then became progressively labeled with tagged tubulin in the distal region after induction. These flagella must have therefore emerged in the hours leading up to induction.

2) It is unlikely that all cells progress through the cell cycle at the same speed (Muniz et al., 2022). As the assembly of a new flagellum is tightly linked to the cell cycle, we can deduce incorporation but we are limited to the observation of general trends rather than pinpoint dynamics of individual cells.

3) Tubulin is tagged with an epitope tag and not a fluorescent tag, which means that we need to fix cells at a given time and we have to infer what happened over the time of induction. These limitations complicate analysis when we want to trace mature flagella over several cell cycles. To summarise, if a cell started the assembly of a new flagellum after induction this flagellum incorporates tagged tubulin along the entire length from the base to the tip. This flagellum was termed a fully green flagellum. Over prolonged induction time this cell will divide, initiate and then complete the assembly of another flagellum that incorporated tagged tubulin along the entire length. However, after induction times that span several cell cycles, it becomes impossible to distinguish between these flagella, as most of them are “fully green”.

We attempted to circumvent this limitation by performing a pulse-chase experiment in which the induction serves as the pulse. Tetracycline was added to the culture for 24 h, so the cells assemble flagella that incorporated tagged tubulin for 2-3 generations (Fig. 24, green arrow 0 -24h). We then proceeded to de-induce the culture by washing the cells four times with PBS, to get rid of tetracycline (Bertiaux et al., 2018). Over time the tet-repressor will be able to bind the tet-operator again, which turns off the expression of tagged tubulin (Bastin et al., 2000). After de-induction the cells were grown in the absence of tetracycline for 48 hours (5-6 cell cycles, washout) and were then harvested for IFA (Fig. 24, red arrow).

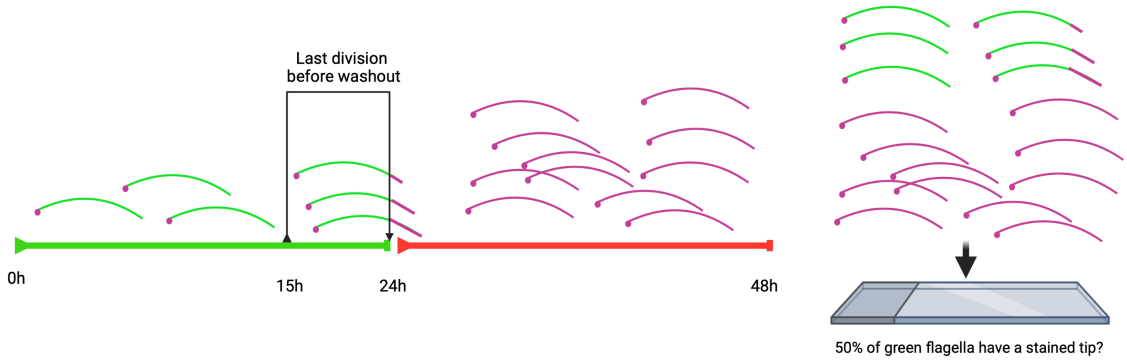

Figure 24 : Pulse-chase experiment. New flagella that are constructed during the first 15 hours of induction should have incorporated Ty-1-tubulin at the tip or along the entire length. Only the flagella in which assembly had started in the last 9 hours (last cell cycle) could not be finished during induction. During the washout of tetracycline, these cells would run out of tagged tubulin and could then only incorporate untagged material. Flagella would therefore be green but become progressively unstained due to the lack of tagged tubulin. Therefore 50% (one cell cycle) of green flagella would have an unstained portion at the tip. The other 50% green flagella, that were made before the last cycle should have been finished while Ty-1-tubulin was available. In that case, this half of the green flagella should stay completely green after the washout period, if they do not elongate in presence of turnover. Figure generated by Biorender.

After 24h fully green flagella were considered labelled (pulse) as we can trace their origin to the time between the beginning of induction and the beginning of the de-induction. Examples of fully green flagella can be seen in Fig. 26A. Observing flagella 48h post de-induction allowed us to track what happened to the flagella that still contained tagged tubulin, while they were grown in the absence of tagged tubulin during the washout. This step marks the chase-aspect of the experiment.

If mature flagella indeed stay locked forever, a substantial proportion of green flagella should remain green along their entire length. If one cell cycle is enough to assemble a new flagellum to full length and then be locked, the proportion of fully green flagella can be estimated to 50%. In that case only the flagella concluded in the last cell cycle of induction (~9h) are not able to complete assembly in the presence of tagged tubulin and are expected to have a negative distal segment (Fig. 24).

Tips of mature flagella incorporate tubulin even after more than one cell cycle

To test for how long, flagella incorporate tubulin after they were assembled, de-induction experiments were performed. For this purpose, expression of Ty-1-tubulin was induced for 24 hours (2-3 cell cycles). After that time, tagged tubulin should be incorporated in the MTs of the cell body as well as old and new flagella. After three cell cycles the proportion of fully green flagella can be estimated to 87.5% (50%➢75%➢87.5%). Then, tetracycline was washed out and the cells grown for 48 hours (5-6 cell cycles) in its absence, hence without tagged tubulin. During the initial induction, samples were taken after 4 and 24 hours and were compared at 48 hours after de-induction. At last, cells after 48-hour de-induction were treated again with tetracycline for 4 hours (re-induction). From all these timepoints, slides were prepared with whole cells, cytoskeletal extracts and flagella extracts. The slides were then stained with BB2 (tagged tubulin), anti-FTZC (transition zone), Mab25 (axoneme) and DAPI (DNA).

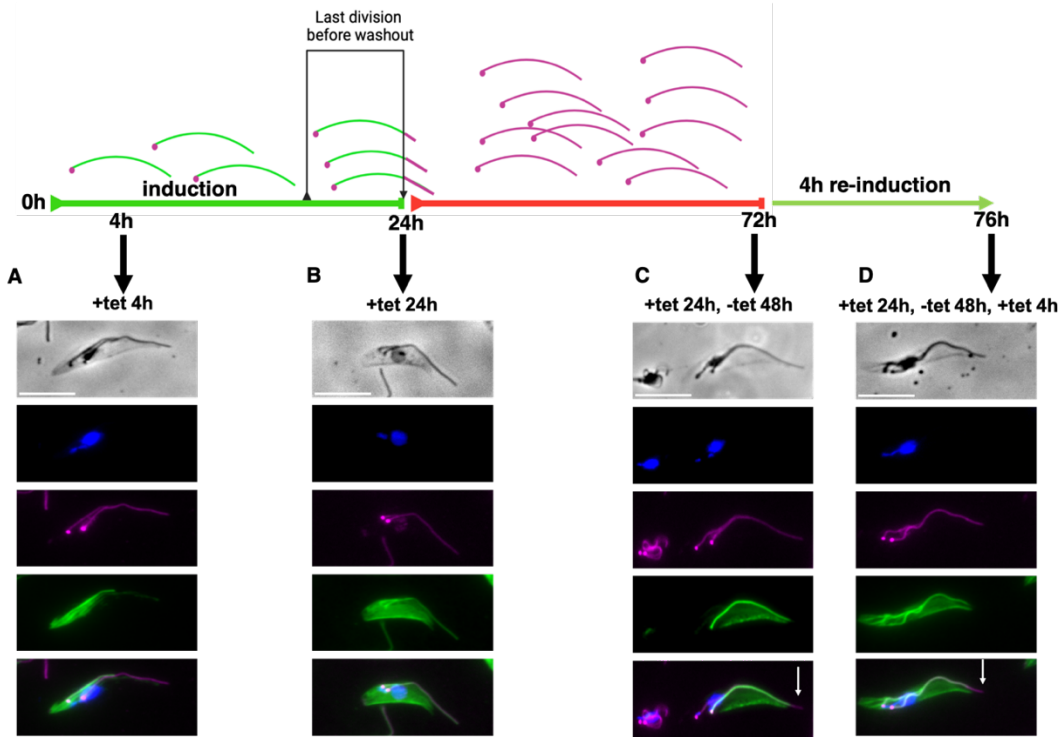

Figure *25* : Cytoskeleton extracts of the inducible Ty-1-tubulin cell line. That were harvested at different times during the washout experiment. One representative cell is shown per timepoint. Samples were stained with BB2 (green, tagged tubulin), Mab25 (magenta, axoneme), FTZC (magenta (dot), transition zone) and DAPI (blue, DNA).

In Fig. 25, a cytoskeleton of one representative cell per timepoint is depicted. The first timepoint was a typical 4-hour induction as described in Fig. (14 -17).

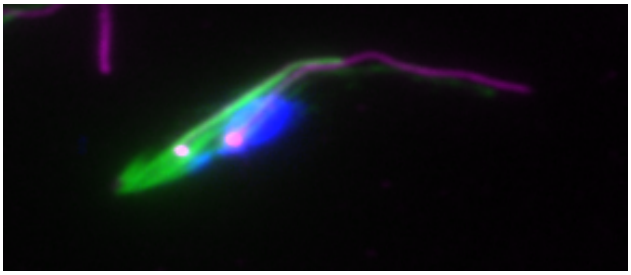

Zoom in of Fig. 25A of a cell 4h post induction. Tagged tubulin is integrated in the NF but not the OF and in the posterior of the cell body.

Tagged tubulin had incorporated in the posterior MTs of the cell body as well as in the new flagellum but only in old flagella of bi-flagellated cells with very short new flagella, coherent with the grow and lock model (Fig. 25, +tet 4h). This pattern was identical to what was described for 4-hour inductions in previous experiments (Fig. 25A).

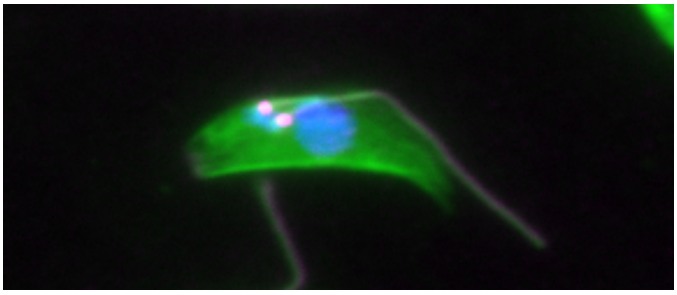

Zoom in of Fig. 25B of a cell 24h post induction. Tagged tubulin is integrated in NF and OF and along the whole cell body.

After 24 hours (Fig. 25B, Fig. 26A), the cells had gone through more than one cell cycle during induction and we started to observe cells that had incorporated tagged tubulin in the entire cell body as well as in both new and old flagella.

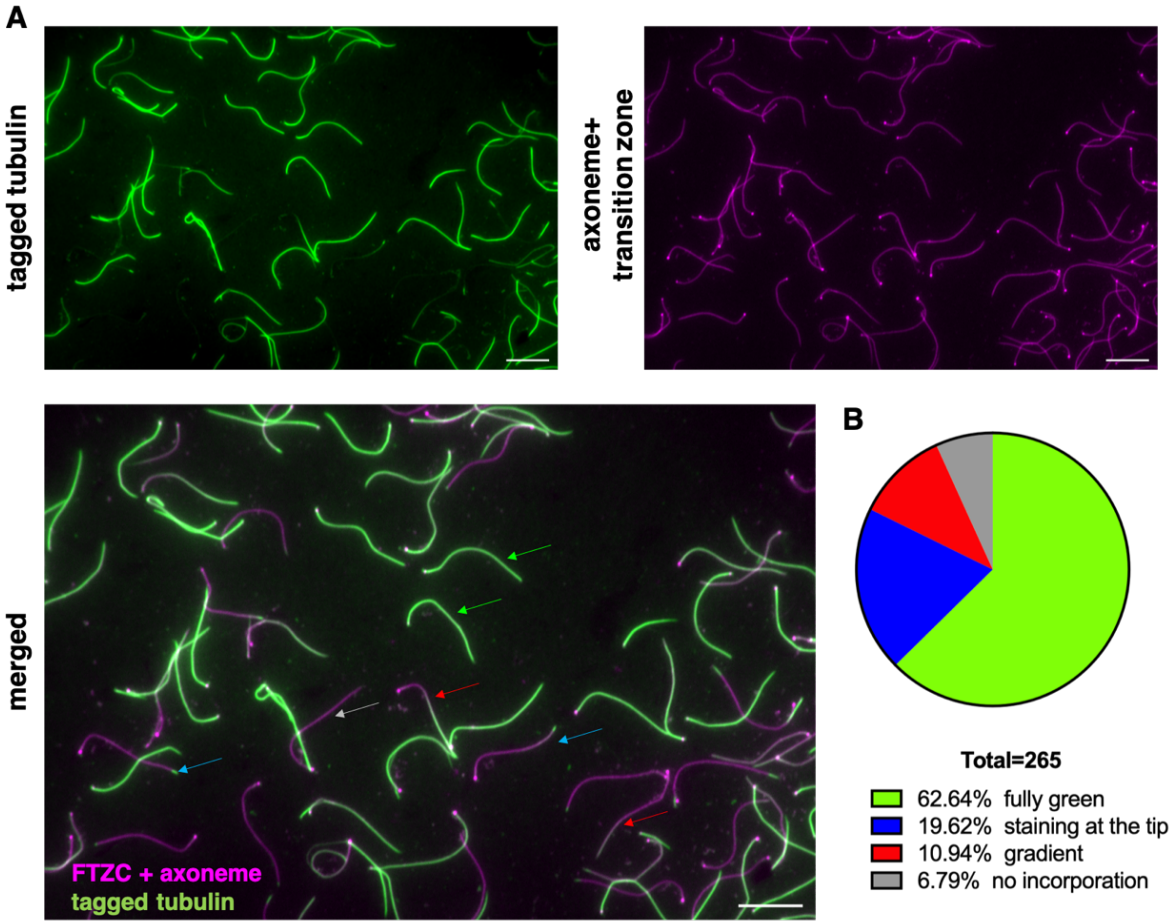

Figure 26 : A: IFA of high salt extracted flagella incubated with tetracycline in for 24 hours. Samples were incubated with the BB2 antibody (green, tagged tubulin), Mab25 (magenta, axoneme) and (magenta (dot), FTZC). B: Proportion of the different species of flagella (mono-flagellated or OF of bi-flagellated cells) found after 24h post induction.

In flagellar extracts, ~63% of flagella were fully green (Fig. 26A, merged, green arrow), ~10% had a green gradient (Fig. 26A, merged, red arrow) and ~20% had incorporated tagged tubulin only at the tip (Fig. 26A, merged, blue arrow). Only 7% of flagella had not incorporated any tagged tubulin at that point (Fig. 26A, merged, grey arrow). A pie chart that summarises these quantifications is shown in Fig. 26B. It was noted that the flagella with a gradient (Fig. 26A, merged, red arrows) have on average a weaker signal than fully stained flagella. This was expected as these flagella were made during the initial hours of induction where the proportion of tagged to untagged tubulin was comparatively lower. To assess induction efficiency, samples with whole cells from the same induction experiment were analysed. After 24 hours, only 5% of cells had not integrated any tagged tubulin in neither flagella or the cell body. We concluded that this is the portion of cells that did not respond to tetracycline. Hence, a majority of flagella from the ones that had not integrated tagged tubulin (Fig. 26A, merged, grey arrow) could be attributed to these non-responders. This suggested, that after 24 hours ~98% of flagella that were capable of integrating tagged tubulin had indeed done so. A representative image of a cytoskeleton extract from cell that had integrated Ty-1-tubulin throughout the whole cell is depicted in Fig. 25B.

For the next timepoint, cells were harvested 48h after tetracycline was removed (72h since the beginning of the experiment). Some of these cells had therefore gone through the initial induction and then through the washout. They could be easily distinguished from the cells that arose after induction by the tagged tubulin that was incorporated. Cells that had not incorporated any tagged tubulin represented a majority at that point. This was expected after a 48-hour washout period because no tagged tubulin was present anymore for the cells to integrate after almost six generations in the absence of tetracycline. Initially, we observed some flagella where tagged tubulin staining becomes progressively less intense along the flagellum. In contrast to the situation for flagella with a gradient of tagged tubulin after induction, where the proportion of tagged vs. untagged tubulin increases with time (Fig. 26A, merged,

red arrows), this was attributed to a decreasing proportion of tagged vs untagged material. This was a good indicator that tagged tubulin was indeed becoming progressively scarcer. Whole cells and cytoskeletons were then investigated that still contained tagged tubulin and must have emerged during the initial induction.

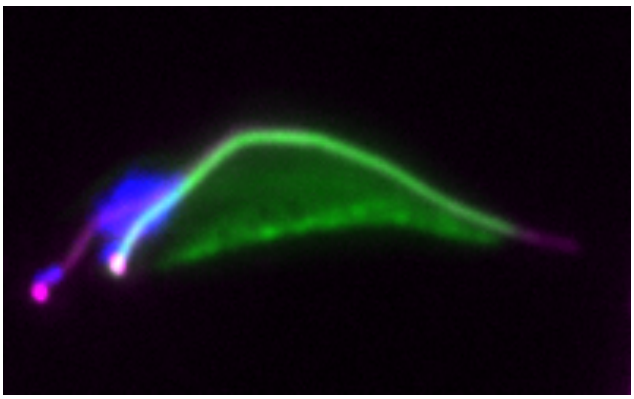

Zoom in of Fig. 25C of a cell 48h post washout. Tagged tubulin is integrated in the OF but not the NF resembling the mirror image of a short induction. The tip of the old flagellum is not stained with tagged tubulin

These cells exhibit tagged tubulin in the anterior MTs of the cell body and in the mature but not the new flagellum. The posterior part of the cell has not incorporated Ty-1-tubulin (Fig. 25C). Remarkably, the presence of tagged material after the washout is the mirror image of a short induction (4h). Taken together, this means, that tagged tubulin was successfully washed out and cells had incorporated exclusively untagged tubulin.

Flagella after de-induction

The presence of tagged tubulin in flagella after the washout was then assessed in more detail in flagella extracts (Fig. 27).

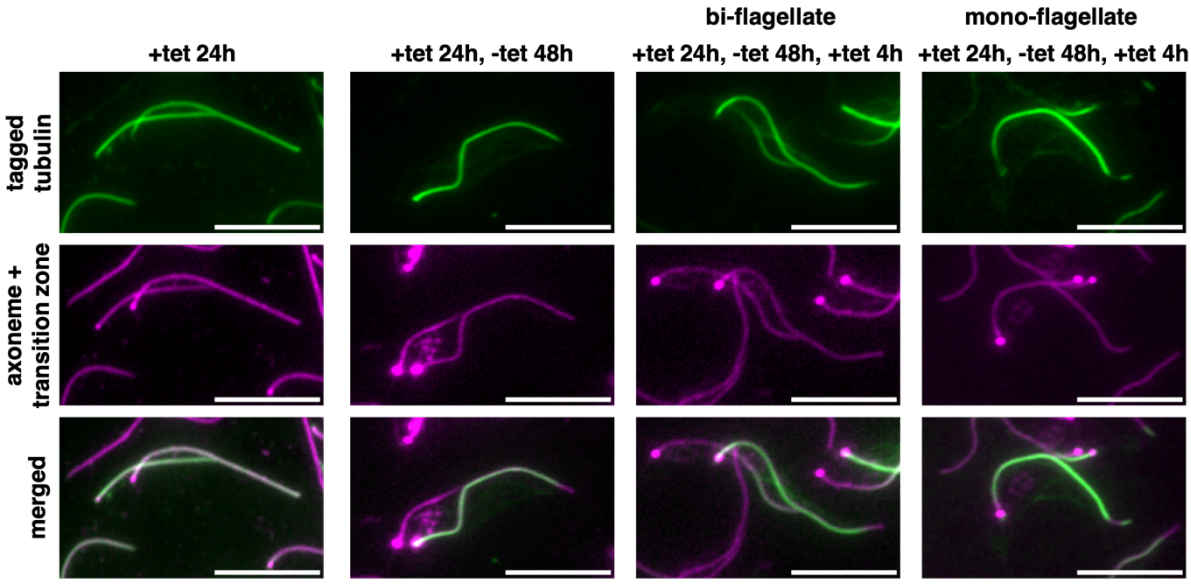

Figure 27 : IFA of high salt extracted flagella that were harvested at different times during the washout experiment. Samples were stained with BB2 (green, tagged tubulin), Mab25 (magenta, axoneme), anti-FTZC (magenta (dot), transition zone). +24h: Cell that was harvested after 24h of induction, tagged tubulin had integrated in NF and OF along the entire length. +24h-48h: Cell that was harvested 48h post de-induction. Tagged tubulin had integrated in the OF but not the NF. The OF has an unstained portion at the tip where only untagged tubulin had incorporated. +24h-48h+4h bi-flagellated cell: Cell was harvested after the re-induction. Tagged tubulin integrated in the distal part of the NF as well as the OF apart from the unstained tip. The tagged tubulin in the NF presumably corresponds to the re-induction. As the NF is only partially green this cell demonstrates that integration of tagged tubulin still follows the grow and lock model in a cell who's OF emerged several generations prior, during the initial induction. +24h-48h+4h mono-flagellated cell: The OF of a mono-flagellated cell has a short portion where tagged tubulin integrated again distal to the unstained portion, presumably during re-induction. Not enough images were acquired to assess these cells quantitatively.

No green new flagella were found in any cells, coherent with the absence of tagged material (Fig. 27, +tet 24h,-tet48h). In contrast, green flagella in isolation (mono-flagellated) or green OF of bi-flagellated cells are still present. We specifically chased the green flagella that were present after the washout to assess if they were subject to integration of untagged material during the washout period. Strikingly, in these green flagella tagged tubulin is absent from the tip in >95% (Fig. 27, +tet 24h,-tet48h) of cases. A ~1-2 μm long portion of untagged flagellum extends beyond the green part. Only 5% of green flagella 48h post washout have integrated tubulin up to the very end of the distal tip. This is observed for flagella of mono-flagellated and OF of bi-flagellated cells.

It appears that almost all green flagella that had emerged during the initial 24h induction (pulse), had been the subject to integration of untagged material during the 48h after the de-induction when assessed by IFA after 72h total. (chase-timepoint).

There were two possible explanations for this observation that we tested: 1) The presence of a constant disassembly re-assembly process (turnover). 2) Finishing the assembly of a flagellum takes several cell cycles, (definitively more than one) and untagged tubulin is progressively added to reach full length. In the next experiments, we attempted to address both hypotheses.

To test for turnover, we wanted to see if the green old flagella that had an unstained tip were able to integrate tagged tubulin again after several cell cycles. Therefore, we added tetracycline again for 4 hours after the 48-hour washout period.

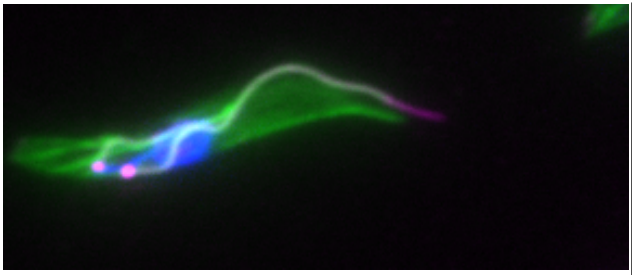

Zoom in of Fig. 25D of a cell that was re-induced with 48h post washout by addition of tetracycline for 4h (total of 76h). This cell had integrated tagged tubulin in NF and the OF as well as the entire cell body. Only the unstained tip of the OF did not integrate tagged tubulin.

The focus was set on green old flagella with an unstained tip of bi-flagellated cells that had incorporated tagged tubulin in the new flagellum (Fig. 25D, Fig. 27: +tet24h,-tet 48h,+tet4h, bi-flagellate). Similar to previously described 4-hour inductions, integration at distal portion is only observed in new flagella, but not at the unstained tip. This means that access to the old flagellum is still prevented, as expected from the grow and lock model. We cannot exclude however, that these flagella became unlocked and then locked again. After all, they had incorporated untagged material at the tip during the 48h post de-induction.

If the reason for the unstained tip was due to the circumstance that 24 hours (2-3 generations) was not enough to finish a flagellum we expected a slight increase in fully green flagella when the initial induction was longer. Therefore, we attempted to maintain the cells induced for 48h (5-6 generations) or 72h (8-9 generations) and then de-induce them. Instead of the just 24h (2-3 generations) described so far. Should more than 2-3 generations be needed to finish a flagellum we would expect that the number of flagella with unstained tips slightly decreases after prolongation of the initial induction time to 5-6 (48h) or 8-9 (72h) generations.

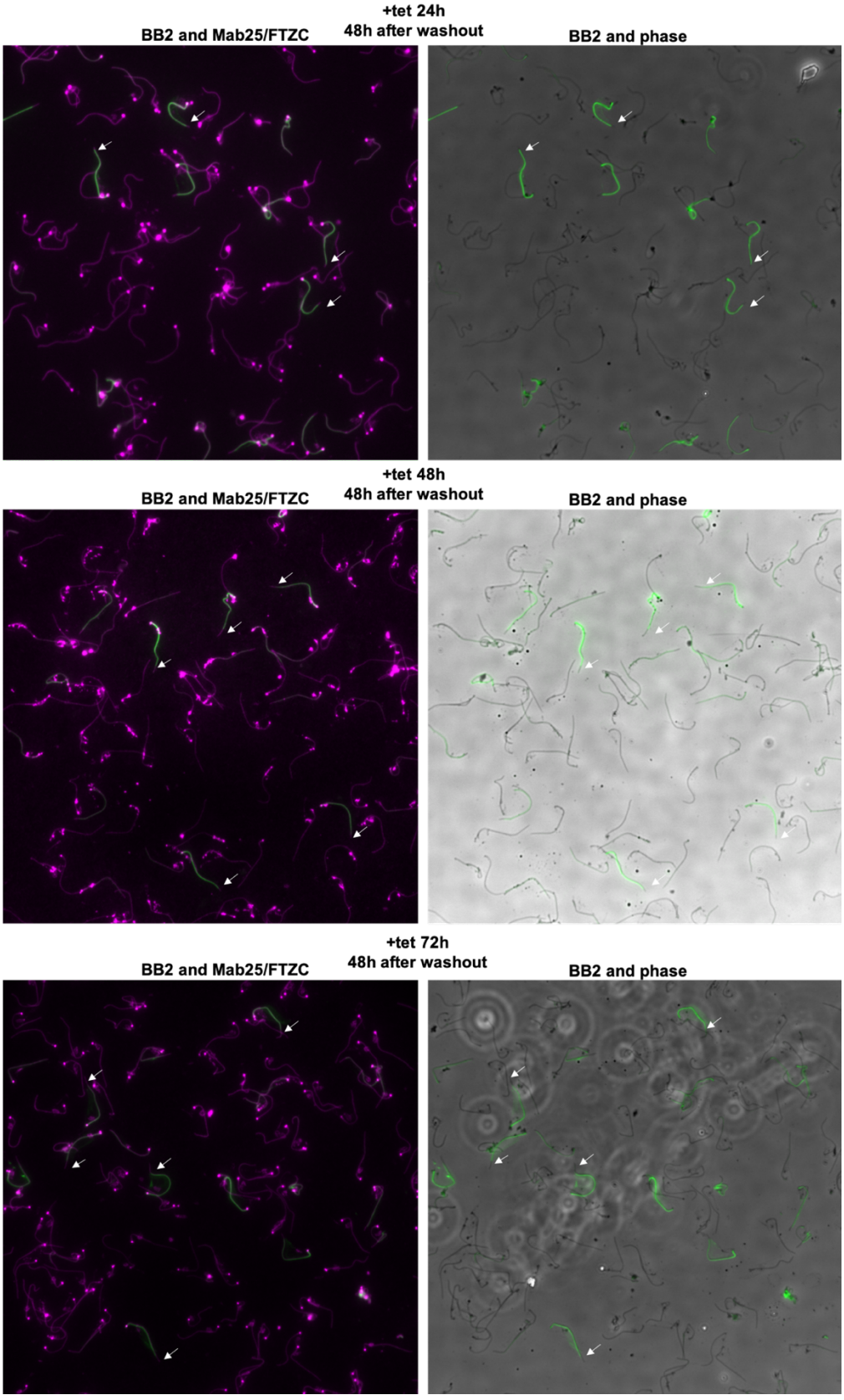

Figure 28 : IFA of high salt extracted flagella incubated with tetracycline in for 24 / 48 / 72 hours and subjected to a tetracycline washout for 48 hours after. Samples were incubated with the BB2 antibody (green, tagged tubulin), Mab25 (magenta, axoneme) and (magenta (dot), FTZC).

In these conditions however, >95% of green flagella from longer initial inductions have an unstained portion at the tip (Fig. 28, 48h + 72h). On the contrary, the length of the unstained tip slightly increases on average in conditions with prolonged initial induction.

In summary, tagged tubulin could be washed out and cells started to integrate exclusively untagged material again. The localization of tagged material after the washout is the mirror image of a short induction with tagged tubulin present in mature but not new flagella and at the anterior but not posterior MTs of the cell body. A vast majority of green old flagella have incorporated untagged material 48h post de-induction and only few fully green OF were observed. This number did not increase even in conditions of prolonged initial induction. In bi-flagellated cells that were re-induced with tetracycline for 4, only the new flagellum incorporates tagged tubulin at the tip.

Taken together, these results suggest a process in which mature flagella integrate tubulin even after several cell cycles had passed but only while they are not bi-flagellated. Since the overall length of green flagella 48h post de-induction did not meaningfully increase a disassembly process might be present that is limited to the flagellar tip. The described results are coherent with constant disassembly process and a cell cycle dependent re-assembly process at the flagellar tip (Balance-point model). Indeed, some isolated green flagella (not in bi-flagellated cells) had incorporated tagged tubulin at the end of the unstained tip (Fig. 27, +tet24h,-tet 48h,+tet4h, mono-flagellated cell). Due to the limitations of an epitope tag which cannot be traced as dynamically as a fluorescent protein we could not measure this for tubulin directly.

Old axonemes are locked in bi-flagellated BSF trypanosomes (preliminary)

Assembly of the BSF flagellum differs in several aspects from the assembly of the procyclic form flagellum. First, the flagellum of BSFs is 25 μm in length (Tyler, 2001) and therefore ~20% longer compared to the one of procyclic forms (~20 μm). Secondly, the NF of BSF is assembled to full length of the OF before the cells divide, whereas procyclic forms need to finish the NF after cell division. Lastly, the flagellar connector that attaches the NF tip to the old flagellums axoneme in procyclic forms is absent in the BSF stage. Instead, the NF is embedded into a groove inside the cell (Hughes et al., 2013). This is very relevant as it complicates analysis of flagella isolates, in which the cell body is absent.

We were curious if other stages of *T.brucei* adhere to the grow and lock model. As BSFs can be readily cultured and are amenable to genetic manipulation similar to procyclic forms we decided to start our investigation there. the inducible tagged tubulin system was introduced into pleomorphic Antat BSF strain. We first transfected the cells with the Ty1-tubulin-pHD430 construct and selected the cells with phleomycin. The cells were then screened and subjected to clonal dilution. After that the tetracycline repressor was introduced by transfection with the pHD360 vector (Wirtz and Clayton, 1995). As this expression system has been developed for the procyclic stage, we are working on another construct for ectopic inducible expression of tagged tubulin that has been optimised for the expression in the BSF stage.

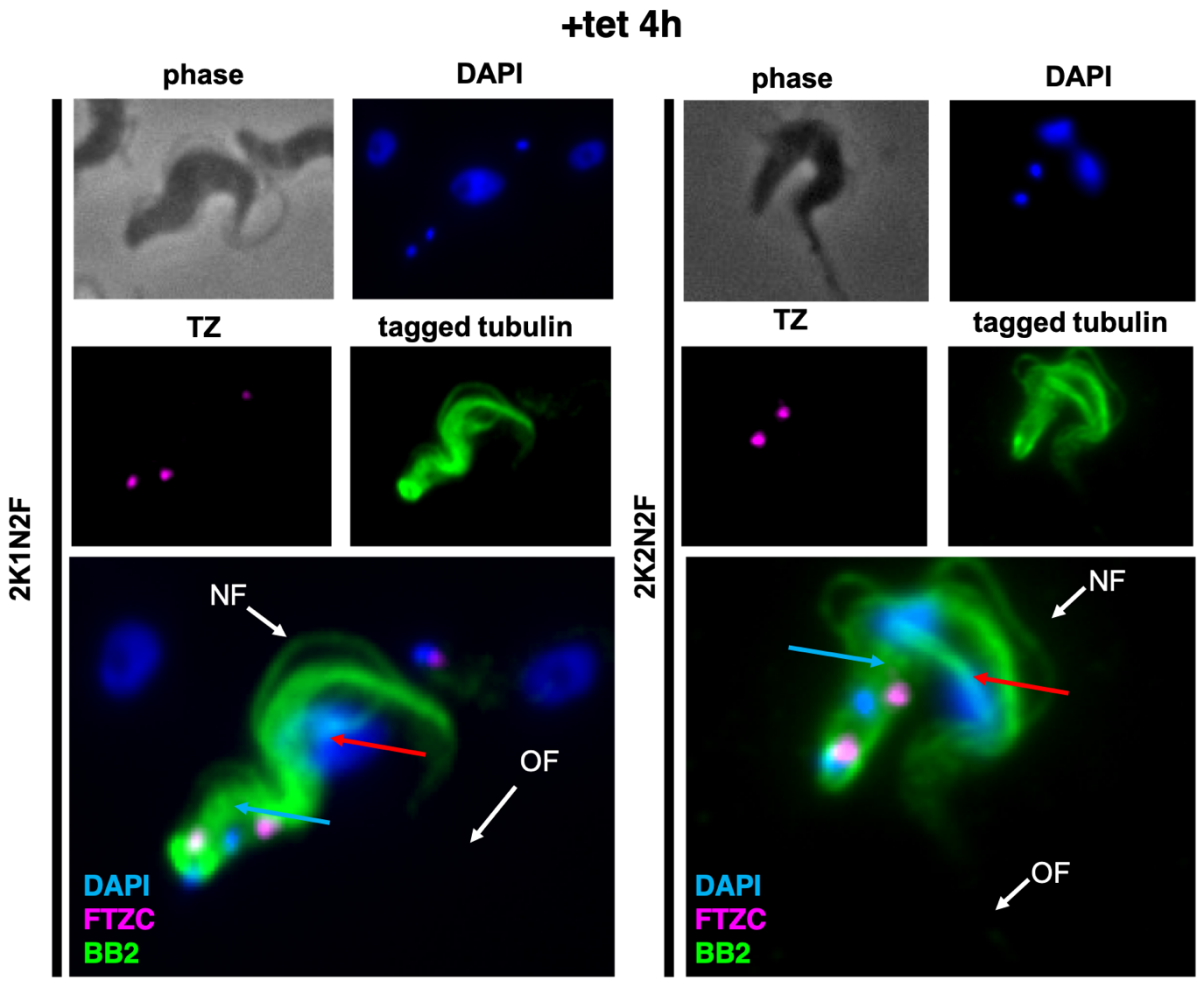

Figure 29 : IFA of whole cells fixed with 4% paraformaldehyde (PFA) 4 hours post tetracycline induction. Slides were stained with the BB2 antibody (tagged tubulin), anti-FTZC (transition zone) and DAPI (DNA). Integration can be observed in the MTs of the cell body (blue arrows), the mitotic spindle (red arrows) and the NF (white arrow, NF) but not the OF (white arrow OF). The axonemal marker we used for procylic forms did not yield satisfactory staining of the flagellum.

Regardless, we observed that tagged tubulin can be inducible expressed in the BSF stage with the current system. After induction, tagged tubulin is incorporated in the MTs of the cell body, the flagellum as well as the mitotic spindle. When expression was induced for 4 hours, tagged tubulin was incorporated in the cell body, the mitotic spindle and the NF but not the OF (Fig. 29). We noted that is more difficult to track the NF and the OF of BSF as the flagella are longer and the cells more difficult to fix in one plane. Therefore, we are currently working on a reliable protocol for flagellar and cytoskeleton extracts of BSF and a BSF adapted expression system. Nonetheless, the preliminary results depicted in Fig. 29 suggest that incorporation of tagged tubulin follows the grow and lock model in bi-flagellated cells.

Results

Methods

Cell line culture and transfection:

Procyclic trypanosome strain 427 were cultured in SDM-79 medium (GE Healthcare Cat No.: SH3A8023.01) pH 7.4, complemented with 10% fetal bovine serum and Hemin (7.5 mg/l). Cells were grown to densities between 5 x 10^6 – 1 x 10^7. A total of 4 x 10^7 was harvested and then transfected with 10 μg of linearized plasmid using an Amaxa nucleofector II (Burkard et al. 2011). To obtain the α-Ty1-tubulin cell line two rounds of transfection were carried out. 4 x 10^7 cells were transfected with the pHD430 1xTy1-tub and then selected with phleomycin (2.5 μg/ml) for 10 days. The upcoming wells were harvested and screened for the presence of tagged tubulin by IFA using the BB2 antibody (Bastin et al., 1996). Positive wells were further cloned out with serial dilutions and screened in similar fashion. Clones with expression of the tag in >90% of cells were then transfected as described above with the pHD360 (Wirtz and Clayton, 1995) vector that contains the Tet repressor. Cells were selected with hygromycin (25 μg/ml) for 10 days. The 24-well plates were then split in two sets, one set was incubated with tetracycline. All plates were then subjected to IFA with the BB2 antibody. Wells that had estimated >70% presence of signal in tetracycline induced conditions and <5% positive in non-induced conditions were selected and subject to clonal dilution. After 7 – 10 days cells were harvested and tested in the same manner. Clones were chosen with induction rate >85% and leakiness <1%. Induction experiments were performed with the addition of 1μg/ml tetracycline.

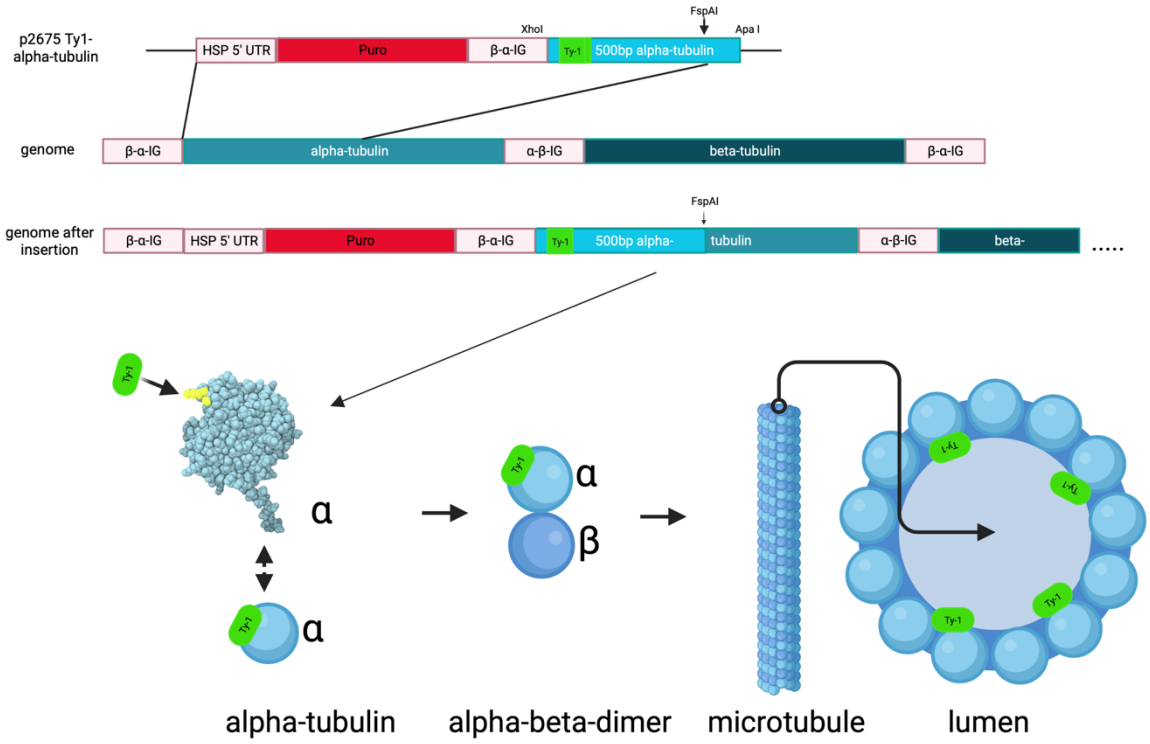

Figure 1 : Vector design of alpha-tubulin in situ tagging. Intragenic Ty-1-tag was inserted 1 AA after the acetylated lysine (K40), so the tag ends up facing the lumen of the MTs. Tagged tubulin was first inserted into a construct for in situ-expression. A heat shock protein (HSP) 5'UTR downstream of the puromycin resistance gene was followed by the beta-alpha-tubulin intergenic region and then the first 500bp of the alpha-tubulin ORF with the inserted Ty-1-tag. After recombination, Ty-1-tagged tubulin will end up flanked by its natural 5' UTR and its endogenous 3' UTR. Graph generated by biorender.

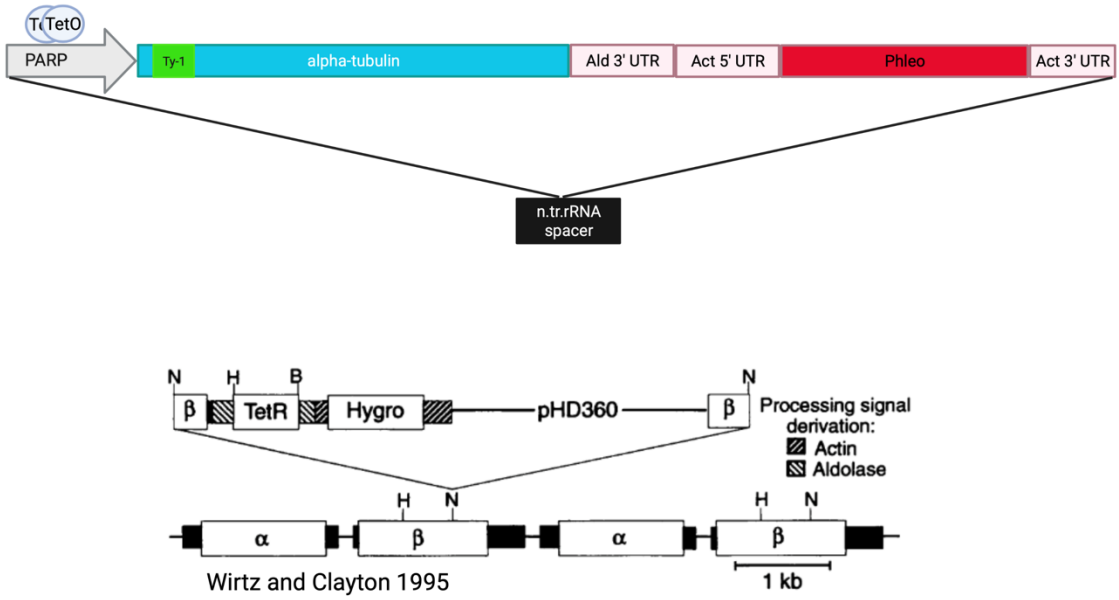

Figure 2 : Vector design to inducible express tagged tubulin. First the whole ORF of alpha-tubulin that carries the Ty-1-tag 1 AA after the acetylated lysine (K40) was cloned into a pHD430 vector downstream of the PARP (procyclin) promoter that has inserted two copies of the Tetracycyline operator (tetO). The tagged alpha-tubulin is followed by the aldolase 3' UTR and then the phleomycin resistance gene flanked by the actin 5' and 3' UTRs. The cells were first transfected with this vector then screened and subjected to clonal dilution. In a subsequent transfection the pHD360 vector was introduced that incorporates the Tet-repressor into a tubulin locus. Selection was carried out with hygromycin. As the expression of the tagged tubulin and the phleomycin gene on the pHD430 are not independent phleomycin was not added. Since the repressor would shut off the expression of both, which would require the addition of tetracycline as well.

Vectors:

To test if the expression of an internal tag of alpha-tubulin is feasible in *Trypanosoma brucei*, a vector was designed for the endogenous expression of a 1xTy-epitope positioned in the acetylation loop of alpha-tubulin. A fragment was designed where one or two Ty-1 tags were inserted after the threonine (position T41) in the first 500 bp of the alpha-tubulin open reading frame (ORF). The fragment was synthesized with XhoI and ApaI flanking sites and cloned into p2675 (reviewed in Kelly et al. 2007) by GeneCust (Boynes, France) (see Fig. 1). The resulting vectors were linearized with FspAI (4891–4898bp of p2675-alpha-TubTy1) before transfection. To monitor incorporation of alpha-tubulin a vector was designed that contained the full ORF of alpha-tubulin under the regulation of a tetracycline operator with one epitope of the Ty-1 tag (Bastin et al. 1996). A fragment was designed in which the whole open reading frame of alpha-tubulin carries one copy of the Ty-1-tag inserted after the threonine (T41) (Sirajuddin et al., 2014). This fragment was synthesized and cloned between HindIII and BamHI sides of a pHD430-mNeonGreen-Ty1-IFT172 (pHD 430 derivative, Wirtz and Clayton 1995) by GeneCust (Boynes, France) (see Fig.2). Prior to transfection the plasmid was linearized with NotI.

Immunofluorescence assays:

Procyclic cells were grown to densities between 5 x 10^6 – 1 x 10^7 and harvested by centrifugation (1500g for 8min). For whole cell analysis, the cells were pipetted onto poly-L-lysine coated slides (epredia, REF J2800AMNZ, Gerhard Menzel GmbH) and left to air-dry for 10 – 15 minutes. They were then fixed with methanol at -20°C for 5 min. To extract cytoskeletons, cells were pipetted onto poly-L-lysine coated slides and left to settle for 10 minutes in a humid chamber. Extraction was achieved with treatment of 1% Nonidet P-40 in PEM buffer (2 mM EGTA; 1mM $MgSO_4$; 0.1 M, pH6.9, PIPES) for 5 minutes. Slides were then washed once with PBS and the cytoskeletons fixed with Methanol at -20°C for 5 minutes.

Extraction of flagella was achieved by further treating the cytoskeletons. They were washed once in PBS followed by treatment with 1.1M NaCl for two times 5 – 15 minutes, each with a PBS washing step after. Following methanol fixation, the slides were left in PBS to re-hydrate for 15 minutes. Slides were then treated with the different primary antibodies; BB2 mouse monoclonal antibody (Bastin et al. 1996, undiluted) was used against Ty-1 tagged alpha-tubulin, FTZC rabbit polyclonal antibody ((Bringaud et al., 2000) 1:2000 in 0.1%BSA in PBS or in supernatant of BB2 hybridoma) was used as a marker for the transition zone, Mab 25 mouse monoclonal IgG2a (Dacheux et al., 2012), 1:4 in 0.1% BSA in PBS or BB2 hybridoma supernatant) was used as an axonemal marker. Slides were then washed 3 times in PBS and treated with secondary antibodies: α-mouse IgG1 coupled to Alexa Fluor488 (AF488) (Jackson ImmunoResearch Laboratories, #Cat: 115-545-205), α-mouse IgG2a coupled to Cy5 (Jackson ImmunoResearch Laboratories, #Cat: 115-175-206), α-rabbit coupled to AF647 (Jackson ImmunoResearch Laboratories, #Cat: 711-605-152). After three washing steps in PBS the nuclei and kinetoplasts were stained with DAPI (10 μg/ml in PBS) for 1 minute. Slides were then washed once and shortly air-dried before mounting the coverslips with ProLong™ Gold antifade reagent (P36930, invitrogen by Thermo Fisher Scientific). Images were acquired with a 100x objective of the Leica DMI4000 microscope (NA=1.4, photometrics PRIME 95B™ back illuminated scientific CMOS camera) and analyzed with ImageJ (Schindelin et al., 2012).

Western blot analysis:

Procyclic cells were grown to densities between 5 x 10^6 – 1 x 10^7 and harvested by spinning for 8 min at 1500g. The pellet was washed once in PBS. For whole cells 1x10^7 cells were boiled at 100°C in 100 μl hot Laemmli buffer for 5min. For cytoskeletal and soluble fraction cells were harvested by spinning, washed once in PBS and then spun down again. The supernatant was discarded and the pellet resuspended in 1% NP-40 in PEM buffer containing protease inhibitor (Roche cOmplete Mini EDTA free, #Cat: 11826153001). The solution was

incubated for 2 minutes and then spun down at full speed for 30 seconds. For the soluble fraction 50 µl of the supernatant were transferred and then boiled in 50µl of 2x hot Laemmli buffer at 100°C for 5 minutes. To obtain the cytoskeleton fraction the pellet was resuspended in 100 µl of hot Laemmli buffer and boiled at 100°C for 5 minutes. Before loading onto sodium dodecyl sulfate-polyacrylamide gel (SDS-PAGE) gels the samples were spun down at full speed for 5 minutes, to precipitate the DNA. Proteins were separated in Mini-PROTEAN TGX Precast gels from BIO-RAD (7.5% cat: #4561021 or 4 – 15% gradient gel cat: #4561083) with the BIO-RAD running system in Tris / Glycine / SDS – buffer (BIO-RAD cat: #1610772). Proteins were then transferred onto Nitrocellulose or PVDF membranes (Trans-Blot Turbo Transfer Pack BIO-RAD cat: #1704158 and #1704156) using the Trans-Blot Turbo transfer system of BIO-RAD. Membranes were then washed once in PBS-Tween (0.1%) and blocked for 1 hour at room temperature in 5% milk powder in PBS. After blocking, the membranes were washed once in 2.5% milk PBS. The membranes were then treated with different antibodies: To detect Ty-1 tagged tubulin BB2 (mouse monoclonal, 1/10 diluted in 2.5% milk PBS) was used. To detect polyglutamylated tubulin Poly-E (rabbit polyclonal 1/10000 in 2.5% milk PBS, original publication by Shang et al. 2002, obtained from Rogowski et al. 2010) and GT335 (mouse monoclonal 1/1000, (Wolff et al., 1992)) were used. To detect tyrosinated tubulin, YL1/2 (rat monoclonal 1/1000, original publication by (Kilmartin et al., 1971) obtained from Thermo Fisher scientific cat: # MA1-80017) was used. To detect alpha-tubulin, TAT-1 (mouse monoclonal 1:500, (Woods et al., 1989) was used. To detect acetylated tubulin, C3B9 (1/50 Woods et al., 1989) and 6-11B-1 (mouse monoclonal IgG2b, invitrogen Thermo Fisher Scientific cat:# **32-2700**) were used. The membranes were incubated for 1 hour at room temperature or overnight at 4°C. After primary antibody incubation, the blots were washed in 0.1% Tween in PBS 3 times for 10 minutes. Secondary antibodies were added in 2.5% milk in PBS: ECL™ Anti-mouse IgG, Horseradish Peroxidase-Linked (Amersham™ from Cytiva, #Cat: NA931-100 µl, 1 : 10`000), Anti-rabbit IgG, Horseradish Peroxidase-Linked (Amersham™ from Cytiva, #Cat: NA934-100 µl, 1 : 10`000), Anti-rat IgG, Horseradish Peroxidase-Linked

(Amersham™ from Cytiva, #Cat: NA935-1 ml, 1 : 10`000) and the blots incubated at room temperature for 1 hour. Membranes were then washed in 0.1% Tween in PBS 3 times for 10 minutes. The blots were then incubated with ECL Select™ Western Blotting Detection Reagent for 5 minutes and revealed with an Amersham™ ImageQuant 800.

Tetracycline induction and washout of α-Ty1-tub pHD360 cell line:

To measure the assembly rate of the axoneme, a culture between 5 x 10^6 – 1 x 10^7 cells/ml was split into five flasks. Tetracycline (1μg / ml) was added to a new flask in 30 min intervals to obtain a time course of 2 – 4h. Cells were then harvested at the same time by centrifugation and subject of analysis by IFA and western blot. De-Induction experiments were performed to monitor the disappearance of Ty-1-tubulin over several cell cycles. A culture in logarithmic growth phase was induced with tetracycline and diluted to 2 x 10^6 every 24h. After 48h de-induction was started: the cells were washed with medium (supplemented with 10% FBS and Hemin) four times and then placed into fresh medium. Cells were diluted every 24h to 2 x 10^6 cells/ml and monitored by IFA at 24h, 48 and 72h post de-induction. From every time point whole cells, cytoskeletal and flagella extracts were harvested as described in the immunofluorescence assay section. To determine the timing of the locking event an experiment was carried out where cell division was inhibited ahead of tetracycline addition. A culture was diluted to 4 x 10^6 cells/ml and then grown in the presence of 10mM teniposide (Sigma cat: #SML0609 – 10MG) for 15h. Tetracycline was then added to the culture and samples taken at 6h and 9h. Cells were then analysed by IFA as described previously.

Measuring of flagella length:

The length of flagella was measured in the fluorescent channels of pictures from flagella extracts (as described above). Length was assessed in the individual channels of composites from BB2 and FTZC/Mab25 (the latter two on the same wavelength). Length was measured

with the segmented line tool of ImageJ. Whole length of mature flagella was measured from the proximal part of the FTZ-C marker to the distal tip of the Mab25 portion. The green new flagellum and the green portion of the mature flagellum (Fig. 2 and 5) were measured in the “BB2 channel”. Images were normalized for the individual experiments and the green new flagellum was measured from the proximal part to to tip (without regards to FTZC position). The green portion of the old flagellum (Results Fig. 21) or new flagellum from the proximal portion (beginning of the gradient) to the tip.

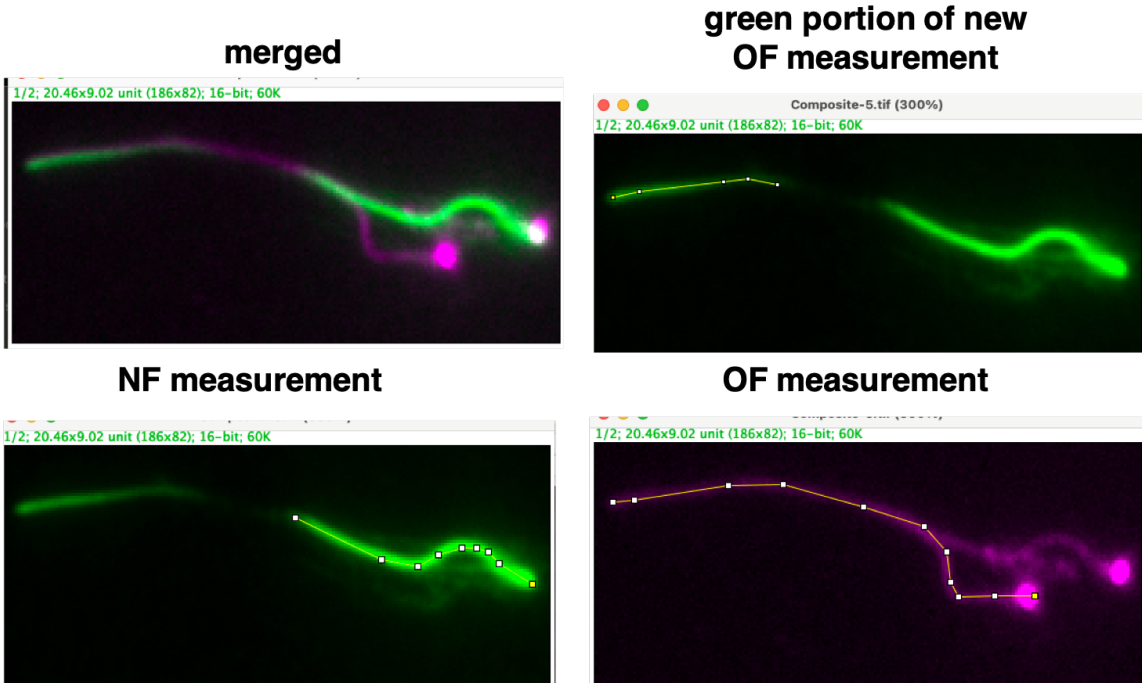

Figure 3 : Illustration how the different parts of bi-flagellated cells were measured. Segmented line was drawn in ImageJ and then measured with the M command.

LC/MS/MS to asses tagged tubulin acetylation

Purification of flagella

3 x 10^7 cells were harvested and washed in SDM-79 without serum for 3 times. They were then resuspended in 300 μl of 1% NP-40 in PEM buffer containing protease inhibitor (Roche cOmplete Mini EDTA free, #Cat: 11826153001) and 1 μl benzonase and then incubated for 15 min at RT. After that they were spun down and resuspended again in 1% NP-40 in PEM buffer containing protease inhibitor without benzonase. Samples were incubated at RT for 2 minutes and then spun down and washed in PEM buffer. Incubation in 1% NP-40 in PEM buffer followed by washing was repeated twice more and the samples spun down at full speed. They were then resuspended in 1ml of 1M NaCl and incubated for 15 min. The samples were then spun down and washed in PBS and the NaCl treatment repeated one more time. After a last washing step, the samples were resuspended in water and the purity of the preparation was assessed at the microscope. The samples were then spun down and all supernatant was removed. The pellet containing purified flagella was stored at -80 degrees.

LC/MS/MS carried out by the massspectrometry plattform at IP Pasteur.

The peptides were reconstituted in 2% ACN, 0.1% FA. LC-MS/MS analysis of digested peptides was performed on an Orbitrap Fusion Lumos mass spectrometer (Thermo Fisher Scientific, Bremen) coupled to an EASY-nLC 1000 (Thermo Fisher Scientific). A home-made column was used for peptide separation (C18, 30 cm capillary column picotip silica emitter tip, 75 µm diameter filled with 1.9 µm Reprosil- Pur Basic C18-HD resin (Dr. Maisch GmbH, Ammerbuch-Entringen, Germany)). The column was equilibrated and the samples were loaded in solvent A (0.1 % FA) at 900 bars. The peptides were separated and eluted at 300 nl.min-1 flow using an increasing gradient of solvent B (80% ACN, 0.1 % FA) from 2% to 31% in 70 min, 31% to 60% in 25 min (total length of the chromatographic run was 113 min including high ACN level steps and column regeneration). Mass spectra were acquired in datadependent acquisition mode using the XCalibur 2.2 software (Thermo Fisher Scientific, Bremen) with

automatic switching between MS and MS/MS scans using a 3 s cycle time method. MS spectra were recorded at a resolution of 60000 (at m/z 400) with a target value of 4 Å~ 105 ions over a maximum injection time of 50 ms. The scan range was set from 300 to 1700 m/z. Peptide fragmentation was performed using either CID (collision energy 35%, activation time 10 ms and activation Q 0.25) or EThcD (ETD reaction time 50 ms, supplemental activation using HCD at 20 %). All MSMS were recorded in the Orbitrap cell at a resolution of 15000 (at m/z 400). Intensity threshold for ions selection was set at 1 Å~ 105 ions with charge exclusion of z = 1 and z > 7. Isolation window was set at 1.6 Th. Dynamic exclusion was employed within 25 s.

Methods

Discussion

Introduction

To study flagellum construction and length control, we chose to investigate assembly with the flagellum's main component tubulin. As assembly is a dynamic process we developed a tool that offers flexibility in terms of timing.

We therefore chose to introduce a tagged ectopic copy of alpha-tubulin under the regulation of the tetracycline repressor system, allowing us to inducibly express tagged tubulin and follow flagellar assembly by tracking its main component. Inducible expression offers the temporal resolution needed to observe flagellar elongation but also the option to trace these organelles over more than one generation. The main conundrum of this work is that tagging tubulin in trypanosomes is delicate. Multiple attempts have failed in the past to tag tubulin in a way it gets incorporated into flagella. N- or C-terminal tagging was not successful, so we looked for other possible sites. We have chosen to tag alpha-tubulin with an intragenic Ty-1-tag inside a the acetylation loop, a structure that is oriented towards the MT lumen and seems to be invisible for most interacting partners (Janke and Magiera, 2020; Soppina et al., 2012). This approach has been successfully carried out in yeast and mammalian cells and up to 17 AA could be introduced one AA after the acetylated lysine (K40) without impairing tubulin function or the cells viability (Schatz et al., 1987; Sirajuddin et al., 2014).

Here we report, that tubulin tagged with this method, can be inducible expressed and is incorporated into MTs as efficiently as endogenous untagged tubulin. Furthermore, this system allowed us to further validate but also challenge aspects of the grow and lock model.

Tagged tubulin is incorporated into MTs as efficiently as untagged tubulin.

Our first goal was to develop a strategy that allowed us to judge if the presence of a Ty-1-tag inside alpha-tubulins acetylation loop is compatible with the protein's integration into MTs. We designed a construct for *in situ* tagging that did not alter the regulatory UTRs of alpha-tubulin. As we cannot rule out that previous attempts had failed due to the untimely expression of the tagged tubulin, this was done to avoid artifacts related to the transcription of tagged tubulin rather than the presence of the tag inside the protein. We therefore chose a construct in which the first 500bp of the alpha-tubulin ORF, encoding the epitope tag, would recombine into the context of the regular tubulin-UTR. With the selected construct, the tagged gene should be positioned downstream of the beta-alpha-intergenic region upstream of the endogenous 3'UTR of alpha-tubulin.

Since it was published that up to 17 AA can be introduced into the acetylation loop (Schatz et al., 1987), we attempted to tag tubulin with one or two 10 amino acid-long Ty-1-tags. These experiments revealed that up to 20AA can be inserted into the acetylation loop of *T. brucei* alpha-tubulin without impairing its incorporation in microtubules, its function or cell viability. When we compared tubulin localization after clonal dilution, we noticed that the signal was more uniform between individual cells. As this construct can recombine into forty loci, it is conceivable that the tagged tubulin construct could have recombined multiple times in some cells. This would be an explanation for the heterogeneity between individual cells that disappeared after clonal dilution.

With the use of detergent extracted cytoskeletons, we were able to show that tagged tubulin is indeed incorporated into MTs and not just soluble in the cytoplasm. Based on fractionation and WB analysis, this integration was as efficient as the integration of untagged tubulin. A curious observation we made, was that the relative signal between the flagellar MTs and the MTs of the cell body was more intense in flagella for tagged tubulin than it was for the TAT-1

antibody that recognises an epitope towards alpha-tubulins C-terminus (Fig. 1, TAT-1 epitope red). The MTs of the flagellum are doublets decorated with many accessory proteins while the MTs of the cell body are singlets. It is possible that the epitopes on MTs of the cell body are more accessible for TAT-1 compared to the ones in the flagellum. Indeed, the TAT-1 antibody should, according to literature (Woods et al., 1989), recognize all forms of alpha-tubulin, but the actual impact of PTM has not been investigated. However, it only stains the mitotic spindle very weakly or not at all. BB2 on the other hand labels tagged tubulin inside the mitotic spindle very well and so do antibodies that recognise acetylated tubulin (C3B9 and 6-11-B1)(Sasse et al JS1988) (Piperno and Fuller, 1985; Woods et al., 1989) (Fig. 1, K40 acetylation highlighted in cyan). These antibodies bind in the proximity of the acetylated lysine and therefore recognise an epitope very close to where tagged tubulin was inserted, one AA after the acetylated lysine (Fig. 1, Ty-1-tag, highlighted in green). Taken together, it is conceivable that the TAT-1 epitope is differentially accessible between different MT based structures.

When we tested the presence of acetylation on tagged tubulin we noticed that antibodies that recognize this modification did not yield a second band corresponding to tagged tubulin on WB. Since it has been reported that all alpha-tubulin is acetylated we hypothesize that the absence is owed to the fact that C3B9 and 6-11B-1 can no longer recognise their epitope due to the insertion of the tag one AA after the acetylated lysine. Indeed, mass spectrometry revealed that Ty-1-tag specific peptides were in fact acetylated.

We then proceeded to compare the integration of tagged tubulin into the cytoskeleton by WBs stained with the TAT-1 antibody and found that the profile of tagged tubulin in whole cells, detergent extracted and soluble fractions matched the one of endogenous tubulin very well. This we could show as the Ty-1-tagged protein migrated slightly above the endogenous tubulin and could therefore be distinguished. An observation similar to the one made for Ty-1-tagged PFR2 (Bastin et al., 1999). Both proteins shifted on WBs by a size difference not expected for the added molecular weight of 1.2 kDa per Ty-1-eptiope. Unexpected but nonetheless useful to investigate the presence of PTMs on tagged tubulin.

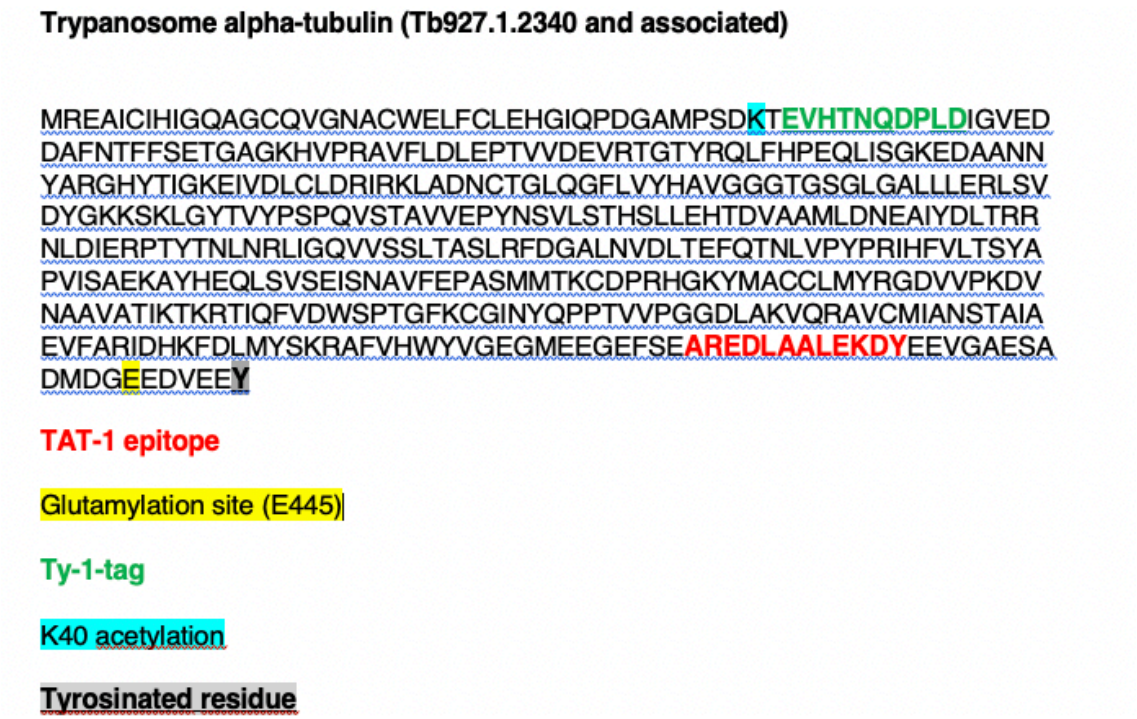

Figure 1 : AA sequence of the *T.brucei* alpha-tubulin ORF including the intragenic Ty-1-tag (green). Marked are specific sites known for PTMs and antibody binding epitopes: Red: The epitope recognized by the alpha-tubulin specific TAT-1 antibody, Yellow: Glutamylation site at Glutamate pos E445, Cyan: The acetylated lysine K40. Grey: The tyrosine residue that is subject to de-tyrosination and re-tyrosination.

Tagged tubulin can be used to follow assembly dynamics of MTs

As integration of in situ tagged tubulin was successful we proceeded to introduce an ectopic copy of tagged tubulin under the regulation of a tetracycline operator. The tetracycline repressor was then added in a subsequent transfection. Repression of tagged tubulin expression was efficient and leakiness was only observed in few cells. After the addition of tetracycline, tagged tubulin was expressed and localized to known MT based structures, namely the flagellar MTs, the MTs of the subpellicular array and the mitotic spindle.

We also observed tagged tubulin localized on the cells dorsal side along the flagellum in the vicinity of the new flagellum FAZ. Similar to what was seen when Sheriff et al. 2014 induced the expression of YFP-tagged tubulin.

This indicates integration of new tubulin in the ultimate proximity of the FAZ while the new flagellum is made. New tubulin might be integrated in the adjacent MTs of the subpellicular array, as the FAZ is positioned in a gap between the singlets. But this localisation could also correspond to the four MTs of the MT quartet (Introduction Fig. 7), which is also positioned in this gap.

We could reproduce the pattern observed by Sheriff and colleagues with cytoskeleton extracts although we have not performed co-localization with FAZ markers. As we have not performed high-resolution microscopy with antibodies that co-localize with the microtubule quartet either, we cannot claim that this structure incorporated tagged tubulin as well.

Based on our results from WBs we knew that tagged tubulin was available ~1 hour after induction, the inducible system provided therefore enough sensitivity to track MT assembly dynamics at shorter induction times 2-4h.

In these experiments newly, produced tagged tubulin integrated in the posterior part of the cell body. Its presence then extends in anterior direction over longer induction time. Our results therefore re-produce the localization of Sheriff and colleagues, as recently produced YFP-tagged tubulin in their experiments localized in the posterior of the cell (Introduction Fig. 10 compared to Results Fig. 13+14).

Additionally, our findings also further validated YL1/2 as a marker for recently assembled tubulin. This antibody recognizes the tyrosinated residue at the end of the protein (Fig. 1, tyrosinated residue highlighted in grey) and also stains the cell posterior as well as the new flagellum similar to early inductions of tagged tubulin.

However, this antibody has limitations, as is not known how fast the de-tyrosination reaction is. Indeed, in our hands tagged tubulin was present in the mitotic spindle after just 2 - 2.5 hours post induction, YL1/2 however, does not stain the spindle (Sherwin et al., 1987a; Sherwin and Gull', 1989; van der Laan et al., 2019). This indicates that de-tyrosination of spindle MTs is rather fast in this structure.

Furthermore, re-tyrosination, although not present in flagella, could bias the interpretation when investigating the presence of newly synthesized tubulin. Lastly, the YL1/2 antibody cross reacts with other proteins such as RP2 in the area between the BB and the TZ (Andre et al., 2014; Jung et al., 2021).

We did perform co-localization with a commercial YI1/2 antibody and observed very convincing co-localization when tagged tubulin was induced for 4 hours. However, the manufacturer of the rat-derived YI1/2 antibody mentioned possible cross-reactivity with mouse antibodies. As the tag specific BB2 antibody is a mouse Igg1 antibody we remain cautious to derive conclusions from this experiment, as we indeed observed some minor cross reactivity when different combinations of mouse and rat specific secondary antibodies were tested.

Taken together the integration of tagged tubulin after induction is coherent with what is reported in the literature for recently assembled tubulin. Integration into the cytoskeleton was as efficient as untagged tubulin and we even observed that the ratio between cytoskeleton vs. soluble fraction was a little bit higher for tagged tubulin. This is in stark contrast to what was previously reported for N-terminally tagged, ectopically expressed, alpha or beta-tubulin where a substantial portion had not integrated into MTs and remained soluble (Lee et al., 2023; Sheriff et al., 2014). We concluded that the here described inducible expression system is an excellent tool to study MT dynamics.

The assembly rate

As we knew that the inducible system is suitable to track MT dynamics with temporal sensitivity we proceeded to measure the assembly rate of the axoneme. First, we validated that new tubulin is indeed added at the distal tip of growing flagella. We then proceeded to measure the portion in these flagella were tagged tubulin had incorporated.

Based on our measurements we concluded that axoneme elongation of the NF occurs at a linear rate of ~2.9μm / hour. This assembly rate is a bit slower compared to the one that was measured for the PFR at 3.6μm/h (Bastin et al., 1999).

However, the PFR only emerges after the flagellum exits the FP and its assembly is therefore delayed in comparison to the axoneme. It is conceivable that the PFR building blocks can be added at a faster pace as the flagellum stem is already present.

A constant assembly rate is intriguing as it allows us to speculate if flagellum assembly in Trypanosomes adheres to one of the currently described models.

1) The balance point model: Elongation occurs when the assembly rate is larger than the dis-assembly rate. Vice versa, flagella shorten when dis-assembly exceeds assembly.

This strategy offers organisms a dynamic mechanism to adjust flagellar length. Chlamydomonas for example utilizes a constant dis-assembly rate to control the length of their flagella. When they need to maintain a flagellum at a certain length they adjust the assembly rate so it matches the dis-assembly rate. At this point the flagellum does therefore neither shorten nor lengthen.

This would be possible for trypanosomes but as the assembly rate appears to be constant they would need to adjust the dis-assembly rate instead. As shortening has not been observed when the assembly rate was slowed down in trypanosomes this is unlikely to be the case (Bertiaux et al., 2018; Bertiaux and Bastin, 2020).

2) Limited pool model: This model describes how a limited pool of constituents governs the length of the flagellum. When cells run out of building blocks (like tubulin) they cannot elongate the flagellum any further.

However, the limitation of tubulin does not necessarily need to be restricted at the site of production. Tubulin could also be prevented from entering the flagellum or from integration into the axoneme (Equal (or unequal) access-model) (Bertiaux and Bastin, 2020).

In the case of trypanosomes that elongate a NF while maintaining an OF, the access could be restricted in just the OF to avoid competition for a limited pool of constituents. Indeed, this is currently best explanation how trypanosomes control the length of their flagella and summarized as the grow-and-lock model. As we now have suitable system to test which flagella integrate new tubulin we challenged this model.

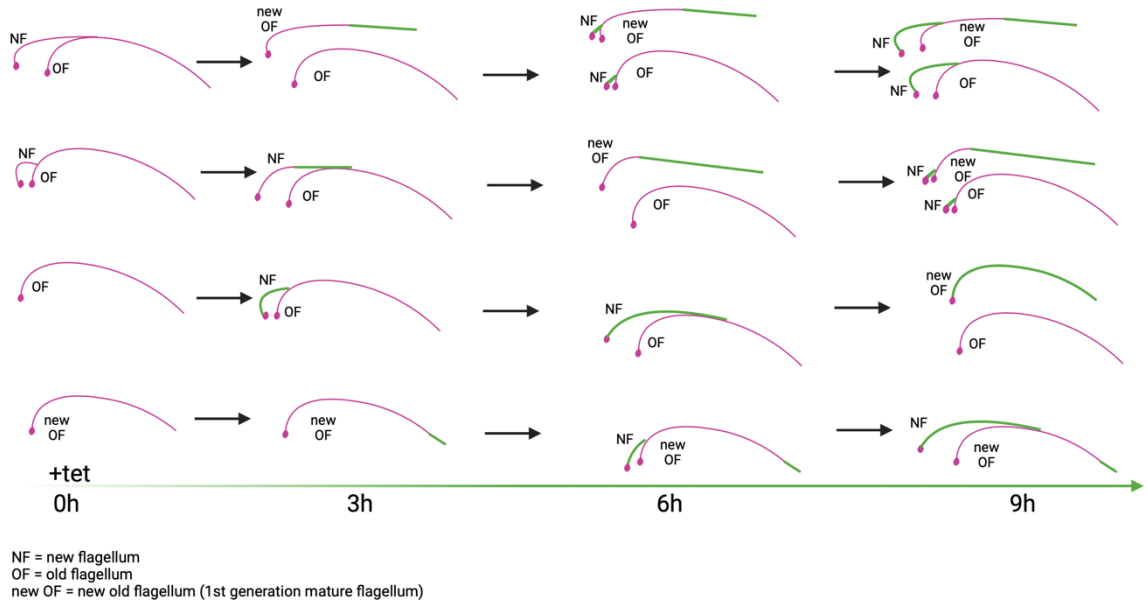

Figure 2 : Model of a 9-hour induction of an asymmetrically dividing culture. 1) In the case of a cell having started assembly of a NF before tagged tubulin was induced, the NF is finished in the presence of tagged tubulin (green). The cell divides and the NF becomes an OF of first generation when its cell starts to assemble a NF on its own. By contrast, Integration of tagged tubulin into the initial OF is not observed if it is permanently locked. 2) Same as scenario 1 but in the case where assembly of NF was less advanced when expression of tagged tubulin was induced. 3) Situation of a uniflagellated cell whose OF was older than one generation and whose assembly is in theory finished before induction. Incorporation of tagged tubulin would only ever be seen in the NF if OF is definitely locked. 4) Same situation but with the flagellum being from first generation (i.e. from the daughter cell that inherited the new flagellum). The flagellum needs to finish assembly after cell division. After its cell starts to make a new flagellum, incorporation of tagged tubulin is seen at the tip of the OF and throughout this new flagellum.

Integration of tagged tubulin in OF of bi-flagellated cells is coherent with the locking model

The main focus of this work lies on how we can track the integration of new tubulin building blocks into new and old flagella. According to the grow-and-lock model, a flagellum is locked after it is constructed to full length. After that it is not subject to further elongation or shortening. NF are constructed alongside the OF up to 80% of the length of the OF, the cells then divide and the NF finishes assembly after division.

Based on the conducted experiments we derived a model how we expect new and old flagella to incorporate tubulin in a regular asymmetrically dividing culture. In the cartoon above four types of cells are depicted, scenarios 1 and 2 are the same but with a shifted timing of NF assembly. Scenario 1 depicts a cell with a mature flagellum that had already started the assembly of a NF a couple of hours before induction. Scenario 2 depicts a cell with a mature flagellum that had already started the assembly of a new flagellum before induction but later compared to scenario 1.

The initially new flagella of scenario 1 and 2 would over time become new old flagella (new OF or 1st generation-OF). According to the locking model old flagella are locked and assembly of new and old flagella can therefore not be simultaneous and must be sequential. Hence, a cell with a partially green NF and a partially green OF cannot exist as expression of tagged tubulin was induced after the NF had already emerged. That means if integration would occur at the tip of the OF this integration would be simultaneous with the elongation of the NF (Fig. 17, type 2a flagellum).

Scenarios 3 and 4 show cells in which assembly of a NF had started post-induction. In scenario 3 the flagellum had to be finished after cell division during induction. If given enough time this cell will start the assembly of a NF that incorporates tagged tubulin along its entire length. These cells will have incorporated tagged tubulin at the tip of the OF as well as the entire NF. In contrast, the cell in scenario 4 finished the assembly of its OF at a timepoint before induction.

If given enough time it will start the assembly of a NF that incorporates tagged tubulin along the entire length but it will not incorporate tagged tubulin in the OF as it was locked pre-induction. The typical duration of a cell in G1-phase (mono-flagellated stage) is ~3h (Ploubidou, et al. 1999.), however, this can be variable between cells (Muniz et al., 2022).

In our experiments, after shorter inductions (<2.5 hours) integration in both NF and OF was not observed. We hypothesize that this duration is not enough for cells to finish a flagellum post-division, then go through G1-phase and start the assembly of a NF (Results Fig. 17C, type 1a flagellum). After longer induction times, cells that incorporated tagged tubulin at the tip of the OF and along the whole length of the short NF, became more common. This finding further strengthened our findings that integration of tagged tubulin in OF occurs before the assembly of a NF was initiated and that OF must therefore be locked pre-NF emergence. In addition, we never observed cells that had integrated tagged tubulin only in the distal portion of both NF and OF. Together, this is strong evidence that OF of bi-flagellated cells indeed adhere to the grow-and-lock model and do not incorporate tubulin while a NF is assembled.

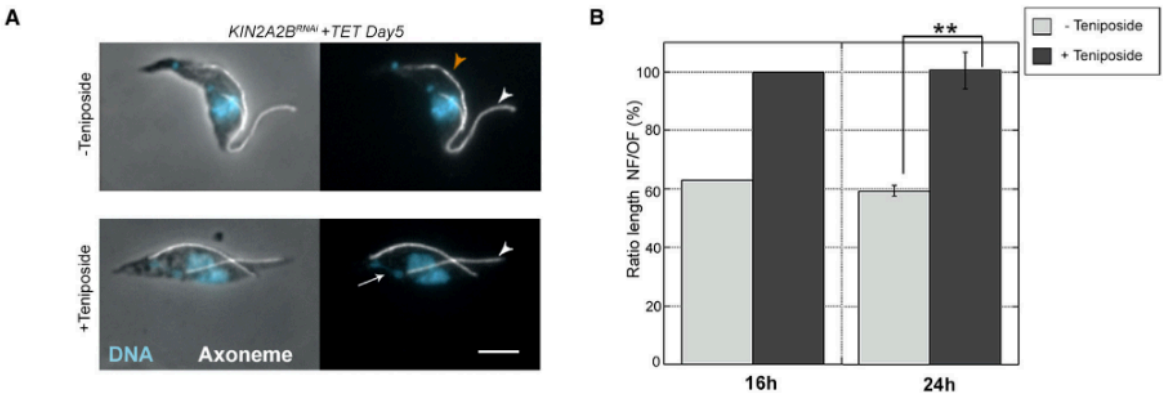

Figure 3 : Teniposide experiments that show the timing of the locking event. In the absence of teniposide NF are constructed to ~60% of the length of the OF. When treated with teniposide, NF can catch up in length to the OF when cell division is inhibited but do not extend further. Meaning these cells constructed their NF to full length and locked it before cell division.

The time at which cells commit to the locking event was determined to be before cell division (Bertiaux et al., 2018). The authors inhibited cell division via the addition of teniposide, a drug that prevents the kinetoplast from segregation and therefore halts division of the entire cell. We reproduced this experiment with the inducible tagged tubulin system by adding teniposide to a culture for 15 hours ahead of tetracycline induction. Judging from our assembly rate experiments, at this stage, both flagella should have had enough time to be constructed to full length and should therefore be locked. If the cells indeed commit to this mechanism ahead of cell division, no integration into NF or OF should be observed. Cells were then induced for 6 hours as this is enough time to observe substantial integration of tagged tubulin into flagella.

In a regular 6-hour induction the cells incorporated tagged tubulin into the posterior cell body as well as in the NF but not the OF and also in the mitotic spindle (Fig. 19).

When cells were treated with teniposide ahead of induction, they were still able to integrate tagged tubulin into the MTs of the cell body, although to a lesser extent compared to untreated. However, the teniposide treated cells did not incorporate tagged tubulin into their flagella in a manner comparably to untreated cells. Apart from integration at some flagellar tips no notable elongation with integrated tagged tubulin was observed. Which was confirmed when the experiment was repeated with flagellar extracts (Fig. 19).

From this we concluded that the integration of tagged tubulin was prevented in NF and OF of cells that could not undergo division. These results are compatible with the ones that led Bertiaux and colleagues to propose that cells commit to locking their flagella ahead of cell division. As NF of cells that were treated with teniposide and could not undergo division caught up in length to the OF but did not exceed it.

We concluded that the absence of tubulin integration in flagella of teniposide treated cells is compatible with the idea that cells commit to locking their flagella before cell division.

Are flagella locked forever?

When quantifying how many flagella had integrated tagged tubulin after 24h of induction we noticed that only a very small proportion had not incorporated any tagged tubulin (2%, Fig. 26) after 24h post-induction. Under the pretense that OF stay locked forever and never integrate new material after they are locked we would expect 25% -12.5% of flagella to not incorporate any tagged tubulin after 2-3 cell cycles.

This was not observed, instead the only type of flagella that we found to adhere to these numbers were flagella that had incorporated tagged tubulin at the distal tip (~1 μm) (Fig. 26, blue arrow). After 9 hours of induction (one cell cycle) this type of OF was with 37% the most abundant type (Fig. 22, type2). Additionally, they were the longest OF type while the new OF (1st generation OF) were the shortest (Fig 22). These new OF could be distinguished because they had integrated tagged tubulin along an increasingly more intense gradient, suggesting that the proportion of tagged vs. untagged material had increased during induction time.

As the length of the NF is a good temporal marker of the cell cycle, we compared the length of NF to the presence or absence of staining at the tip of the corresponding OF. Indeed, when NF length of type1 (absence of green tip) and type 2 (presence of green tip) are compared there is little overlap (Fig. 23A). This could mean that integration of tagged tubulin at the tip in OF of bi-flagellated cells is cell cycle dependent.

Finish of assembly vs. turnover

Since type 3 flagella are the most recently assembled type of OF and also the shortest it is possible that the integration at the tip corresponds to a last elongation step that a flagellum needs to undergo to reach full length. It is conceivable that this occurs during a G1-phase because we know OF of bi-flagellated cells are locked and don't integrate tagged tubulin.

It was observed that after knockdown of a GFP-tagged flagellar component (TAX-2), cells had started to incorporate new material that was not stained with GFP. The length of that portion

was ~1μm. The authors attributed this to post-division axonemal growth and not turn-over as the frequency of these flagella did not exceed ~66% after 24h (Farr and Gull, 2009). This length is consistent with the short portion at the tip observed for type 2 flagella in 9-hour inductions.

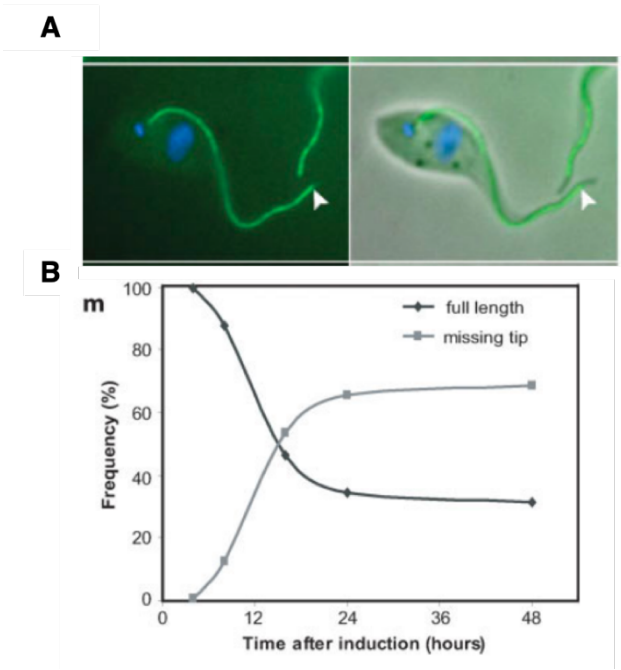

Fig. 4: A: Upon knockdown of TAX-2 a population of flagella arises that incorporated new material at the distal tip of the old flagellum.B: Over time the the number of these flagella increased put plateaued around 66%.

To get an idea to what extent the axoneme has been remodeled after multiple cell cycles, we performed de-induction experiments (pulse-chase) in the inducible tagged tubulin cell line. For that purpose, tetracycline was added for periods of 24 – 72 hours (pulse). Tetracycline was then washed out and the cells grown in its absence for 48 hours. They were then analysed by IFA (chase). After the initial induction, we observed that new and mature flagella had incorporated tagged tubulin from the flagellum base to the distal tip as previously described. For simplicity, we call them “green flagella”. 48 hours after washing out tetracycline (de-induction) when we chased for these green flagella almost all had a portion at the tip (1-2 μm on average) where only untagged tubulin had integrated (Fig. 27,+24h,-48h and Fig. 28). If new flagella would be finished to full length in the first G1-phase after division they should incorporate tagged tubulin up to the end of the distal tip (Fig. 24, fully green flagella). At that point they should be locked.

Only flagella that had emerged during the last cell cycle of the induction did not receive enough time to finish assembly and lock their flagella. These will need to integrate untagged tubulin to finish assembly. Since one cell cycle is one duplication the unfinished flagella should represent around 50% of the green flagella that were chased. The other 50% of chased green flagella should remain fully green as they are locked.

However, the number of fully green flagella was lower than 5%. This suggests that the tip of flagella is subject to incorporation after more than one generation. Even when the initial induction was prolonged more than 95% of chased green flagella had integrated untagged tubulin at the tip. Together this makes it unlikely that NF are finished during their first G1-phase. This was coherent with the fact that OF with a gradient (1st generation OF) were slightly shorter than other OF. Similar to the reasoning of (Farr and Gull 2007) the two most likely explanations for this observation are: 1.) slow finish of assembly over several cell cycles OR 2.) the presence of turn-over.

When tubulin expression was re-induced for 4h in washed-out cells, however, the tip of mature flagella in bi-flagellated cells showed no incorporation (Fig. 25D, Fig. 27 +tet24h,-tet48h+tet4h), indicating that if there is turnover, it is not present in bi-flagellated cells. This also further strengthens our finding that OF of bi-flagellated cells are locked. It also meant that OF from bi-flagellated cells were locked multiple generations after their emergence.

Now the conundrum becomes apparent: Were these flagella locked all the time or did they get unlocked to finish assembly?

In agreement with Farr and Gull we hypothesize that flagella are first assembled as new flagella, but then these flagella have to be finished in subsequent generations. However, if OF of bi-flagellated cells are locked but new OF (1st generation OF) are not full length how does this elongation happen without the removal of the lock?

We suggest the following model: NF are constructed to 80% of the length of OF. The cells divide and the NF has to be finished post division. This process must be halted once the assembly of a new flagellum is initiated, possibly to avoid competition for building blocks like

tubulin. This is consistent with the localization pattern of Cep164C reported by (Atkins et al. 2021). A protein candidate for the locking model that localizes to the transition fibers of the mature flagellum. A knockdown of Cep164C results in cells carrying longer old and shorter new flagella, consistent with the idea that the lock prevents competition between NF and OF. Localization studies show that 60% of mono-flagellated cells do not have Cep164C. This means that the cells need to acquire CEP164C before they can start to assemble a NF. The absence of CEP164C in 60% of G1-phase could correspond to NF after division that did not acquire the protein yet OR it could mark the disappearance from a previously OF that needs to undergo another elongation step.

This begs the question: If new OF can become unlocked again to finish assembly and possess the ability to re-apply the locking mechanism, can flagella from older generations do this too or does this only happen once? If indeed removal and re-application of the lock is a more constant occurrence, we are no longer looking at a process explicable with the absence of turn over. As addition of new tubulin every time when the lock is removed would result in elongation.

Is there evidence for the presence of turnover?

In the previously described washout experiments, 95-99% of all chased green flagella had only untagged tubulin incorporated at the tip. This finding is more consistent with turnover rather than only finishing assembly. If a NF is finished right after the first division the proportion of fully green cells would be 50%, in the next cell cycle 25% then 12.5% and so on and so forth. To reach 5% the finishing of flagellum assembly would need to take 4-5 generations. Additionally, only a minor portion of OF did not integrate tagged tubulin after 24 hours of induction. Together these findings are more consistent with turn-over rather than just post-division assembly.

However, since assembly is not observed in OF of bi-flagellated cells, the presence of constant disassembly in the OF while the NF is made would mean that OF of cells with a relatively

longer NF would have spent relatively more time dis-assembling in the absence of re-assembly. Which would mean that cells with longer new flagella would have to have relatively shorter mature flagella.

Such a correlation however, is not observed (Results Fig. 17, magenta dots) which means if there is disassembly, it is not present at all times. Begging the question, of whether assembly and disassembly, if present at all, are also cell cycle-dependent.

The washout experiments delivered some evidence for this as we found mono-flagellated green flagella with an unstained tip that, after re-induction, had incorporated tagged tubulin again at the distal end of the unstained tip. (Fig. 27, mono-flagellate after re-induction). These experiments have to be repeated to quantify how commonly this occurs, however, the fact that this was seen in mono-flagellated cells is consistent with an elongation during G1-phase.

After consultation of the literature we found a protein that would be consistent with a turnover process. *Trypanosoma brucei* flagellar kinesin 13-2 has been linked to flagellar length control and is localized to the flagellum tip of new and old flagella. Upon knockdown of this protein cells constructed flagella that were to long (Blaineau et al., 2007). Although, a knockout of the same protein did not reproduce this phenotype a minor effect on new flagellum length was observed (Chan and Ersfeld, 2010). Intriguingly, this protein seems to be absent at the tip of old flagella in 2K2N2F cells (Tryptag.org) that are very advanced in the cell cycle. Should TbKif13-2 be involved in disassembly at the flagellum tip this localization might also explain cell cycle dependent absence of integration.

Concluding remarks

We can only speculate on the presence of turn-over at the flagellum tip. What we know is, that integration of tagged tubulin is exclusive to new flagella of bi-flagellated cells and that cells commit to locking their flagella when cell division is inhibited after the addition of teniposide.

But we also observed that a majority of OF incorporated tagged tubulin at their tip after several generations had passed. This integration might be post-division assembly as proposed by Farr and Gull or the presence of cell cycle dependent turn-over, or both. Measuring dis-assembly in the absence of re-assembly is very difficult as absence of proof is not proof of absence, especially if the two processes are cell cycle dependent. In other words, we cannot say if tagged tubulin at the tip was removed or never there to begin with.

Nonetheless, it is conceivable that there is a dis-assembly machinery present for faithful maintenance of length. Old flagella could indeed be subject to integration briefly during G1-phase when NF and OF do not compete for building blocks. Cep164C (the locking protein) is absent in 60% of G1-cells (Atkins et al., 2021) and its transcript peaks at late G1-phase (TriTrypDB.org), compatible with the re-application of the lock before the cell assembles a new flagellum. At last, we did observe mono-flagellated cells that had incorporated tagged tubulin again after 4-hour re-induction post washout. These cells have a very long green portion from the initial induction, followed by an unstained portion where only untagged tubulin had incorporated during the de-induction and then a green spot at the tip that corresponded to the re-induction (Fig. 4). As green cells after 5-6 generations are rare this was not assessed quantitatively, but it means that these flagella had still integrated tubulin at least twice, over several generations after their emergence, which again speaks for turn-over rather than just post-division assembly.

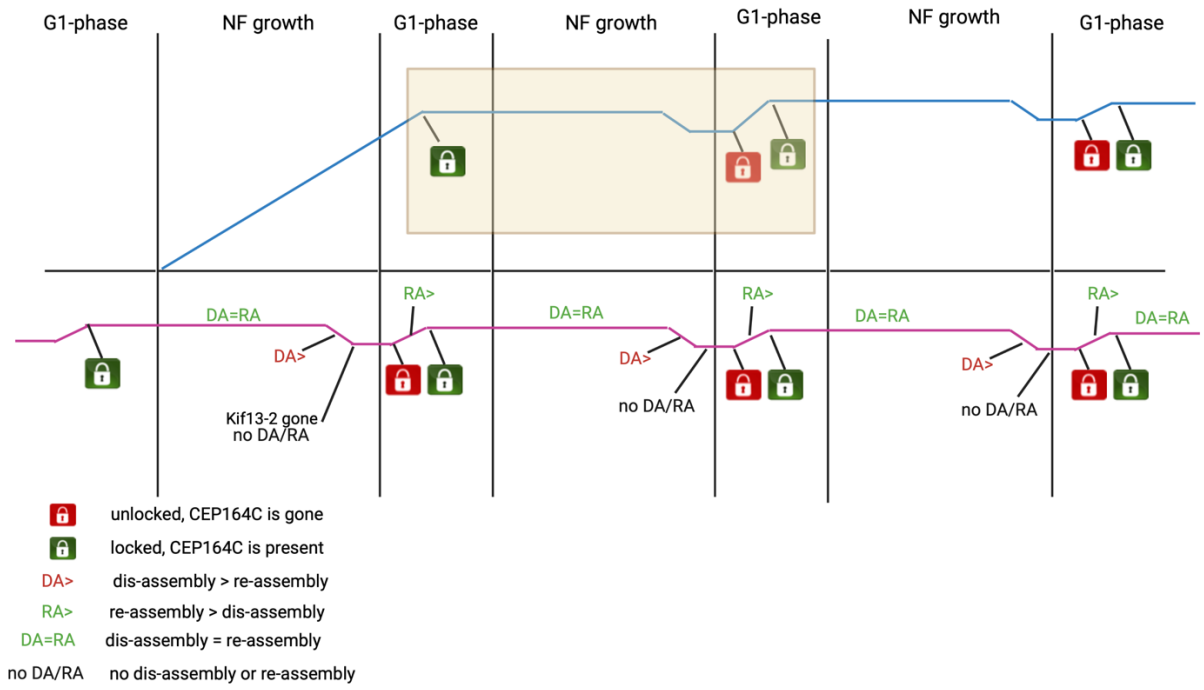

Figure 5 : Cartoon of how turnover could potentially occur in *T.brucei*. Seen in blue is the growth of the NF in magenta the OF. From left to right: The OF assembles to full length in the first G1-phase and is then locked, no further tubulin can gain access to the OF. A NF emerges and is assembled at a constant rate. Meanwhile the length of the OF is maintained at the same length since the assembly rate matches the dis-assembly rate (balance-point). How this could occur is explained in the next graph. At some point all tubulin is depleted and DA is higher than RA. This results in shortening. Towards the end of the NF growth the DA machinery in the OF disappears (for ex. coinciding with disappearance Kif-13-2) and shortening stops. The cells divide and CEP164C disappears from the OF. It can then re-assemble the tip again as it is not competing with the NF anymore and the lock is gone. Simultaneously the NF is elongating in G1-phase as well. At some point later in G1-phase CEP164C is applied to both flagella and they are now both locked.

To summarise, we speculate a model that is compatible with all our described results:
OF are locked in bi-flagellated cells and no more building blocks can enter the OF while the NF is assembled. The building blocks that are left in the OF pool manage to balance dis-assembly and re-assembly up to a point, at which the material is depleted. From this point on dis-assembly shortens the OF until the cells divide and the OF becomes unlocked again. It can then re-integrate new material during G1-phase while it does not compete with a NF. The lock is then re-applied at the end of G1-phase to prevent competition with the assembly of the next NF. At this stage this cycle repeats. Consistent with this hypothesis are the high number of unstained tips after washout (95%), the low number of tips with no integration of tagged tubulin after 24h-induction (2%) and the cell cycle dependent localization of CEP164C and TbKif13-2. As well as the seemingly cell cycle dependent absence of tagged tubulin at the tip of OF in bi-flagellated cells with very long NF.
Such a process cannot be measured with an epitope tag and requires a more dynamic approach, for example a fluorescent tag of a PFR protein in combination with fluorescence recovery after photobleaching (FRAP). Or an even more dynamic system like labeling of HALO-tagged proteins. GFP tagging of tubulin inside the acetylation loop was attempted and had failed (data not shown). It is therefore unlikely that larger tags can be incorporated in this structure. Nonetheless, PFR could be tagged with a HALO tag and the cells incubated with different substrates to test if a pattern of alternating substrates is observed at the flagellum tip. Additionally, we are currently trying to co-over-express alpha and beta-tubulin to investigate if the overabundance of both proteins leads to mis-regulation of flagellar length.

References

Absalon, S., Kohl, L., Branche, C., Blisnick, T., Toutirais, G., Rusconi, F., Cosson, J., Bonhivers, M., Robinson, D., Bastin, P., 2007. Basal body positioning is controlled by flagellum formation in Trypanosoma brucei. PLoS ONE 2. https://doi.org/10.1371/journal.pone.0000437

Alushin, G.M., Lander, G.C., Kellogg, E.H., Zhang, R., Baker, D., Nogales, E., 2014. High-Resolution Microtubule Structures Reveal the Structural Transitions in αβ-Tubulin upon GTP Hydrolysis. Cell 157, 1117–1129. https://doi.org/10.1016/j.cell.2014.03.053

Alves, A.A., Gabriel, H.B., Bezerra, M.J.R., De Souza, W., Vaughan, S., Cunha-e-Silva, N.L., Sunter, J.D., 2020. Control of assembly of extra-axonemal structures: the paraflagellar rod of trypanosomes. J. Cell Sci. 133, jcs242271. https://doi.org/10.1242/jcs.242271

Andre, J., Kerry, L., Qi, X., Hawkins, E., Drižytė, K., Ginger, M.L., McKean, P.G., 2014. An Alternative Model for the Role of RP2 Protein in Flagellum Assembly in the African Trypanosome. J. Biol. Chem. 289, 464–475. https://doi.org/10.1074/jbc.M113.509521

Atkins, M., Týč, J., Shafiq, S., Ahmed, M., Bertiaux, E., Neto, A.L.D.C., Sunter, J., Bastin, P., Dean, S.D., Vaughan, S., 2021. CEP164C regulates flagellum length in stable flagella. J. Cell Biol. 220. https://doi.org/10.1083/jcb.202001160

Bachmaier, S., Giacomelli, G., Calvo-Alvarez, E., Vieira, L.R., Van Den Abbeele, J., Aristodemou, A., Lorentzen, E., Gould, M.K., Brennand, A., Dupuy, J.-W., Forné, I., Imhof, A., Bramkamp, M., Salmon, D., Rotureau, B., Boshart, M., 2022. A multi-adenylate cyclase regulator at the flagellar tip controls African trypanosome transmission. Nat. Commun. 13, 5445. https://doi.org/10.1038/s41467-022-33108-z

Bastin, P., Bagherzadeh, A., Matthews, K.R., Gull, K., 1996. A novel epitope tag system to study protein targeting and organelle biogenesis in Trypanosoma brucei, Molecular and Biochemical Parasitology.

Bastin, P., Macrae, T.H., Francis, S.B., Matthews, K.R., Gull, K., 1999. Flagellar Morphogenesis: Protein Targeting and Assembly in the Paraflagellar Rod of Trypanosomes, MOLECULAR AND CELLULAR BIOLOGY.

Bastin, P., Pullen, T.J., Moreira-Leite, F.F., Gull, K., 2000. Inside and outside of the trypanosome flagellum: a multifunctional organelle.

Bastin, P., Sherwin, T., Gull, K., 1998. Paraflagellar rod is vital for Trypanosome motility. Nature 391, 548–548.

Beneke, T., Madden, R., Makin, L., Valli, J., Sunter, J., Gluenz, E., 2017. A CRISPR Cas9 high-throughput genome editing toolkit for kinetoplastids. R. Soc. Open Sci. 4, 170095. https://doi.org/10.1098/rsos.170095

Berriman, M., Ghedin, E., Hertz-Fowler, C., Blandin, G., Renauld, H., Bartholomeu, D.C., Lennard, N.J., Caler, E., Hamlin, N.E., Haas, B., Böhme, U., Hannick, L., Aslett, M.A., Shallom, J., Marcello, L., Hou, L., Wickstead, B., Cecilia Alsmark, U.M., Arrowsmith, C., Atkin, R.J., Barron, A.J., Bringaud, F., Brooks, K., Carrington, M., Cherevach, I., Chillingworth, T.-J., Churcher, C., Clark, L.N., Corton, C.H., Cronin, A., Davies, R.M., Doggett, J., Djikeng, A., Feldblyum, T., Field, M.C., Fraser, A., Goodhead, I., Hance, Z.,

Harper, D., Harris, B.R., Hauser, H., Hostetler, J., Ivens, A., Jagels, K., Johnson, D., Johnson, J., Jones, K., Kerhornou, A.X., Koo, H., Larke, N., Landfear, S., Larkin, C., Leech, V., Line, A., Lord, A., MacLeod, A., Mooney, P.J., Moule, S., A Martin, D.M., Morgan, G.W., Mungall, K., Norbertczak, H., Ormond, D., Pai, G., Peacock, C.S., Peterson, J., Quail, M.A., Rabbinowitsch, E., Rajandream, M.-A., Reitter, C., Salzberg, S.L., Sanders, M., Schobel, S., Sharp, S., Simmonds, M., Simpson, A.J., Tallon, L., Michael Turner, C.R., Tait, A., Tivey, A.R., Van Aken, S., Walker, D., Wanless, D., Wang, S., White, B., White, O., Whitehead, S., Woodward, J., Wortman, J., Adams, M.D., Martin Embley, T., Gull, K., Ullu, E., David Barry, J., Fairlamb, A.H., Opperdoes, F., Barrell, B.G., Donelson, J.E., Hall, N., Fraser, C.M., Melville, S.E., El-Sayed, N.M., 2005. The Genome of the African Trypanosome Trypanosoma brucei.

Bertiaux, E., Bastin, P., 2020. Dealing with several flagella in the same cell. Cell. Microbiol. 22. https://doi.org/10.1111/cmi.13162

Bertiaux, E., Morga, B., Blisnick, T., Rotureau, B., Bastin, P., 2018. A Grow-and-Lock Model for the Control of Flagellum Length in Trypanosomes. Curr. Biol. 28, 3802-3814.e3. https://doi.org/10.1016/j.cub.2018.10.031

Biebinger, S., Rettenmaier, S., Flaspohler, J., Hartmann, C., Pena-Diaz, J., Wirtz, L.E., Hotz, H.-R., Barry, J.D., Clayton, C., 1996. The PARP Promoter of Trypanosoma Brucei Is Developmentally Regulated in a Chromosomal Context. Nucleic Acids Res. 24, 1202–1211. https://doi.org/10.1093/nar/24.7.1202

Binder, L.I., Rosenbaum, J.L., 1978. The in vitro assembly of flagellar outer doublet tubulin. J. Cell Biol. 79, 500–515. https://doi.org/10.1083/jcb.79.2.500

Birkett, C.R., Foster, K.E., Johnson, L., Gull, K., 1985. Use of monoclonal antibodies to analyse the expression of a multi-tubulin family. FEBS Lett. 187, 211–218. https://doi.org/10.1016/0014-5793(85)81244-8

Blaineau, C., Tessier, M., Dubessay, P., Tasse, L., Crobu, L., Pagès, M., Bastien, P., 2007. A Novel Microtubule-Depolymerizing Kinesin Involved in Length Control of a Eukaryotic Flagellum. Curr. Biol. 17, 778–782. https://doi.org/10.1016/j.cub.2007.03.048

Bramhill, D., Thompson, C.M., 1994. GTP-dependent polymerization of Escherichia coli FtsZ protein to form tubules, Proc. Nati. Acad. Sci. USA.

Briggs, L.J., McKean, P.G., Baines, A., Moreira-Leite, F., Davidge, J., Vaughan, S., Gull, K., 2004. The flagella connector of Trypanosoma brucei: An unusual mobile transmembrane junction. J. Cell Sci. 117, 1641–1651. https://doi.org/10.1242/jcs.00995

Bringaud, Frédéric, Robinson, D.R., Barradeau, S., Biteau, N., Baltz, D., Baltz, T., Bringaud, F., 2000. Characterization and disruption of a new Trypanosoma brucei repetitive flagellum protein, using double-stranded RNA inhibition, Molecular and Biochemical Parasitology.

Broadhead, R., Dawe, H.R., Farr, H., Griffiths, S., Hart, S.R., Portman, N., Shaw, M.K., Ginger, M.L., Gaskell, S.J., McKean, P.G., Gull, K., 2006. Flagellar motility is required for the viability of the bloodstream trypanosome. Nature 440, 224–227. https://doi.org/10.1038/nature04541

Bruce, S.D., n.d. Obituary Notices of Fellows of the Royal Society Volume 1, Issue 1.

Buceta, J., Ibañes, M., Rasskin-Gutman, D., Okada, Y., Hirokawa, N., Izpisúa-Belmonte, J.C., 2005. Nodal Cilia Dynamics and the Specification of the Left/Right Axis in Early Vertebrate Embryo Development. Biophys. J. 89, 2199–2209. https://doi.org/10.1529/biophysj.105.063743

Camara, Mariame, Ouattara, E., Duvignaud, A., Migliani, R., Camara, O., Leno, M., Solano, P., Bucheton, B., Camara, Mamadou, Malvy, D., 2017. Impact of the Ebola outbreak on Trypanosoma brucei gambiense infection medical activities in coastal Guinea, 2014-2015: A retrospective analysis from the Guinean national Human African Trypanosomiasis control program. PLoS Negl. Trop. Dis. 11, e0006060. https://doi.org/10.1371/journal.pntd.0006060

Capewell, P., Cren-Travaillé, C., Marchesi, F., Johnston, P., Clucas, C., Benson, R.A., Gorman, T.-A., Calvo-Alvarez, E., Crouzols, A., Jouvion, G., Jamonneau, V., Weir, W., Stevenson, M.L., O'Neill, K., Cooper, A., Swar, N.K., Bucheton, B., Ngoyi, D.M., Garside, P., Rotureau, B., MacLeod, A., 2016. The skin is a significant but overlooked anatomical reservoir for vector-borne African trypanosomes. eLife 5, e17716. https://doi.org/10.7554/eLife.17716

Casanova, M., de Monbrison, F., van Dijk, J., Janke, C., Pagès, M., Bastien, P., 2015. Characterisation of polyglutamylases in trypanosomatids. Int. J. Parasitol. 45, 121–132. https://doi.org/10.1016/j.ijpara.2014.09.005

Chan, K.Y., Ersfeld, K., 2010. The role of the Kinesin-13 family protein TbKif13-2 in flagellar length control of Trypanosoma brucei. Mol. Biochem. Parasitol. 174, 137–140. https://doi.org/10.1016/j.molbiopara.2010.08.001

Cicconofri, G., Noselli, G., DeSimone, A., 2021. The biomechanical role of extra-axonemal structures in shaping the flagellar beat of Euglena gracilis. eLife 10, e58610. https://doi.org/10.7554/eLife.58610

Clayton, C., 2016. Gene expression in Kinetoplastids. Curr. Opin. Microbiol. 32, 46–51. https://doi.org/10.1016/j.mib.2016.04.018

Cordon-Obras, C., Gomez-Liñan, C., Torres-Rusillo, S., Vidal-Cobo, I., Lopez-Farfan, D., Barroso-del Jesus, A., Rojas-Barros, D., Carrington, M., Navarro, M., 2022. Identification of sequence-specific promoters driving polycistronic transcription initiation by RNA polymerase II in trypanosomes. Cell Rep. 38, 110221. https://doi.org/10.1016/j.celrep.2021.110221

Cross, G.A.M., Kim, H.S., Wickstead, B., 2014. Capturing the variant surface glycoprotein repertoire (the VSGnome) of Trypanosoma brucei Lister 427. Mol. Biochem. Parasitol. 195, 59–73. https://doi.org/10.1016/j.molbiopara.2014.06.004

Dacheux, D., Landrein, N., Thonnus, M., Gilbert, G., Sahin, A., Wodrich, H., Robinson, D.R., Bonhivers, M., 2012. A MAP6-Related Protein Is Present in Protozoa and Is Involved in Flagellum Motility. PLoS ONE 7, e31344. https://doi.org/10.1371/journal.pone.0031344

Daniels, J.-P., Gull, K., Wickstead, B., 2010. Cell Biology of the Trypanosome Genome. Microbiol. Mol. Biol. Rev. 74, 552–569. https://doi.org/10.1128/MMBR.00024-10

Davidge, J.A., Chambers, E., Dickinson, H.A., Towers, K., Ginger, M.L., McKean, P.G., Gull, K., 2006. Trypanosome IFT mutants provide insight into the motor location for mobility of the flagella connector and flagellar membrane formation. J. Cell Sci. 119, 3935–3943. https://doi.org/10.1242/jcs.03203

Dean, S., Moreira-Leite, F., Gull, K., 2019. Basalin is an evolutionarily unconstrained protein revealed via a conserved role in flagellum basal plate function. eLife 8, e42282. https://doi.org/10.7554/eLife.42282

Dean, S., Moreira-Leite, F., Varga, V., Gull, K., 2016. Cilium transition zone proteome reveals compartmentalization and differential dynamics of ciliopathy complexes. Proc. Natl. Acad. Sci. U. S. A. 113, E5135–E5143. https://doi.org/10.1073/pnas.1604258113

Dean, S., Sunter, J.D., Wheeler, R.J., 2017. TrypTag.org: A Trypanosome Genome-wide Protein Localisation Resource. Trends Parasitol. 33, 80–82. https://doi.org/10.1016/j.pt.2016.10.009

Despommier, D.D., Griffin, D.O., Gwadz, R.W., Hotez, P.J., Knirsch, C.A., Photographs, J.K., Griffin, D., 2017. Parasitic Diseases Sixth Edition.

Ersfeld, K., Melville, S.E., Gull, K., 1999. Nuclear and Genome Organization of Trypanosoma brucei. Parasitol. Today 15, 58–63. https://doi.org/10.1016/S0169-4758(98)01378-7

Euteneuer, U., McIntosh, J.R., 1981. Polarity of some motility-related microtubules. Proc. Natl. Acad. Sci. 78, 372–376. https://doi.org/10.1073/pnas.78.1.372

FARINA, M., ATTIAS, M., SOUTO-PADRON, T., DE SOUZA, W., 1986. Further Studies on the Organization of the Paraxial Rod of Trypanosomatids. J. Protozool. 33, 552–557. https://doi.org/10.1111/j.1550-7408.1986.tb05661.x

Farr, H., Gull, K., 2009. Functional studies of an evolutionary conserved, cytochrome b5 domain protein reveal a specific role in axonemal organisation and the general phenomenon of post-division axonemal growth in trypanosomes. Cell Motil. Cytoskeleton 66, 24–35. https://doi.org/10.1002/cm.20322

Franco, J.R., Cecchi, G., Paone, M., Diarra, A., Grout, L., Kadima Ebeja, A., Simarro, P.P., Zhao, W., Argaw, D., 2022. The elimination of human African trypanosomiasis: Achievements in relation to WHO road map targets for 2020. PLoS Negl. Trop. Dis. 16, e0010047. https://doi.org/10.1371/journal.pntd.0010047

Gennerich, A., Vale, R.D., 2009. Walking the walk: how kinesin and dynein coordinate their steps. Curr. Opin. Cell Biol. https://doi.org/10.1016/j.ceb.2008.12.002

Gluenz, E., Povelones, M.L., Englund, P.T., Gull, K., 2011. The Kinetoplast Duplication Cycle in *Trypanosoma brucei* Is Orchestrated by Cytoskeleton-Mediated Cell Morphogenesis. Mol. Cell. Biol. 31, 1012–1021. https://doi.org/10.1128/MCB.01176-10

Goehring, N.W., Hyman, A.A., 2012. Organelle Growth Control through Limiting Pools of Cytoplasmic Components. Curr. Biol. 22, R330–R339. https://doi.org/10.1016/j.cub.2012.03.046

Hajduk, S., Ochsenreiter, T., 2010. RNA editing in kinetoplastids. RNA Biol. 7, 229–236. https://doi.org/10.4161/rna.7.2.11393

Höög, J.L., Huisman, S.M., Sebö-Lemke, Z., Sandblad, L., McIntosh, J.R., Antony, C., Brunner, D., 2011. Electron tomography reveals a flared morphology on growing microtubule ends. J. Cell Sci. 124, 693–698. https://doi.org/10.1242/jcs.072967

Huaˆn, H., Ngoˆ*, N., Tschudi, C., Gull, K., Ullu, E., 1998. Double-stranded RNA induces mRNA degradation in Trypanosoma brucei, Biochemistry.

Huet, D., Blisnick, T., Perrot, S., Bastin, P., 2019. IFT25 is required for the construction of the trypanosome flagellum. J. Cell Sci. 132. https://doi.org/10.1242/jcs.228296

Hughes, L., Towers, K., Starborg, T., Gull, K., Vaughan, S., 2013. A cell-body groove housing the new flagellum tip suggests an adaptation of cellular morphogenesis for parasitism in the bloodstream form of Trypanosoma brucei. J. Cell Sci. 126, 5748–5757. https://doi.org/10.1242/jcs.139139

Janke, C., Magiera, M.M., 2020. The tubulin code and its role in controlling microtubule properties and functions. Nat. Rev. Mol. Cell Biol. https://doi.org/10.1038/s41580-020-0214-3

Jentzsch, J., Sabri, A., Speckner, K., Lallinger-Kube, G., Weiss, M., Ersfeld, K., 2020. Microtubule polyglutamylation is important for regulating cytoskeletal architecture

and motility in Trypanosoma brucei. J. Cell Sci. 133. https://doi.org/10.1242/jcs.248047

Jumper, J., Evans, R., Pritzel, A., Green, T., Figurnov, M., Ronneberger, O., Tunyasuvunakool, K., Bates, R., Žídek, A., Potapenko, A., Bridgland, A., Meyer, C., Kohl, S.A.A., Ballard, A.J., Cowie, A., Romera-Paredes, B., Nikolov, S., Jain, R., Adler, J., Back, T., Petersen, S., Reiman, D., Clancy, E., Zielinski, M., Steinegger, M., Pacholska, M., Berghammer, T., Bodenstein, S., Silver, D., Vinyals, O., Senior, A.W., Kavukcuoglu, K., Kohli, P., Hassabis, D., 2021. Highly accurate protein structure prediction with AlphaFold. Nature 596, 583–589. https://doi.org/10.1038/s41586-021-03819-2

Jung, J., Santi-Rocca, J., Fort, C., Tinevez, J.-Y., Schietroma, C., Bastin, P., 2021. Concentration of intraflagellar transport proteins at the ciliary base is required for proper train injection (preprint). Cell Biology. https://doi.org/10.1101/2021.08.02.454739

Kilmartin, J.V., Wright, B., Mistein, C., 1971. Rat Monoclonal Antitubulin Antibodies Derived by Using a New Nonsecreting Rat Cell Line.

Kohl, L., Robinson, D., Bastin, P., 2003. Novel roles for the flagellum in cell morphogenesis and cytokinesis of trypanosomes. EMBO J. 22, 5336–5346. https://doi.org/10.1093/emboj/cdg518

Kozminski, K.G., Beech, P.L., Rosenbaum, J.L., 1995. The Chlamydomonas kinesin-like protein FLA10 is involved in motility associated with the flagellar membrane. J. Cell Biol. 131, 1517–1527. https://doi.org/10.1083/jcb.131.6.1517

Kozminski, K.G., Johnson, K.A., Forscher, P., Rosenbaum, J.L., 1993. A motility in the eukaryotic flagellum unrelated to flagellar beating. Proc. Natl. Acad. Sci. 90, 5519–5523. https://doi.org/10.1073/pnas.90.12.5519

Lacey, S.E., Foster, H.E., Pigino, G., 2023. The molecular structure of IFT-A and IFT-B in anterograde intraflagellar transport trains. Nat. Struct. Mol. Biol. 30, 584–593. https://doi.org/10.1038/s41594-022-00905-5

Lacomble, S., Vaughan, S., Gadelha, C., Morphew, M.K., Shaw, M.K., McIntosh, J.R., Gull, K., 2010. Basal body movements orchestrate membrane organelle division and cell morphogenesis in *Trypanosoma brucei*. J. Cell Sci. 123, 2884–2891. https://doi.org/10.1242/jcs.074161

Lacomble, S., Vaughan, S., Gadelha, C., Morphew, M.K., Shaw, M.K., McIntosh, J.R., Gull, K., 2009. Three-dimensional cellular architecture of the flagellar pocket and associated cytoskeleton in trypanosomes revealed by electron microscope tomography. J. Cell Sci. 122, 1081–1090. https://doi.org/10.1242/jcs.045740

Langousis, G., Hill, K.L., 2014. Motility and more: The flagellum of Trypanosoma brucei. Nat. Rev. Microbiol. https://doi.org/10.1038/nrmicro3274

Lee, K.J., Li, Z., 2021. The CRK2-CYC13 complex functions as an S-phase cyclin-dependent kinase to promote DNA replication in Trypanosoma brucei. BMC Biol. 19. https://doi.org/10.1186/s12915-021-00961-1

Lee, K.J., Zhou, Q., Li, Z., 2023. CRK2 controls cytoskeleton morphogenesis in Trypanosoma brucei by phosphorylating β-tubulin to regulate microtubule dynamics. PLoS Pathog. 19. https://doi.org/10.1371/journal.ppat.1011270

Lemos, M., Mallet, A., Bertiaux, E., Imbert, A., Rotureau, B., Bastin, P., 2020. Timing and original features of flagellum assembly in trypanosomes during development in the tsetse fly. Parasit. Vectors 13. https://doi.org/10.1186/s13071-020-04026-0

L'hernault, S.W., Rosenbaum, J.L., 1983. Chlamydomonas a-Tubulin Is Posttranslationally in the Flagella during Flagellar Assembly Modified.

Li, S., Fernandez, J.J., Marshall, W.F., Agard, D.A., 2012. Three-dimensional structure of basal body triplet revealed by electron cryo-tomography. EMBO J. 31, 552–562. https://doi.org/10.1038/emboj.2011.460

Li, Z., Wang, C.C., 2006. Changing roles of aurora-B kinase in two life cycle stages of Trypanosoma brucei. Eukaryot. Cell 5, 1026–1035. https://doi.org/10.1128/EC.00129-06

Mandelkow, E.-M., Mandelkow, E., Milligan, R.A., 1991. Microtubule Dynamics and Microtubule Caps: A Time-resolved Cryo-Electron Microscopy Study.

Marshall, W.F., Rosenbaum, J.L., 2001. Intraflagellar transport balances continuous turnover of outer doublet microtubules. J. Cell Biol. 155, 405–414. https://doi.org/10.1083/jcb.200106141

Meyer, H., De Souza, W., 1976. Electron Microscopic Study of *Trypanosoma cruzi* Periplast in Tissue Cultures. I. Number and Arrangement of the Peripheral Microtubules in the Various Forms of the Parasite's Life Cycle*. J. Protozool. 23, 385–390. https://doi.org/10.1111/j.1550-7408.1976.tb03792.x

Muniz, R.S., Campbell, P.C., Sladewski, T.E., Renner, L.D., De Graffenried, C.L., 2022. Revealing spatio-temporal dynamics with long-term trypanosomatid live-cell imaging. PLOS Pathog. 18, e1010218. https://doi.org/10.1371/journal.ppat.1010218

Myler, P.J., Glick', D., Feagin, J.E., Morales, T.H., Stuart, K.D., n.d. Structural organization of the maxicircle variable region of Trypanosoma brucei: identification of potential replication origins and topoisomerase 11 binding sites.

Nehlig, A., Molina, A., Rodrigues-Ferreira, S., Honoré, S., Nahmias, C., 2017. Regulation of end-binding protein EB1 in the control of microtubule dynamics. Cell. Mol. Life Sci. https://doi.org/10.1007/s00018-017-2476-2

Nogales, E., Wang, H.W., 2006. Structural mechanisms underlying nucleotide-dependent self-assembly of tubulin and its relatives. Curr. Opin. Struct. Biol. https://doi.org/10.1016/j.sbi.2006.03.005

Nogales, E., Wolf, S.G., Downing, K.H., 1998. Structure of the tubulin dimer by electron crystallography, NATURE.

Ogbadoyi, E.O., Robinson, D.R., Gull, K., 2003. A High-Order *Trans* -Membrane Structural Linkage Is Responsible for Mitochondrial Genome Positioning and Segregation by Flagellar Basal Bodies in Trypanosomes. Mol. Biol. Cell 14, 1769–1779. https://doi.org/10.1091/mbc.e02-08-0525

O'Toole, J.F., Bruggeman, L.A., Madhavan, S., Sedor, J.R., 2017. The Cell Biology of APOL1. Semin. Nephrol. 37, 538–545. https://doi.org/10.1016/j.semnephrol.2017.07.007

Pays, E., Coquelet, H., Tebabi, P., Pays, A., Jefferies, D., Steinert, M., Koenig, E., Williams, R.O., Roditi, I., 1990. Trypanosoma brucei: constitutive activity of the VSG and procyclin gene promoters. EMBO J. 9, 3145–3151. https://doi.org/10.1002/j.1460-2075.1990.tb07512.x

Peter J Schatz, ', Georges, G.E., Solomon, F., Botstein', D., 1987. Insertions of up to 17 Amino Acids into a Region of ox-Tubulin Do Not Disrupt Function In Vivo Downloaded from, MOLECULAR AND CELLULAR BIOLOGY.

Pigino, G., 2021. Intrafl agellar transport, R530 Current Biology.

Piperno, G., Fuller, M.T., 1985. Monoclonal Antibodies Specific for an Acetylated Form of a-Tubulin Recognize the Antigen in Cilia and Flagella from a Variety of Organisms.

Ploubidou, A., n.d. Cell cycle checkpoints in trypanosomes.

Poon, S.K., Peacock, L., Gibson, W., Gull, K., Kelly, S., 2012. A modular and optimized single marker system for generating Trypanosoma brucei cell lines expressing T7 RNA polymerase and the tetracycline repressor. Open Biol. 2. https://doi.org/10.1098/rsob.110037

Portman, N., Lacomble, S., Thomas, B., McKean, P.G., Gull, K., 2009. Combining RNA Interference Mutants and Comparative Proteomics to Identify Protein Components and Dependences in a Eukaryotic Flagellum. J. Biol. Chem. 284, 5610–5619. https://doi.org/10.1074/jbc.M808859200

Rachel, R.A., Li, T., Swaroop, A., 2012. Photoreceptor sensory cilia and ciliopathies: focus on CEP290, RPGR and their interacting proteins. Cilia 1, 22. https://doi.org/10.1186/2046-2530-1-22

Ralston, K.S., Hill, K.L., 2006. Trypanin, a Component of the Flagellar Dynein Regulatory Complex, Is Essential in Bloodstream Form African Trypanosomes. PLoS Pathog. 2, e101. https://doi.org/10.1371/journal.ppat.0020101

Rath, A., Glibowicka, M., Nadeau, V.G., Chen, G., Deber, C.M., 2009. Detergent binding explains anomalous SDS-PAGE migration of membrane proteins. Proc. Natl. Acad. Sci. 106, 1760–1765. https://doi.org/10.1073/pnas.0813167106

Rico, E., Jeacock, L., Kovářová, J., Horn, D., 2018. Inducible high-efficiency CRISPR-Cas9-targeted gene editing and precision base editing in African trypanosomes. Sci. Rep. 8, 7960. https://doi.org/10.1038/s41598-018-26303-w

Robinson, D., Gull, K., 1991. Basal body movements as a mechanism for mitochondrial genome segregation in the trypanosome cell cycle. Nature 352, 731–733.

Rose, C., Casas-Sánchez, A., Dyer, N.A., Solórzano, C., Beckett, A.J., Middlehurst, B., Marcello, M., Haines, L.R., Lisack, J., Engstler, M., Lehane, M.J., Prior, I.A., Acosta-Serrano, Á., 2020. Trypanosoma brucei colonizes the tsetse gut via an immature peritrophic matrix in the proventriculus. Nat. Microbiol. 5, 909–916. https://doi.org/10.1038/s41564-020-0707-z

Rotureau, B., Ooi, C.-P., Huet, D., Perrot, S., Bastin, P., 2014. Forward motility is essential for trypanosome infection in the tsetse fly: Trypanosome motility is essential in tsetse flies. Cell. Microbiol. 16, 425–433. https://doi.org/10.1111/cmi.12230

Rotureau, B., Subota, I., Bastin, P., 2011. Molecular bases of cytoskeleton plasticity during the Trypanosoma brucei parasite cycle. Cell. Microbiol. 13, 705–716. https://doi.org/10.1111/j.1462-5822.2010.01566.x

Rotureau, B., Subota, I., Buisson, J., Bastin, P., 2012. A new asymmetric division contributes to the continuous production of infective trypanosomes in the tsetse fly. Development 139, 1842–1850. https://doi.org/10.1242/dev.072611

Rotureau, B., Van Den Abbeele, J., 2013. Through the dark continent: African trypanosome development in the tsetse fly. Front. Cell. Infect. Microbiol. 3. https://doi.org/10.3389/fcimb.2013.00053

Sasse, R., Gull, K., 1988. Tubulin post-translational modifications and the construction of microtubular organelles in Trypanosoma brucei.

Schatz, P.J., Georges, G.E., Solomon, F., Botstein', D., 1987. Insertions of up to 17 Amino Acids into a Region of ox-Tubulin Do Not Disrupt Function In Vivo. MOL CELL BIOL 7.

Schindelin, J., Arganda-Carreras, I., Frise, E., Kaynig, V., Longair, M., Pietzsch, T., Preibisch, S., Rueden, C., Saalfeld, S., Schmid, B., Tinevez, J.-Y., White, D.J., Hartenstein, V., Eliceiri, K., Tomancak, P., Cardona, A., 2012. Fiji: an open-source platform for biological-image analysis. Nat. Methods 9, 676–682. https://doi.org/10.1038/nmeth.2019

Schneider, A., Plessmann, U., Weber, K., 1997. Subpellicular and flagellar microtubules of *Trypanosoma brucei* are extensively glutamylated. J. Cell Sci. 110, 431–437. https://doi.org/10.1242/jcs.110.4.431

Schneider, A., Sherwin, T., Sasse, R., Russell, D.G., Gull, K., Seebeck, T., 1986. Subpellicular and Flagellar Microtubules of Trypanosoma brucei brucei Contain the Same a-Tubulin Isoforms.

Seebeck, T., Whittaker, P.A., Imboden, M.A., Hardman, N., Braun, R., 1983. Tubulin genes of Trypanosoma brucei: a tightly clustered family of alternating genes. Proc. Natl. Acad. Sci. 80, 4634–4638. https://doi.org/10.1073/pnas.80.15.4634

Shaw, S., DeMarco, S.F., Rehmann, R., Wenzler, T., Florini, F., Roditi, I., Hill, K.L., 2019. Flagellar cAMP signaling controls trypanosome progression through host tissues. Nat. Commun. 10, 803. https://doi.org/10.1038/s41467-019-08696-y

Shaw, S., Knüsel, S., Abbühl, D., Naguleswaran, A., Etzensperger, R., Benninger, M., Roditi, I., 2022. Cyclic AMP signalling and glucose metabolism mediate pH taxis by African trypanosomes. Nat. Commun. 13, 603. https://doi.org/10.1038/s41467-022-28293-w

Sheriff, O., Lim, L.F., He, C.Y., 2014. Tracking the biogenesis and inheritance of subpellicular microtubule in trypanosoma brucei with inducible YFP- α-tubulin. BioMed Res. Int. 2014. https://doi.org/10.1155/2014/893272

Sherman, D.R., Janz, L., Hug, M., Clayton, C., 1991. Anatomy of the parp gene promoter of Trypanosoma brucei. EMBO J. 10, 3379–3386. https://doi.org/10.1002/j.1460-2075.1991.tb04902.x

Sherwin, T., Gull, K., 1989. The cell division cycle of Trypanosoma brucei timing of event markers and cytoskeletal modulations.

Sherwin, T., Gull', K., 1989. Visualization of Detyrosination along Single Microtubules Reveals Novel Mechanisms of Assembly during Cytoskeletal Duplication in Trypanosomes, Cell.

Sherwin, T., Schneider, A., Sasse, R., Seebeck, T., Gull, K., 1987a. Distinct Localization and Cell Cycle Dependence of COOH Terminally Tyrosinolated a-Tubulin in the Microtubules of Trypanosoma brucei brucei.

Sherwin, T., Schneider, A., Sasse, R., Seebeck, T., Gull, K., 1987b. Distinct Localization and Cell Cycle Dependence of COOH Terminally Tyrosinolated a-Tubulin in the Microtubules of Trypanosoma brucei brucei.

Shi, H., Chamond, N., Djikeng, A., Tschudi, C., Ullu, E., 2009. RNA Interference in Trypanosoma brucei. J. Biol. Chem. 284, 36511–36520. https://doi.org/10.1074/jbc.M109.073072

Shimogawa, M.M., Ray, S.S., Kisalu, N., Zhang, Y., Geng, Q., Ozcan, A., Hill, K.L., 2018. Parasite motility is critical for virulence of African trypanosomes. Sci. Rep. 8. https://doi.org/10.1038/s41598-018-27228-0

Sinclair, A.N., Huynh, C.T., Sladewski, T.E., Zuromski, J.L., Ruiz, A.E., de Graffenried, C.L., 2021. The Trypanosoma brucei subpellicular microtubule array is organized into functionally discrete subdomains defined by microtubule associated proteins. PLoS Pathog. 17. https://doi.org/10.1371/journal.ppat.1009588

Sirajuddin, M., Rice, L.M., Vale, R.D., 2014. Regulation of microtubule motors by tubulin isotypes and post-translational modifications. Nat. Cell Biol. 16, 335–344. https://doi.org/10.1038/ncb2920

Soppina, V., Herbstman, J.F., Skiniotis, G., Verhey, K.J., 2012. Luminal Localization of α-tubulin K40 Acetylation by Cryo-EM Analysis of Fab-Labeled Microtubules. PLoS ONE 7. https://doi.org/10.1371/journal.pone.0048204

Stuart, K., Allen, T.E., Heidmann, S., Seiwert, S.D., 1997. RNA Editing in Kinetoplastid Protozoa. MICROBIOL MOL BIOL REV 61.

Sunter, J.D., Dean, S., Wheeler, R.J., 2023. TrypTag.org: from images to discoveries using genome-wide protein localisation in Trypanosoma brucei. Trends Parasitol. 39, 328–331. https://doi.org/10.1016/j.pt.2023.02.008

Sunter, J.D., Gull, K., 2016. The Flagellum Attachment Zone: 'The Cellular Ruler' of Trypanosome Morphology. Trends Parasitol. https://doi.org/10.1016/j.pt.2015.12.010

Taylor, A.E.R., Godfrey, D.G., 1969. A New Organelle of Bloodstream Salivarian Trypanosomes. J. Protozool. 16, 466–470. https://doi.org/10.1111/j.1550-7408.1969.tb02302.x

Thomashow, L.S., Milhausen, M., Rutter, W.J., Agabian, N., 1983. Tubulin genes are tandemly linked and clustered in the genome of trypanosoma brucei. Cell 32, 35–43. https://doi.org/10.1016/0092-8674(83)90494-4

Thomson, R., Finkelstein, A., 2015. Human trypanolytic factor APOL1 forms pH-gated cation-selective channels in planar lipid bilayers: Relevance to trypanosome lysis. Proc. Natl. Acad. Sci. 112, 2894–2899. https://doi.org/10.1073/pnas.1421953112

Thomson, R., Genovese, G., Canon, C., Kovacsics, D., Higgins, M.K., Carrington, M., Winkler, C.A., Kopp, J., Rotimi, C., Adeyemo, A., Doumatey, A., Ayodo, G., Alper, S.L., Pollak, M.R., Friedman, D.J., Raper, J., 2014. Evolution of the primate trypanolytic factor APOL1. Proc. Natl. Acad. Sci. 111. https://doi.org/10.1073/pnas.1400699111

Tilney, L.G., Bryan, J., Bush, D.J., Fujiwara, K., Mooseker, D.B.M., Snyder, D.H., 1973. MICROTUBULES : EVIDENCE FOR 13 PROTOFILAMENTS.

Trépout, S., Tassin, A.M., Marco, S., Bastin, P., 2018. STEM tomography analysis of the trypanosome transition zone. J. Struct. Biol. 202, 51–60. https://doi.org/10.1016/j.jsb.2017.12.005

Tu, X., Wang, C.C., 2005. Coupling of Posterior Cytoskeletal Morphogenesis to the G1/S Transition in the Trypanosoma brucei Cell Cycle □ D. Mol. Biol. Cell 16, 97–105. https://doi.org/10.1091/mbc.E04

Tyler, K., 2001. Anisomorphic Cell Division by African Trypanosomes. Protist 152, 367–378. https://doi.org/10.1078/1434-4610-00074

Uzureau, P., Uzureau, S., Lecordier, L., Fontaine, F., Tebabi, P., Homblé, F., Grélard, A., Zhendre, V., Nolan, D.P., Lins, L., Crowet, J.-M., Pays, A., Felu, C., Poelvoorde, P., Vanhollebeke, B., Moestrup, S.K., Lyngsø, J., Pedersen, J.S., Mottram, J.C., Dufourc, E.J., Pérez-Morga, D., Pays, E., 2013. Mechanism of Trypanosoma brucei gambiense resistance to human serum. Nature 501, 430–434. https://doi.org/10.1038/nature12516

Van Den Hoek, H., Klena, N., Jordan, M.A., Alvarez Viar, G., Righetto, R.D., Schaffer, M., Erdmann, P.S., Wan, W., Geimer, S., Plitzko, J.M., Baumeister, W., Pigino, G., Hamel, V., Guichard, P., Engel, B.D., 2022. In situ architecture of the ciliary base reveals the stepwise assembly of intraflagellar transport trains. Science 377, 543–548. https://doi.org/10.1126/science.abm6704

van der Laan, S., Lévêque, M.F., Marcellin, G., Vezenkov, L., Lannay, Y., Dubra, G., Bompard, G., Ovejero, S., Urbach, S., Burgess, A., Amblard, M., Sterkers, Y., Bastien, P.,

Rogowski, K., 2019. Evolutionary Divergence of Enzymatic Mechanisms for Tubulin Detyrosination. Cell Rep. 29, 4159-4171.e6. https://doi.org/10.1016/j.celrep.2019.11.074

Vanhamme, L., Poelvoorde, P., Nolan, D.P., Lins, L., Xong, H.V., Jacquet, A., Moguilevsky, N., Dieu, M., Kane, J.P., Baetselier, P.D., Brasseur, R., Pays, E., 2003. Apolipoprotein L-I is the trypanosome lytic factor of human serum 422.

Varga, V., Moreira-Leite, F., Portman, N., Gull, K., 2017. Protein diversity in discrete structures at the distal tip of the trypanosome flagellum. Proc. Natl. Acad. Sci. U. S. A. 114, E6546–E6555. https://doi.org/10.1073/pnas.1703553114

Vaughan, S., Gull, K., 2016. Basal body structure and cell cycle-dependent biogenesis in Trypanosoma brucei. Cilia. https://doi.org/10.1186/s13630-016-0023-7

Vickerman, K., 1985. DEVELOPMENTAL CYCLES AND BIOLOGY OF PATHOGENIC TRYPANOSOMES, British Medical Bulletin.

Vickerman, K., Tetley, L., Hendry, K.A.K., Michael, C., Turner, R., 1988. Biology of African trypanosomes in the tsetse fly, Biology of the Cell.

Vincensini, L., Blisnick, T., Bastin, P., 2011. 1001 model organisms to study cilia and flagella. Biol. Cell 103, 109–130. https://doi.org/10.1042/BC20100104

Wang, H.W., Nogales, E., 2005. Nucleotide-dependent bending flexibility of tubulin regulates microtubule assembly. Nature 435, 911–915. https://doi.org/10.1038/nature03606

Wedel, C., Förstner, K.U., Derr, R., Siegel, T.N., 2017. GT -rich promoters can drive RNA pol II transcription and deposition of H2A.Z in African trypanosomes. EMBO J. 36, 2581–2594. https://doi.org/10.15252/embj.201695323

Wheeler, R.J., 2021. A resource for improved predictions of Trypanosoma and Leishmania protein three-dimensional structure. PLOS ONE 16, e0259871. https://doi.org/10.1371/journal.pone.0259871

Winey, M., O'Toole, E., 2014. Centriole structure. Philos. Trans. R. Soc. B Biol. Sci. https://doi.org/10.1098/rstb.2013.0457

Wirtz, E., Clayton, C., 1995. Inducible Gene Expression in Trypanosomes Mediated by a Prokaryotic Repressor. Science 1179–1183.

Wirtz, E., Hoek, M., Cross, G.A.M., 1998. Regulated processive transcription of chromatin by T7 RNA polymerase in Trypanosoma brucei. Nucleic Acids Res. 26, 4626–4634. https://doi.org/10.1093/nar/26.20.4626

Wolff A, de Néchaud B, Chillet D, Mazarguil H, Desbruyères E, Audebert S, Eddé B, Gros F, Denoulet P., 1992. Distribution of glutamylated alpha and beta-tubulin in mouse tissues using a specific monoclonal antibody, GT335. Eur J Cell Biol 1992 Dec592425-32 PMID 1493808.

Woods, A., Sherwin, T., Sasse, R., Macraef, T.H., Baines, A.J., Gull, K., 1989. Definition of individual components within the cytoskeieton of Trypanosoma brucei by a library of monoclonal antibodies.

Woodward, R., Gull, K., 1990. Timing of nuclear and kinetoplast DNA replication and early morphological events in the cell cycle of *Trypanosoma brucei*. J. Cell Sci. 95, 49–57. https://doi.org/10.1242/jcs.95.1.49

Zhang, J., Wang, H., Imhof, S., Zhou, X., Liao, S., Atanasov, I., Hui, W.H., Hill, K.L., Zhou, Z.H., 2021. Structure of the trypanosome paraflagellar rod and insights into non-planar motility of eukaryotic cells. Cell Discov. 7, 51. https://doi.org/10.1038/s41421-021-00281-2

References

Zhou, Q., Hu, H., Li, Z., 2014. New insights into the molecular mechanisms of mitosis and cytokinesis in trypanosomes, in: International Review of Cell and Molecular Biology. Elsevier Inc., pp. 127–166. https://doi.org/10.1016/B978-0-12-800097-7.00004-X

Abstract

Flagella are membrane wrapped microtubule-based protrusions of the cell that play roles in motility, signaling, cell morphogenesis and division. An important property of these organelles is their length. Mis-regulation of flagellar length can impair function of the flagellum, the cell or even the entire organism. We chose African trypanosomes to investigate what regulates flagellar length, with a focus on the timing of assembly. When comparing the cell morphology between the different life cycle stages it becomes apparent that the length of the flagellum is not a constant and almost every life cycle stage has its own intricate flagellar length. However, length between cells of the same life cycle stage does not significantly change, initial assembly aside. This suggests that these parasites have evolved a mechanism that allows them to regulate flagellar length very precisely. We chose to investigate the timing of assembly with the flagellums most important building block tubulin. Studies with tagged tubulin in the trypanosome flagellum have so far been difficult as terminally tagged tubulin does not incorporate into the axoneme. We chose a new approach by tagging tubulin intragenic in an intricate structure called the acetylation loop as this strategy was successfully carried out in yeast and mammalian cells. We could show that tubulin tagged with this approach is indeed a formidable marker to track microtubule assembly dynamics in the flagellum as well as other microtubule-based structures. Assembly follows the recently proposed Grow and Lock-model with an important addition. We found compelling evidence that the very tip of flagella is subject to integration several generations after their emergence and that this happens most likely during the G1-phase of the cell cycle.

Keywords: Flagellar length, Grow and Lock model, tubulin, inducible expression

Résumé

Les flagelles sont des protubérances cellulaires enveloppées d'une membrane et basées sur des microtubules, qui jouent un rôle dans la motilité, la signalisation, la morphogenèse et la division cellulaires. Une propriété importante de ces organites est leur longueur. Une mauvaise régulation de la longueur des flagelles peut nuire au fonctionnement du flagelle, de la cellule, voire de l'organisme tout entier. Nous avons choisi les trypanosomes africains pour étudier ce qui régule la longueur des flagelles, en nous concentrant sur le moment de l'assemblage. En comparant la morphologie cellulaire entre les différents stades du cycle de vie, il devient évident que la longueur du flagelle n'est pas une constante et que presque chaque stade du cycle de vie a sa propre longueur de flagelle. Cependant, la longueur entre les cellules d'un même stade du cycle de vie ne change pas de manière significative, à l'exception de l'assemblage initial. Cela suggère que ces parasites ont développé un mécanisme qui leur permet de réguler très précisément la longueur des flagelles. Nous avons choisi d'étudier la chronologie de l'assemblage à l'aide de la tubuline, le principal élément constitutif des flagelles. Les études sur la tubuline marquée dans le flagelle du trypanosome ont jusqu'à présent été difficiles car la tubuline marquée de façon terminale ne s'incorpore pas dans l'axonème. Nous avons choisi une nouvelle approche en marquant la tubuline de manière intragénique dans une structure complexe appelée boucle d'acétylation, car cette stratégie a été appliquée avec succès dans des cellules de levure et de mammifère. Nous avons pu montrer que la tubuline marquée avec cette approche est en effet un marqueur formidable pour suivre la dynamique d'assemblage des microtubules dans le flagelle ainsi que dans d'autres structures basées sur les microtubules. L'assemblage suit le modèle "Grow and Lock" récemment proposé, avec un ajout important. Nous avons trouvé des preuves irréfutables que l'extrémité des flagelles est sujette à l'intégration plusieurs générations après leur émergence et que cela se produit très probablement pendant la phase G1 du cycle cellulaire.

Mots-clés : Longueur flagellaire, modèle de croissance et de verrouillage, tubuline, expression inductible